

Annual Technical Progress Report: E-BEAM TESTING AND EVALUATION OF SUPERPOLISHED HIGH QUALITY DEVELOPMENTAL MIRRORS

Covering the Period:
21 November 1989 - 21 November 1990

Submitted Under:
Contract No. DASG60-90-C-0002

UNITED STATES ARMY STRATEGIC DEFENSE COMMAND
P.O. Box 1500
Huntsville, AL 35807-3801

19980302 085

BMDOTIC BRIDGE DESIGN INFORMATION CENTER



spire

DISTRIBUTION STATEMENT A

Approved for public release;
Distribution Unlimited

U2892

Report Number: AR-10125

Accession Number: 2892

Title: E-beam Testing and Evaluation of
Superpolished High Quality

Developmental Mirrors

Contract Number: DASG60-90-C-002

Corporate Author or Publisher: Spire Corporation, Bedford, MA 01730

Report Prepared For: U.S. Army Strategic Defense Command,
Huntsville, AL 35807-3801

Publication Date: Dec 01, 1990

Pages: 00100

Comments on Document: Annual Technical Progress Report.

Descriptors, Keywords: Test Evaluation Beam Mirror DEW
Fabrication Material

Annual Technical Progress Report
E-BEAM TESTING AND EVALUATION OF SUPERPOLISHED
HIGH QUALITY DEVELOPMENTAL MIRRORS

Covering the Period:
21 November 1989 - 21 November 1990

Submitted under:
Contract No. DASG60-90-C-0002

Prepared for:
UNITED STATES ARMY STRATEGIC DEFENSE COMMAND
P.O. Box 1500
Huntsville, AL 35807-3801

Submitted by:
SPIRE CORPORATION
Patriots Park
Bedford, MA 01730

BMDOTIC

The views, opinions and/or findings contained in this report are those of the author(s) and should not be construed as an official Department of the Army position, policy or decision unless so designated by other official documentation.

TABLE OF CONTENTS

<u>Section</u>		<u>Page</u>
1	INTRODUCTION	1
2	PROGRAM PLAN	2
2.1	Phase I	2
2.2	Phase II	3
3	YEAR 1 PROGRESS	6
3.1	21 November 1989 Through 21 December 1989	6
3.1.1	Draft of Program Plan	7
3.1.2	Safety Reports	7
3.1.3	Detector Array Feasibility Study	7
3.1.4	Interferometry	8
3.1.5	Vacuum System	8
3.1.6	Scatterometer Optical Train	8
3.2	1 January 1990 Through 28 February 1990	11
3.2.1	Technical "Kickoff" Meeting of 7 February 1990	11
3.2.2	System Safety Hazard Analysis Report	11
3.2.3	Interferometry and Vibration Isolation Systems	11
3.2.4	Electron Beam Generator: Routine Maintenance	12
3.2.5	Reflective Optical Train for Scatterometer	12
3.3	1 March 1990 Through 31 March 1990	14
3.3.1	Electron Beam Maintenance and Diode Servicing	14
3.3.2	Vacuum System Performance	16
3.3.3	Interferometry Demonstration Using High Speed Camera	16
3.3.4	Optical Table	17
3.3.5	Engineering Design Tasks	17
3.4	1 April 1990 Through 31 May 1990	21
3.5	1 June 1990 Through 31 July 1990	24
3.5.1	Optical System Profile	24
3.5.2	Optical System Calibration	26
3.5.3	Review of Final System	30
3.6	1 August 1990 Through 31 August 1990	33
3.6.1	e-Beam Calibration	33
3.6.2	Scatterometer/Vacuum Chamber	34
3.6.3	BRDF Data	34
3.6.4	BRDF Data Acquisition and Sample Manipulator Software	35

TABLE OF CONTENTS (Concluded)

<u>Section</u>	<u>Page</u>
3.7 1 September 1990 Through 30 September 1990	36
3.7.1 Cryogenic Rad-Hard Testing	36
3.7.1.1 Be O50-01: 1.5-inch Diameter Be Mirror	38
3.7.1.2 Be O50-04: 1.5-inch Diameter Be Mirror	44
3.7.1.3 POCT 56-W1-M1-1: Two-inch Diameter Be Mirror	49
3.7.1.4 POCT 2V-A-67-A: Two-inch Diameter Be Mirror	59
3.7.1.5 POCT 56-W1-M1-2: Two-inch Diameter Be Mirror	68
3.7.2 Summary and Discussion of Results	73
3.8 1 October 1990 Through 30 November 1990	78
3.8.1 New Systems	78
3.8.2 Technical Review Meeting	79
 4 STATUS OF PROGRAM MILESTONES	79
 5 INVENTORY OF MIRRORS AT SPIRE	80
 APPENDIX A - DRAFT PROCEDURAL CHECKLISTS	
 APPENDIX B - MIRROR INVENTORY AT SPIRE CORPORATION AS OF 30 NOVEMBER 1990	

LIST OF ILLUSTRATIONS

<u>Figure</u>		<u>Page</u>
1	Contract Milestones	1
2	Milestone #3 Tasks Initiate e-Beam Tests	2
3	Test Procedure for Two-inch Mirrors	4
4	Milestone #4 Tasks	5
5	Phase II Program Schedule	5
6	Schematic of Scatterometer Optics	9
7	Spot Diagram at Test Mirror	10
8	Spot Diagram at Detector	10
9	BRDF Measurements of ZnSe and GaAs	13
10	Voltage and Current Traces from SPI-PULSE 5000 e-Beam Accelerator	15
11	Interferometry Test at 2000 Hz Camera Rate	18
12	Interferometry Test at 4000 Hz Camera Rate	19
13	Interferometry Test at 10,000 Hz Camera Rate	20
14	Sketch of Interferometer and Scatterometer Optical Table	21
15	CO ₂ Laser Spot Images	23
16	Laser Burn Spots Near Detector Plane	23
17	System Profile Without Final Field Stop or GaAs Window	25
18	System Profile With 0.75-inch Field Stop	25
19	System Profile With Final Beam Stop and GaAs Window in Place	26

LIST OF ILLUSTRATIONS (Continued)

<u>Figure</u>		<u>Page</u>
20	Uncalibrated BRDF Measurements on IR Reflectance Standard	28
21	BRDF Measurements Calibrated to IR Reflectance Standard	28
22	Calibrated CRYOSCAT System Profile	29
23	Comparison of New Reflective System Profile to Old Refractive Optical System	30
24	BRDF Measurement of Reflectance Standard on FASCAT Scatterometer	31
25	Comparison of CRYOSCAT and FASCAT BRDF Measurements on Rockwell RI 94 Mirror	32
26	Comparison of Current and Old System BRDF Measurements on RI 94 Mirror	32
27	Photograph of Assembled CRYOSCAT System	34
28	BRDF Measurements on Mirror RI 94 From Fully Assembled CRYOSCAT System	35
29	Geometry of e-Beam Test Sites on Be Mirrors	39
30	BRDF Measurements on Mirror Be O50-01 at Site A (0.17 cal/cm ² e-beam irradiation)	40
31	BRDF Measurements of Mirror Be O50-01 at Site B (0.28 cal/cm ² e-beam irradiation)	41
32	Nomarski Photomicrographs of Mirror Be O50-01 at Site A (0.17 cal/cm ² e-beam fluence)	42
33	Nomarski Photomicrographs of Mirror Be O50-01 at Site B (0.28 cal/cm ² e-beam fluence)	43
34	BRDF Measurements of Mirror Be O50-04 at Site A (0.28 cal/cm ² e-beam fluence)	45

LIST OF ILLUSTRATIONS (Continued)

<u>Figure</u>		<u>Page</u>
35	BRDF Measurements of Mirror Be O50-04 at Site B (0.45 cal/cm ² e-beam fluence)	46
36	Nomarski Photomicrographs of Mirror Be O50-04 at Site A (0.28 cal/cm ²)	47
37	Nomarski Photomicrographs of Mirror Be O50-04 at Site B (0.45 cal/cm ²)	48
38	BRDF Measurements of Mirror POCT 56-W1-M1-1 at Site A (0.27 cal/cm ²)	50
39	BRDF Measurement of Mirror POCT 56-W1-M1-1 at Site B (0.33 cal/cm ²)	52
40	BRDF Measurements of Mirror POCT 56-W1-M1-1 at Site C (0.45 cal/cm ²)	53
41	BRDF Measurements of Mirror POCT 56-W1-M1-1 at Site D (central position receiving only indirect e-beam irradiation)	54
42	Nomarski Photomicrograph of Mirror POCT 56-W1-M1-1 at Site A (0.27 cal/cm ²)	55
43	Nomarski Photomicrograph of Mirror POCT 56-W1-M1-1 at Site B (0.33 cal/cm ²)	56
44	Nomarski Photomicrograph of Mirror POCT 56-W1-M1-1 at Site C (0.45 cal/cm ²)	57
45	Nomarski Photomicrograph of Mirror POCT 56-W1-M1-1 at Site D (central position, no direct e-beam irradiation)	58
46	BRDF Measurements on Mirror POCT 2V-A-67-A at Site A (0.27 cal/cm ²)	60
47	BRDF Measurements on Mirror POCT 2V-A-67-A at Site B (0.37 cal/cm ²)	62
48	BRDF Measurements on Mirror POCT 2V-A-67-A at Site C (0.45 cal/cm ²)	62

LIST OF ILLUSTRATIONS (Concluded)

<u>Figure</u>		<u>Page</u>
49	BRDF Measurements on Mirror POCT 2V-A-67-A at Site D (central position, no direct irradiation)	63
50	Nomarski Photomicrographs of Mirror POCT 2V-A-67-A at Site A (0.27 cal/cm ²)	64
51	Nomarski Photomicrographs of Mirror POCT 2V-A-67-A at Site B (0.33 cal/cm ²)	65
52	Nomarski Photomicrographs of Mirror POCT 2V-A-67-A at Site C (0.45 cal/cm ²)	66
53	Nomarski Photomicrographs of Mirror POCT 2V-A-67-A at Site D (mirror center, no direct irradiation)	67
54	BRDF Measurements on Mirror POCT 56-W1-M1-2 at Site A (0.27 cal/cm ²)	69
55	BRDF Measurements on Mirror POCT 56-W1-M1-2 at Site B (0.37 cal/cm ²)	71
56	BRDF Measurements on Mirror POCT 56-W1-M1-2 at Site C (0.45 cal/cm ²)	72
57	BRDF Measurements on Mirror POCT 56-W1-M1-2 at Site D (center of mirror, no direct irradiation)	73
58	Nomarski Photomicrographs of Mirror POCT 2V-A-67-A at Site A (0.27 cal/cm ²)	74
59	Nomarski Photomicrographs of Mirror POCT 2V-A-67-A at Site B (0.37 cal/cm ²)	75
60	Nomarski Photomicrographs of Mirror POCT 2V-A-67-A at Site C (0.45 cal/cm ²)	76
61	Nomarski Photomicrographs of Mirror POCT 2V-A-67-A at Site D (center of mirror, no direct irradiation)	77
62	New System Components	78

LIST OF TABLES

<u>Table</u>		<u>Page</u>
1	Selected Properties of GaAs and ZnSe	14
2	Electron Beam Energy Fluence	33
3	BRDF Data at $\pm 7.5^\circ$ for Mirror Be O50-01	40
4	BRDF Data at $\pm 7.5^\circ$ for Mirror Be O50-04	45
5	BRDF Data at $\pm 7.5^\circ$ for Mirror POCT 56-W1-M1-1	51
6	BRDF Data at $\pm 7.5^\circ$ for Mirror POCT 2V-A-67-A	61
7	BRDF Data at $\pm 7.5^\circ$ for Mirror POCT 56-W1-M1-2	70

1. INTRODUCTION

The technical tasks for this program have been divided into two main phases. Phase I involves all equipment refits and system qualification tests necessary for the addition of advanced capabilities (i.e., interferometry and cryo-deposit deposition/monitoring). This phase has been scheduled during the first full year of the contract period. Phase II, during the remaining two years, has been scheduled entirely for performing various test procedures on two- and seven-inch diameter mirrors. At the writing of this report, almost all Phase I tasks have been completed, and Phase I should be completed close to schedule.

There are nine milestones to be reached during this three-year period. The milestones are scheduled as shown in Figure 1. Milestones 1 through 4 are associated with the addition of new testing capabilities to the CRYOSCAT facility, namely interferometry and cryo-deposit deposition/monitoring. Completion of Milestone 4 will mark the end of Phase I. Phase II will entail regularly scheduled testing of two- and seven-inch diameter mirror coupons and samples. Section 2 of this report outlines the three-year schedule for this program. Section 3 provides a chronological report of progress during the first 12 months of the contract period. Section 4 gives the status of remaining tasks and milestones. An appendix includes a first draft of procedural checklists for facility operations.

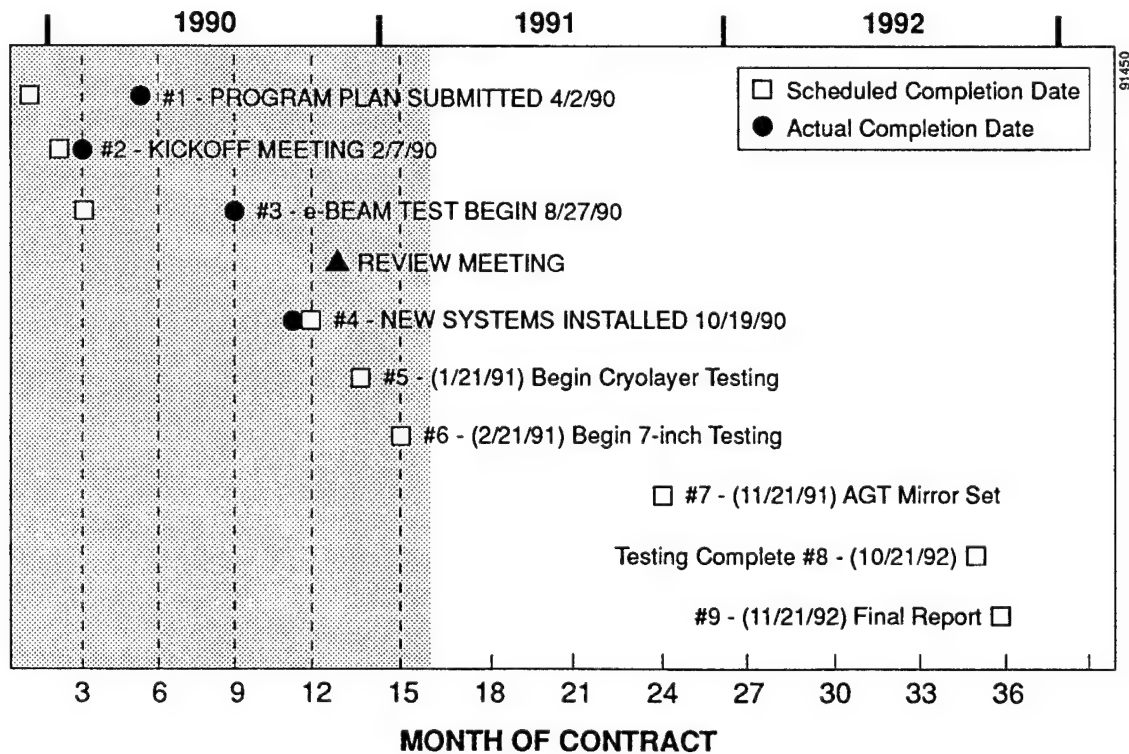


FIGURE 1. CONTRACT MILESTONES

2. PROGRAM PLAN

The following is the original version of the program plan with all tasks aimed at meeting the nine contract milestones:

2.1 Phase I

MILESTONE 1. SUBMISSION OF PROGRAM PLAN

The first milestone is submission of the Program Plan. Prior to the completion of Milestone 1, Safety Hazard Analysis and Description of Proposed Actions and Alternatives (DOPAA) reports were to be prepared and submitted.

MILESTONE 2. TECHNICAL "KICKOFF" MEETING

Milestone 2 is the technical "kickoff" meeting held at Spire on 7 February 1990. This meeting enabled Spire to present the program plan and to discuss all aspects of the effort.

MILESTONE 3. INITIATE E-BEAM TESTING

Milestone 3 marks the beginning of two-inch diameter mirror testing. This window will be open for most of the contract period. Limited testing was performed as new systems were incorporated into the facility. As shown in Figure 2, there were three main tasks to be completed before reaching Milestone 3.

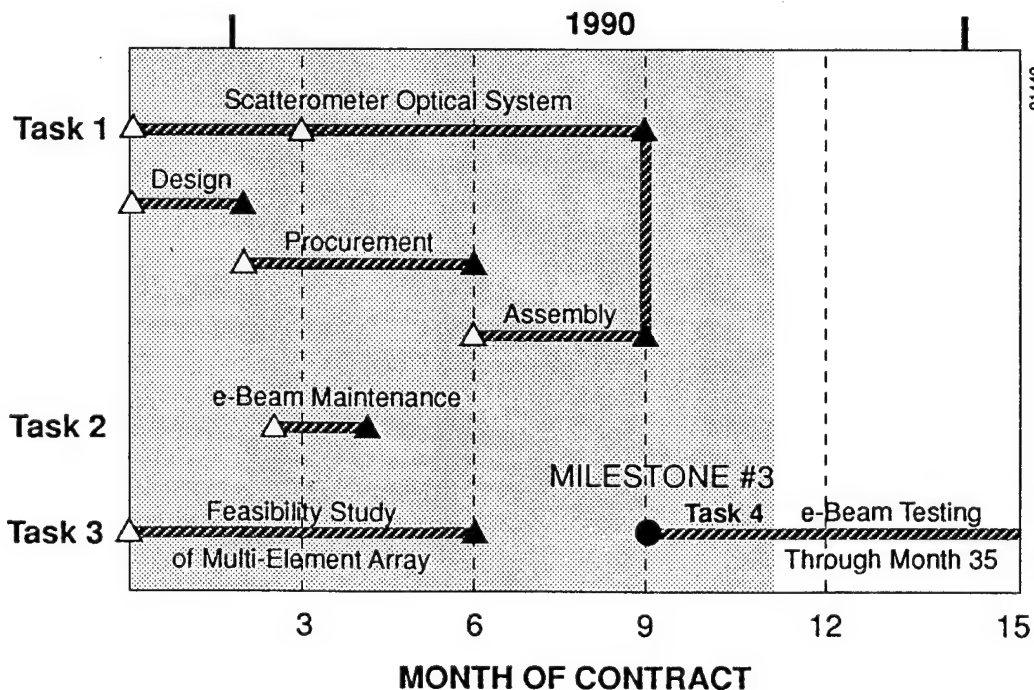


FIGURE 2. MILESTONE #3 TASKS INITIATE e-BEAM TESTS.

Task 1 was the design and installation of a low profile optical train for improved scatterometer performance at near specular angles (SOW Task 1, Subtask 1.1). The modified system was designed as a primarily reflective, rather than refractive, optical system. This type of system is less prone to stray light limitations from bulk and surface scatter by refractive optical elements. The geometry of the system was designed to minimize system profile. A single refractive element was necessary as a vacuum window; Optimization of this window and its associated scatter is critical to the overall performance of the scatterometer.

A comparative set of experiments on ZnSe (an industry standard for IR windows) and GaAs (a promising candidate material) was conducted to determine which is best for the laser beam vacuum window.

Task 2 was completed at Milestone 3. This task (SOW Task 1, Subtask 1.2) involved general servicing and maintenance of the electron beam generator. Vacuum seals were replaced and the diode assembly recalibrated.

Task 3 (SOW Task 1, Subtask 1.3) was initiated at the start of the contract, with scheduled completion in Month 6. This task investigated the feasibility of using a multi-element fixed array of HgCdTe detectors and a high-speed signal processing system as part of the scatterometer. High-speed data acquisition will be a key factor in achieving program testing goals for Years 2 and 3.

Upon reaching Milestone 3, Task 4 (SOW Task 1) was begun. This task includes all tests performed on two-inch diameter mirror coupons during the entire term of the contract. Testing was limited during the first year due to extended periods of down-time required for the installation and qualification of the new systems. Testing procedures for two-inch mirrors is shown in Figure 3.

MILESTONE 4. INSTALLATION AND QUALIFICATION OF NEW SYSTEMS

This milestone will be reached when all new systems are installed and qualified. There are several subtasks involved in reaching this point. Task 5 (SOW Task 2, Subtasks 2.1 through 2.5) includes all subtasks for the design, approval, construction, and qualification of the advanced systems. These are outlined in Figure 4.

The addition of an interferometer to the facility required some planning. A substantial amount of mechanical vibration present in the laboratory must be compensated before the interferometer system could be made operational. Two months were spent examining possible solutions to this problem with the help of both the interferometer manufacturers and vibration isolation experts. The solution is described later in this report.

2.2 Phase II

Years 2 and 3 are outlined in Figure 5. The first two months of Year 2 will involve preliminary testing of all the systems operating as a single facility for the first time. This will allow for procedural development and more detailed planning.

TEST PROCEDURE
<ul style="list-style-type: none">• Cleaning• Photomicroscopy (virgin)• Installation into CRYOSCAT• Room temperature BRDF (all sites)• Bake out vacuum over night• Cool down to 20 K• Cold Virgin BRDF (all sites)• Irradiate three sites• Cold post BRDF (all sites)• Warm to room temperature over night• Room temperature BRDF (all sites)• Vent chamber and remove mirror• Photomicroscopy

91453

FIGURE 3. TEST PROCEDURE FOR TWO-INCH MIRRORS.

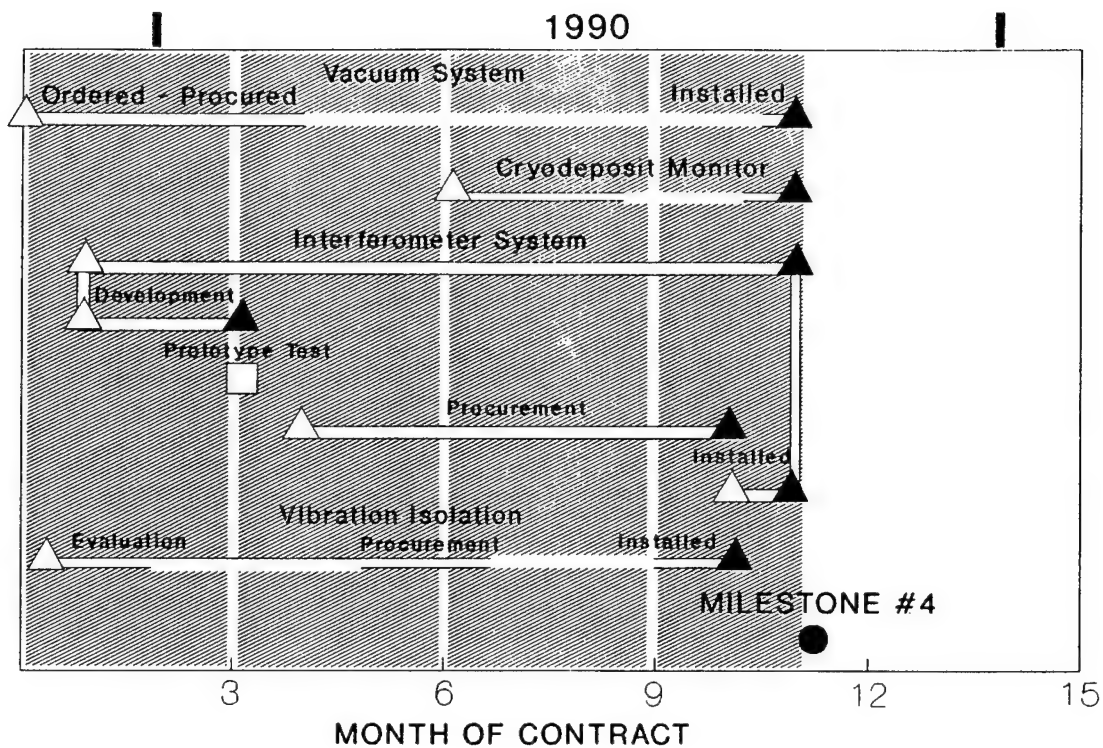


FIGURE 4. MILESTONE #4 TASKS.

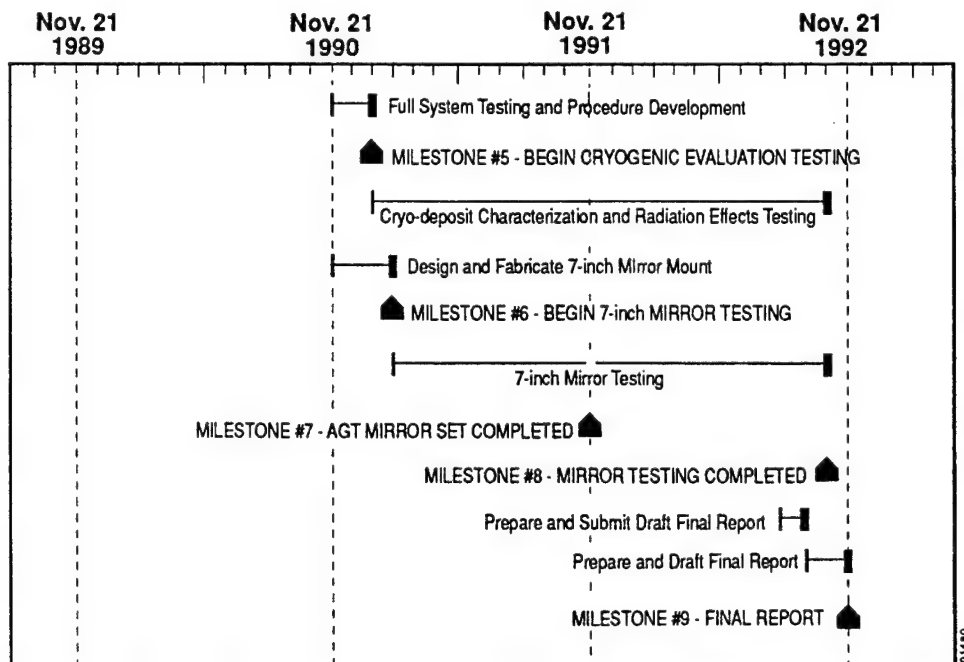


FIGURE 5. PHASE II PROGRAM SCHEDULE.

MILESTONE 5. INITIATE FULL-SCALE TESTING

Beginning in Month 14, the CRYOSCAT facility will be fully committed to testing, characterizing, and evaluating mirrors. The mirrors, both two- and seven-inches in diameter, will be subjected to various testing procedures. Tests will include scatterometry and interferometry of their reflecting surface while at room and cryogenic temperatures, with and without cryo-deposit formations, before and after e-beam irradiation.

MILESTONE 6. INITIATE SEVEN-INCH MIRROR TESTING

Testing/characterization of seven-inch mirrors will begin in Month 15 after appropriate mounting hardware has been fabricated. The interferometer will be of great assistance in the development of a stress-free mount for these mirrors. The procedures used to test large mirrors will be established during the first three months of Year 2. Intermediate tasks for the testing of seven-inch mirrors will depend heavily upon the state of the data acquisition system when testing begins. If the current detection and signal processing systems remain in place, the procedures for seven-inch mirrors will be the same as those for two-inch mirrors (Figure 3).

MILESTONE 7. COMPLETE TESTS OF AGT MIRRORS

By the end of Month 24, a complete set of AGT mirrors will be fully tested and the results documented. This set of mirrors will be furnished by the contracting office and should arrive at Spire no later than Month 19 to allow sufficient time for all tests to be performed and completed on schedule.

MILESTONES 8 AND 9. COMPLETE TESTING AND FINAL REPORT

All mirror testing under this contract will be completed by Month 35. The final month of the program will be devoted to preparing the final technical and other relevant reports.

REPORTING

Monthly technical reports will be filed from Months 2 through 35 except at year-end when annual technical reports will be submitted. Funds and man-hour expenditure as well as contract funds status reports will be filed for each month of the contract period.

3. YEAR 1 PROGRESS

3.1 21 November 1989 Through 21 December 1989

- Draft of program plan
- Safety analysis reports drafted
- Multi-element detector feasibility study initiated
- Design analysis of interferometer system begun

- 10-inch cryopump vacuum system ordered
- Scatterometer optical train designed and ordered

3.1.1 Draft of Program Plan

A three-year program plan was drafted and submitted for approval and/or alteration. The schedule of work was planned in accordance with the milestone requirements of the contract and the statement of work.

Year 1 of the program was dominated by activities aimed at improving and qualifying the test equipment. The first half of Year 1 was devoted to the installation, qualification, and use of a new reflective (rather than refractive) scatterometer. This new system was designed to measure BRDF more accurately and at angles closer to specular than its predecessor. The addition of the interferometric and cryo-deposit monitoring/deposition systems in the latter half of the year will require an extended period of downtime. Years 2 and 3 of the program will be devoted to full-time mirror testing at a maximum throughput rate which will be determined by data acquisition capabilities and available resources.

3.1.2 Safety Reports

In accordance with contract requirements, Spire prepared the System Safety Hazard Analysis Report and the Description of Proposed Actions and Alternatives (DOPAA). These reports were prepared by Spire's safety office and the scientific staff.

3.1.3 Detector Array Feasibility Study

The speed, accuracy, and repeatability of the CRYOSCAT facility's data acquisition system is of critical importance for a successful testing and evaluation program. The primary product of these tests is the BRDF measurement of superpolished, high-quality Be mirrors. Through the use of a highly accurate, computer-controlled sample manipulator and the deployment of a low-scatter, low-profile optics train, the CRYOSCAT facility is able to perform highly accurate BRDF measurements at a significant throughput rate. Increasing the speed at which BRDF data can be obtained, without sacrificing accuracy, is absolutely necessary to allow for additional in-situ experiments to be performed (i.e., interferometry and cryo-deposit deposition) during the eight- to ten-hour cryogenic testing window.

The original detection/signal-processing system of CRYOSCAT is capable of performing all necessary scatter measurements required by the previous contract in eight to ten hours. However, the relatively slow data acquisition process of this single element scanning detector cannot operate fast enough to accommodate the additional tests to be performed during the cryogenic cycle and still maintain a reasonable degree of accuracy and repeatability. Therefore, a study was initiated by Spire Corporation through Electro-Optical Systems, Inc. of Phoenixville, Pennsylvania, to determine the feasibility of a proposed multi-element detector which utilizes a high speed signal processing system.

Preliminary calculations estimated that the testing rate (in number of mirrors tested per year) would double, while cutting actual cryogenic BRDF testing time in half for each mirror. This would provide the necessary time for the additional in-situ cryogenic tests. The detector array would also improve BRDF measurement accuracy and repeatability without increasing operating costs.

3.1.4 Interferometry

The incorporation of an interferometry system into the CRYOSCAT facility has produced a unique resource in optical metrology. Mirrors under simulated operational environments now can be analyzed by surface figure measurements in addition to scatter measurements before and after e-beam irradiation. All tests can be performed entirely in-situ during a single thermal cycle.

Spire, working with Zygo Corporation (Middletown, CT), has assembled a system that incorporates a high speed camera, interferometer, and an in-situ reference flat. Zygo assembled a prototype system that does not require any significant vibration isolation of the mechanical systems to acquire accurate interferograms. Demonstration tests performed in February 1990 determined that further vibration isolation would not be required.

3.1.5 Vacuum System

The base vacuum pressure within the CRYOSCAT test facility will be improved (decreased) by replacing the eight-inch cryopump with a ten-inch cryopump. This pump and all necessary hardware items were ordered and were scheduled to be incorporated into the facility.

3.1.6 Scatterometer Optical Train

The beam forming optics train of the scatterometer was designed to utilize low-scatter reflective optics to reduce the system scatter profile. The ZnSe vacuum window remains the only refractive element in the field-of-view of the detector.

Figure 6 is a diagram of the beam-forming optics in the scatterometer. The CO₂ laser beam is collimated and directed to an off-axis parabolic mirror which focuses the beam through a pinhole. The pinhole "point-source" is then imaged at the detector plane by a concave mirror. The beam passes through the vacuum window and is incident on the test mirror. The large distance between the concave mirror and the detector, along with the 5 mm spot size at the test mirror, provide for a slow optical system which is nearly collimated. The detector scans from the specular position to 10° off specular (both sides). All optical elements in the field-of-view of the detector are vignettted (no longer seen by the detector) well before the detector reaches 1° from specular. Only the ZnSe vacuum window remains in the field-of-view for positions past 1°. Bulk scatter, produced when the beam passes through the vacuum window, now determines the system scatter profile and, therefore, the minimum measurable BRDF angle.

Experiments were conducted to compare ZnSe and GaAs as vacuum window materials. ZnSe is the industry standard for the 10.6 micron wavelength; GaAs was chosen from available

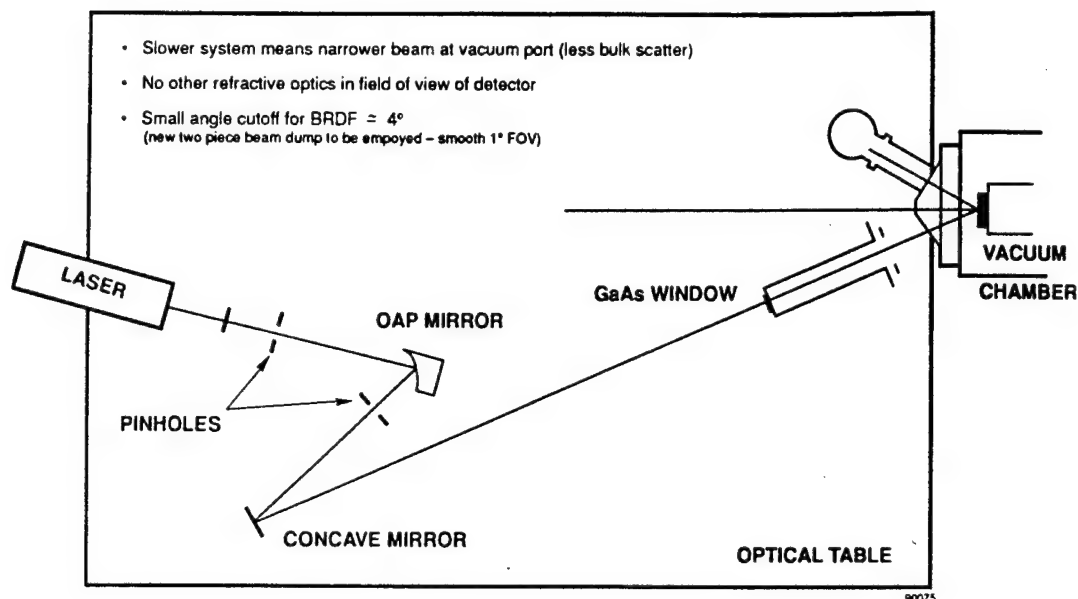


FIGURE 6. SCHEMATIC OF SCATTEROMETER OPTICS.

IR transmissive materials as the best possible substitute which meets all design requirements (i.e., could perform as a vacuum window at 10.6 microns while exposed to continuous wave laser operation at approximately 5 watts of power).

Figures 7 and 8 are spot diagrams generated by optical system software in the design of the scatterometer. These show the image of the systems entrance pupil, fully illuminated by a uniform laser beam, at the test mirror and at the detector. They can be thought of as cross-sectional views of the laser beam energy distribution at each surface. Figure 7 shows that the beam shape and energy distribution remain unchanged and that there are no significant aberrations. The beam is approximately 5 mm in diameter and circular at the test mirror. The best focus of the system is placed at the detector plane. This spot size (Figure 8) is approximately 0.5 mm, which corresponds to the width of the detector element.

All necessary optics and mounting hardware were ordered, and the scatterometer was scheduled to be operational by the end of February 1990. Once assembled, it will be tested and qualified. Design calculations estimate that, with a good low-scatter vacuum window in place, the system scatter profile should be insignificant past 1.5° off-specular.

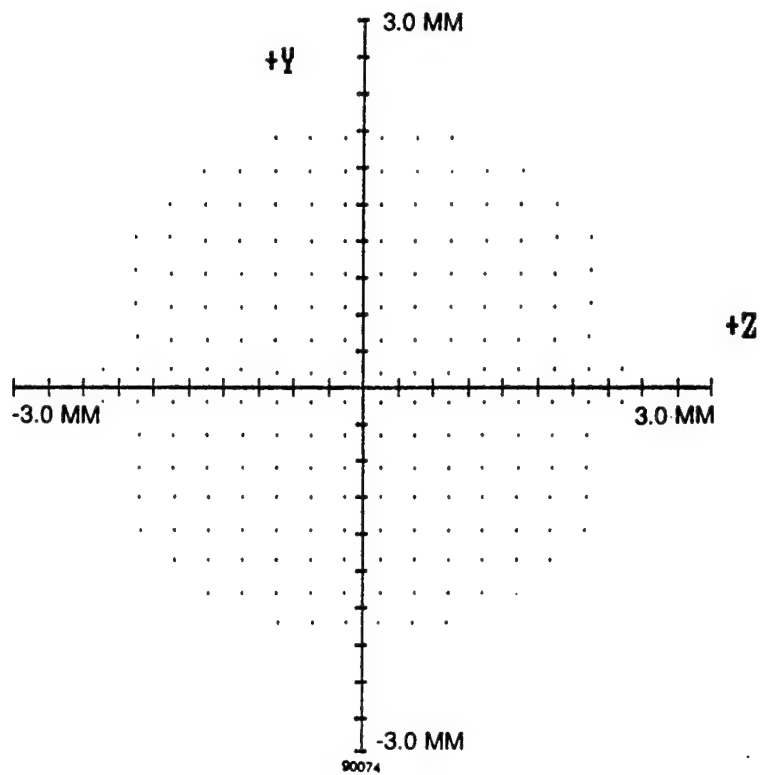


FIGURE 7. SPOT DIAGRAM AT TEST MIRROR.

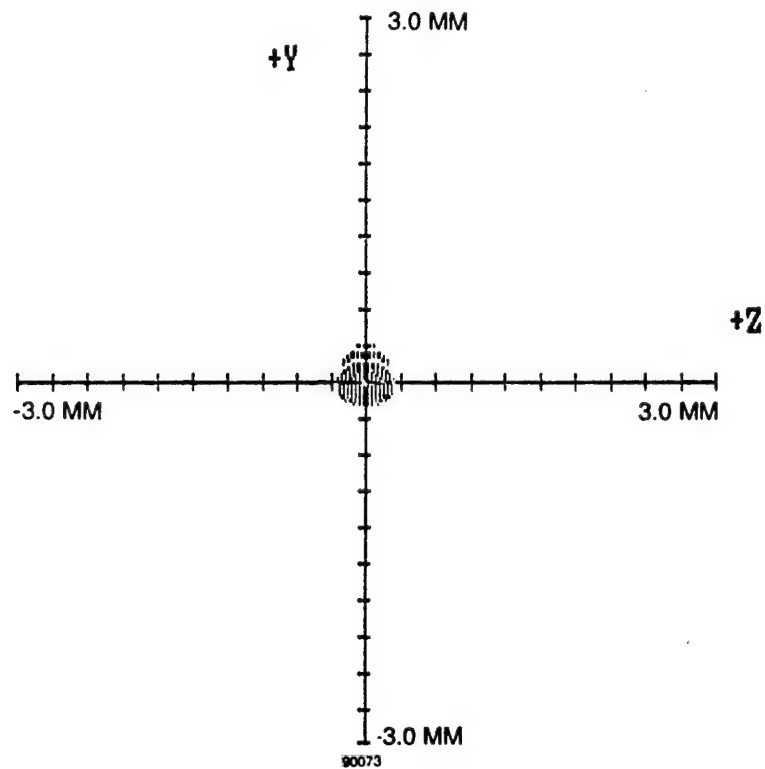


FIGURE 8. SPOT DIAGRAM AT DETECTOR.

3.2 1 January 1990 Through 28 February 1990

- Summary of technical "kickoff" meeting
- Summary of Safety Hazard Analysis Report
- Status of interferometry and vibration isolation systems
- e-Beam maintenance
- Construction of reflective optical train

3.2.1 Technical "Kickoff" Meeting of 7 February 1990

The technical "kickoff" meeting was held at Spire Corporation on 7 February 1990. The following persons were present:

Osama H. El-Bayoumi, RADC/ESM Hanscom AFB, (617) 377-3693
Ward Halverson, Spire Corporation, (617) 275-6000
Ed Johnson, Spire Corporation, (617) 275-6000
Roger Little, Spire Corporation, (617) 275-6000
Claud E. Martin, CSSD-SD-P, (205) 895-3773
Joseph R. McNeely, ORNL, (615) 576-8246
Brian W. Murray, Spire Corporation, (617) 275-6000
Robert C. Sullivan, Spire Corporation, (617) 275-6000
Donald L. Weinberg, Nicholas Research Corporation, (703) 893-7920
James A. Wells, Teledyne Brown Engineering, (205) 726-1592

The program plan was presented, reviewed, and discussed in detail. The major topics of discussion during this meeting included early tests of seven-inch diameter mirrors, the reflective optical train and sensitivity requirements for BRDF measurements, GaAs versus zinc selenide (ZnSe) as a low scatter vacuum window, data acquisition and signal processing capabilities, interferometry and vibration isolation requirements.

3.2.2 System Safety Hazard Analysis Report

The System Safety Hazard Analysis Report was released on 9 February 1990. This report was prepared in accordance with the data item description (DID) DI-SAFT-80101. It identifies specific hazards associated with performing the tasks of this contract and describes operating procedures used to manage these hazards.

3.2.3 Interferometry and Vibration Isolation Systems

On 27 February, Zygo Corporation demonstrated the interferometer system they designed using a high speed, frame shuttered camera. The primary objectives of the design and development effort was to build an interferometer that was capable of functioning while the test sample was vibrating. The vibration spectrum present in the laboratory is strong and covers a broad frequency range. The test sample is at the end of a 42-inch pendulum, which further complicates the vibration motion relative to the interferometer. Such a system would minimize,

if not eliminate, the necessity for an expensive mechanical vibration isolation system for the CRYOSCAT facility.

The demonstration equipment consisted of a modified version of Zygo's PTI Mainframe interferometer, which is robust and used for industrial testing of optics in large volume. The frame-shuttered camera has a variable speed aperture; it can be operated in normal mode or at high speed (60 to 10000 Hz). The demonstration experiment was performed on the CRYOSCAT facility while under operational conditions. A two-inch mirror was mounted in the vacuum chamber at a pressure of 2×10^{-7} torr. All equipment that is a possible source of mechanical vibration was turned on. Interferograms were taken with the mirror at room temperature and then cooled to 77 K. The camera was set at various speed settings to evaluate its performance.

The camera demonstrated that it could capture interferometric figures accurately while the camera was set at 4000 Hz or faster. Slower speed produced blurred pictures that could not be considered accurate. Operation of this camera at 4000 Hz or 10000 Hz will allow for interferometric studies in-situ on mirrors while under regular testing conditions without further isolating the apparatus from mechanical vibrations. Zygo recommended, however, that the camera be used within the MARK-II model interferometer because of the limited space available within the PTI model and the need for a camera with sufficient imaging resolution for testing seven-inch mirrors.

3.2.4 Electron Beam Generator: Routine Maintenance

The SPI-PULSE™ 5000 pulsed e-beam generator requires general maintenance to insure optimum performance. This work began at the end of February and was scheduled for completion in the first week of March. The tungsten mesh anode of the diode requires replacement after each 120-150 firings. This was done following the regular maintenance and the diode was recalibrated to insure that proper energy spectrum and fluence levels were being produced.

3.2.5 Reflective Optical Train for Scatterometer

During late January, experiments were performed to evaluate the performance of GaAs as a window material and compare it to the performance of ZnSe. This window remains the only refractive (transmissive) optical element in the path of the laser beam before it strikes the test mirror. The bulk scatter of the laser beam in this material contributes to the system's scatter profile and limits scatterometer performance. Preliminary tests consisted of a comparison of bidirectional transmissive distribution function (BTDF) values for both materials over the near-specular range.

BTDF is similar to BRDF except that it measures light that is scattered in transmission rather than reflection. These initial tests show that GaAs outperforms ZnSe in the near specular range as close as 1.5 degrees from specular. Figure 9 shows BTDF plots for both materials along with the scatterometer system profile. This figure shows that ZnSe produces scattered light at

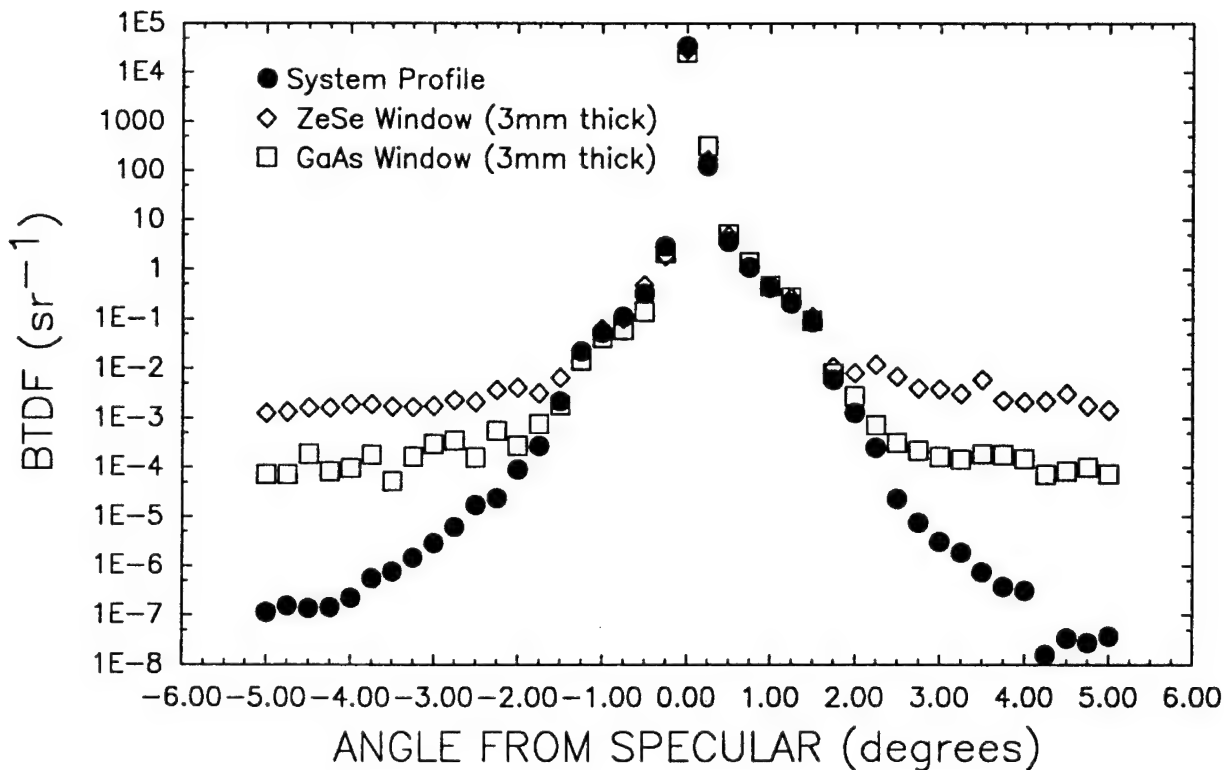


FIGURE 9. BRDF MEASUREMENTS OF ZnSe AND GaAs - BOTH WINDOWS WERE 3 mm THICK AND Ar-COATED ON BOTH SIDES. Note the lower scatter levels produced by GaAs past 1.5°.

levels above the instrument system profile approximately 1.5 degrees from specular. GaAs, however, produced considerably lower scattering levels than ZnSe throughout the entire range past 1.5 degrees, showing that it will be useful in reducing the overall scatter profile.

Further tests were conducted before GaAs could be used to replace ZnSe as a vacuum window. Available data on the mechanical and optical properties of GaAs are extremely limited. The data that are available indicated that GaAs is harder and more rigid than ZnSe, possesses a higher index of refraction, and should be thermally stable. Tests on the performance of this material while subjected to vacuum and long exposure to the high powered CO₂ laser beam were performed.

Table 1 compares the known mechanical and optical properties of the two materials,⁽¹⁾ and represents what is believed to be the most recent figures. GaAs is stronger, harder, and is more thermally conductive than ZnSe. It has higher refractive index (not a serious concern) and is not transparent in the visible wavelength range. Its density, solubility, and coefficient of linear expansion are about the same as ZnSe.

TABLE 1. SELECTED PROPERTIES OF GaAs AND ZnSe.

	<u>GaAs</u>	<u>ZnSe</u>
Density	5.4 g/cc	5.3 g/cc
Knoop Hardness	750 kg/mm ²	100 kg/mm ²
Young's Modulus	84 GN/m ²	66 GN/m ²
Solubility	Insoluble	Insoluble
Thermal Conductivity	48 W/m°C	18 W/m°C
Maximum Temperature	250°C	250°C
dl/dt	6E-6/°C	7E-6/°C
Refractive Index (n)	3.278 (@ 10 microns)	2.407 (@ 10 microns)
dn/dt (@ 10 microns)	+150E-6/°C	+57E-6/°C

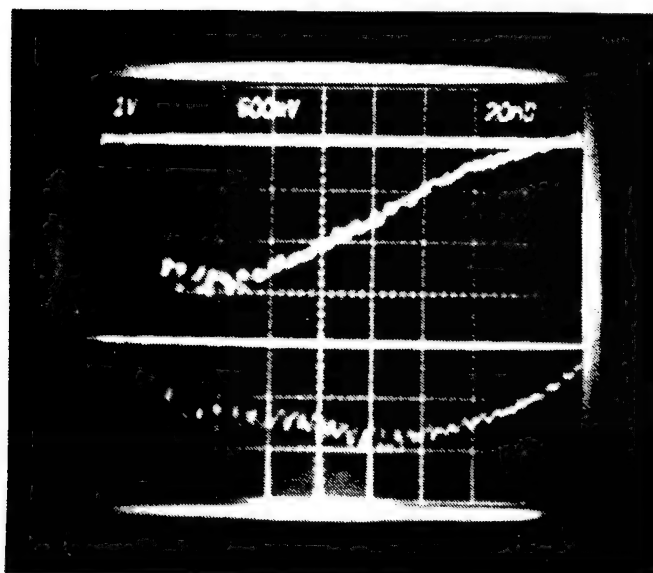
3.3 1 March 1990 Through 31 March 1990

- E-beam generator status
- Vacuum system performance
- Interferometry test results
- Vibration isolation requirements with new interferometer
- Status of engineering design projects

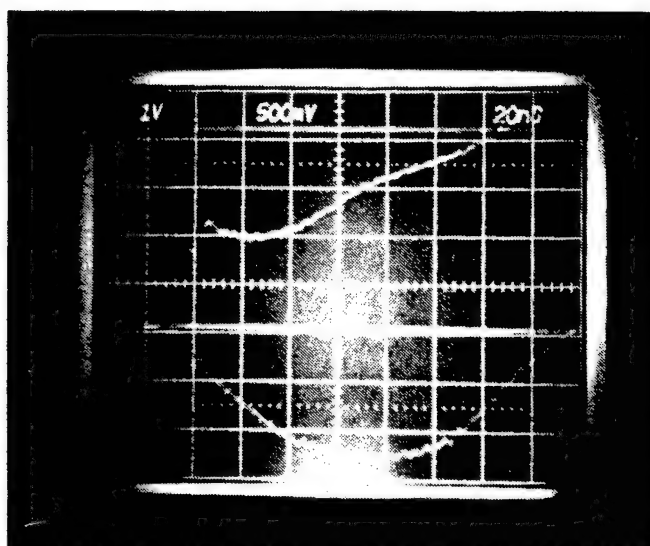
3.3.1 Electron Beam Maintenance and Diode Servicing

The SPI-PULSE™ 5000 shown in Figure 10 is an electrical transmission line. Maintenance of the interior of the line must be carried out occasionally for optimum electrical performance. The SPI-PULSE™ 5000 has been operating continuously for more than five years without servicing without major problems. Although no diagnostic indicators pointed toward immediate difficulties, the long period of continuous service experienced by this machine prompted Spire to perform full maintenance to insure that the e-beam generator would function properly through the three years of the contract.

The entire operation, from separation of the machine from the vacuum chamber to reconnection, required two weeks. The interior of the machine was in excellent condition. Insulating grease and rings were replaced and all moving parts checked, cleaned, and refurbished as needed. All electrical connections were checked and the machine was reassembled. Surfaces that were used for "O"-ring seals were found to have scratches and deformations that could give poor vacuum performance. Therefore, all "O"-rings that separate the high pressure atmosphere within the e-beam generator from the ultra-high vacuum of the test chamber were replaced and "O"-ring surfaces were remachined smooth and flat.



a)



b)

FIGURE 10. VOLTAGE AND CURRENT TRACES FROM SPI-PULSE 5000 e-BEAM ACCELERATOR. (a) Before servicing; (b) After servicing.

The tungsten diode of the e-beam generator was replaced, and the e-beam generator was then reconnected to the vacuum chamber and pressurized. The vacuum environment of the chamber was monitored, but no evidence of a leak was found. The diode gap was set, and voltage and current traces of the pulses were taken to determine e-beam pulse quality. Figure 10(b) shows a voltage/current trace taken at the conclusion of these maintenance procedures. Not only does the pulse conform to required pulse-widths and amplitudes, it is also considerably more quiet and stable than the somewhat "noisy" pulses observed prior to servicing as shown in Figure 10(a). The improvement is mainly due to better electrical grounding connections within the generator and does not affect electron beam energy spectrum.

3.3.2 Vacuum System Performance

A low 10^{-7} torr level leak was observed during the previous contract period (1988-89). Nitrogen used to pressurize the e-beam generator would leak into the ultra-high vacuum chamber past several "O"-ring seals. The scratches and deformations found on the flat "O"-ring surface were clearly the cause of this leak. By remachining these surfaces and replacing the "O"-rings, the vacuum performance of the test chamber was improved.

When service procedures were completed on the e-beam generator, the machine was reconnected to the vacuum chamber assembly. The vacuum chamber was sealed and all peripheral systems except the scatterometer were attached. After pumping the chamber down to a low 10^{-7} torr level vacuum, the residual gas analyzer was set to monitor the level of nitrogen gas as the e-beam machine was pressurized. While a minor increase of the nitrogen partial pressure was observed at the beginning of the procedure, it immediately stabilized and recovered. This indicates that some nitrogen still enters the vacuum chamber, but at a considerably lower rate than before servicing.

The final pressure obtained in the vacuum chamber after bake-out was 1.5×10^{-7} torr, which is 25% lower than the best vacuum obtained previously. The residual gas spectrum is dominated by nitrogen with traces of water, oxygen, and carbon dioxide. The (5:1) ratio of nitrogen to oxygen observed may indicate a minor leak; this is not considered serious enough for further action. The presence of nitrogen during the pressurization process is due to the electrically insulating teflon rings used in the SPI-PULSE™ 5000, which are somewhat porous. Further improvement in vacuum is expected when the much larger 10-inch cryopump is installed.

3.3.3 Interferometry Demonstration Using High Speed Camera

Late in February, Zygo Corporation demonstrated the interferometer/high-speed camera system that they had designed and built at our request. The experiments were conducted, and the data received and evaluated by Spire during the month of March. These data were then forwarded to SDC's technical program monitor for evaluation along with our recommendation for acceptance of the equipment package.

The demonstration was to determine if the interferometer system could effectively capture reproducible interferograms of a mirror surface while the mirror was attached to the CRYOSCAT's long liquid helium (LHe) coldfinger. The problem to be overcome was the severe

mechanical vibration and displacement of the test mirror while under operational conditions within the CRYOSCAT apparatus. If interferometry could not be performed while the mirror was mounted in the CRYOSCAT, extensive and expensive vibration isolation equipment would have to be designed and installed.

The results of the interferometer system tests were very encouraging. As shown in Figure 11, the high-speed, frame-shuttered camera at a speed of 2,000 Hz produced fringe patterns that appear similar but noisy enough to yield different wavefront aberrations (shapes) each time an interferogram was taken. The fringe pattern on the left is interpreted by the software to yield the wavefront map on the right. Although the fringe patterns appear almost identical, the wavefronts calculated from the interferograms of a single surface varied considerably from measurement to measurement. This indicated that the noise produced by the mirror's motion and vibration was sufficient to prevent the interferometer from capturing an accurate picture of the mirror surface.

Interferograms (or fringe patterns) created with the camera operating at 4000 Hz produced wavefront maps that were almost identical. Figure 12 shows the graphical results of these measurements. Calculations and analyses of these fringes indicate that, with the camera set at 4,000 Hz, the interferometer reproduced the wavefront from measurement to measurement with sufficient repeatability to allow quantitative analysis of figure characteristics.

Measurements taken with the camera set at its highest speed of 10,000 Hz proved to be even more accurate and repeatable. Figures 13 shows fringe patterns and wave-front maps taken several minutes apart; each shows identical fringe patterns and maps. At this speed, the camera captures an image of the laser wavefront before the mirror can move a distance that blurs the picture. Operating this interferometer/camera system at 10,000 Hz guarantees our ability to measure and analyze the effects of cryogenic temperature, cryo-deposit formations, and e-beam irradiations on the optical figure of the mirror.

3.3.4 Optical Table

An optical table for the interferometer system and scatterometer optics was designed and ordered through TMC, Inc. (Peabody, MA). The two-piece table (8' x 4' and 6' x 4' with a notch around the vacuum chamber) is 18-inches thick and supported by a basic leg system without isolation pistons. Figure 14 is a sketch of this table.

3.3.5 Engineering Design Tasks

The addition of a 10-inch cryopump and gate valve to the CRYOSCAT test chamber required modification to the support structure to which every system is connected. This was modified to accommodate the larger, heavier pump and gate valve. The cryo-deposit deposition/monitoring system required additional viewports and feedthroughs on the vacuum chamber. A 10-inch blank-off flange has been modified to provide the required access. The interferometer system requires a reference transmission flat mounted inside the vacuum chamber. The reference flat and the interferometer output must be precisely aligned and rigidly mounted

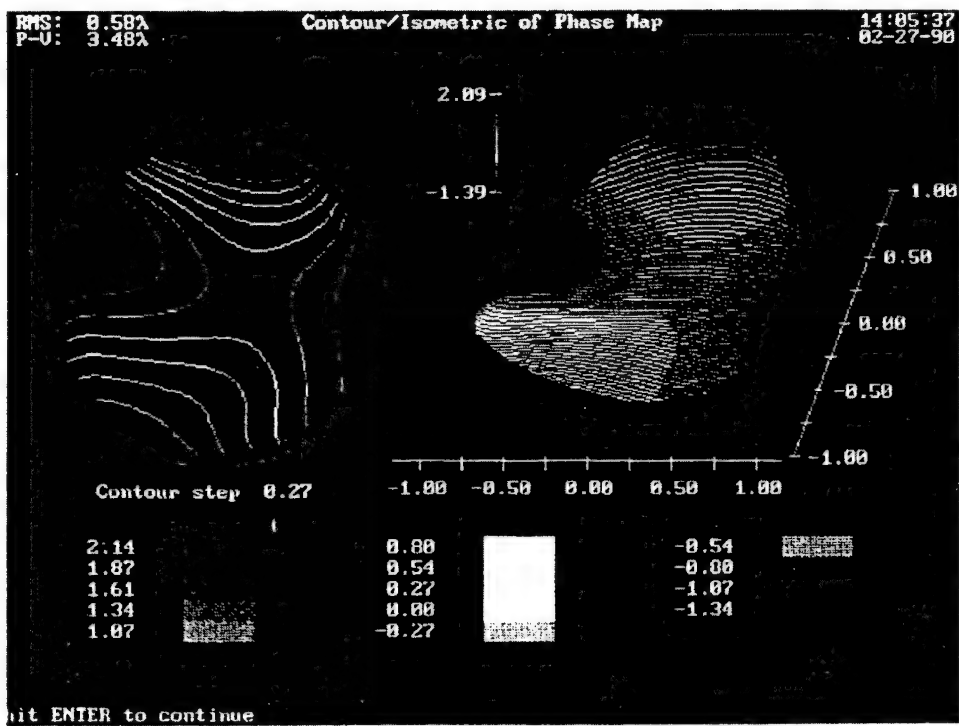
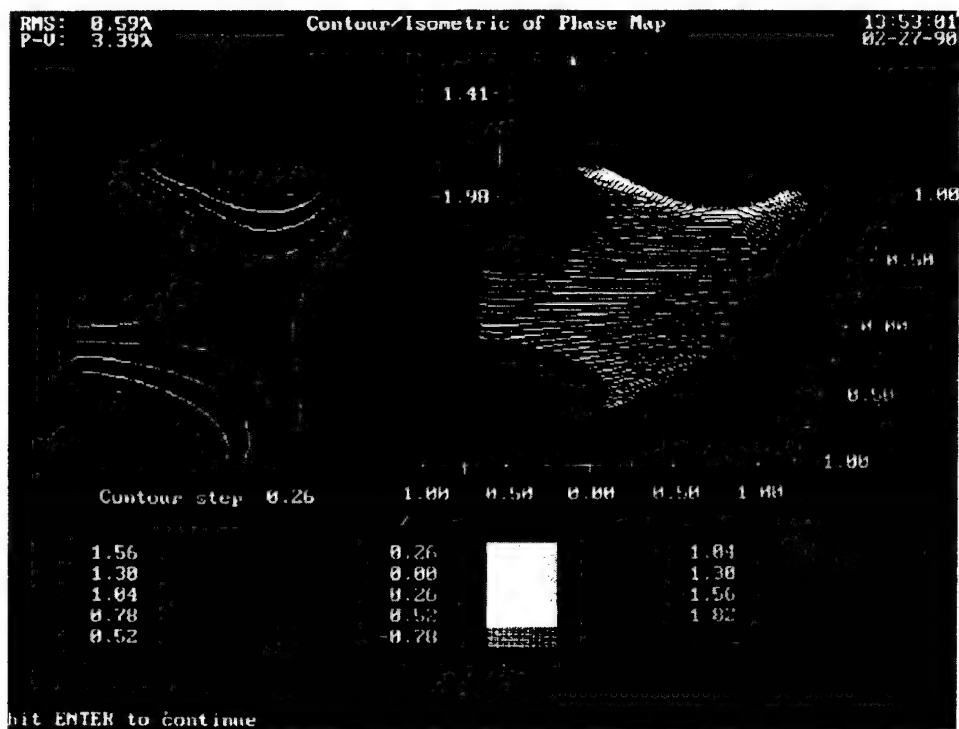


FIGURE 11. INTERFEROMETRY TEST AT 2000 Hz CAMERA RATE.

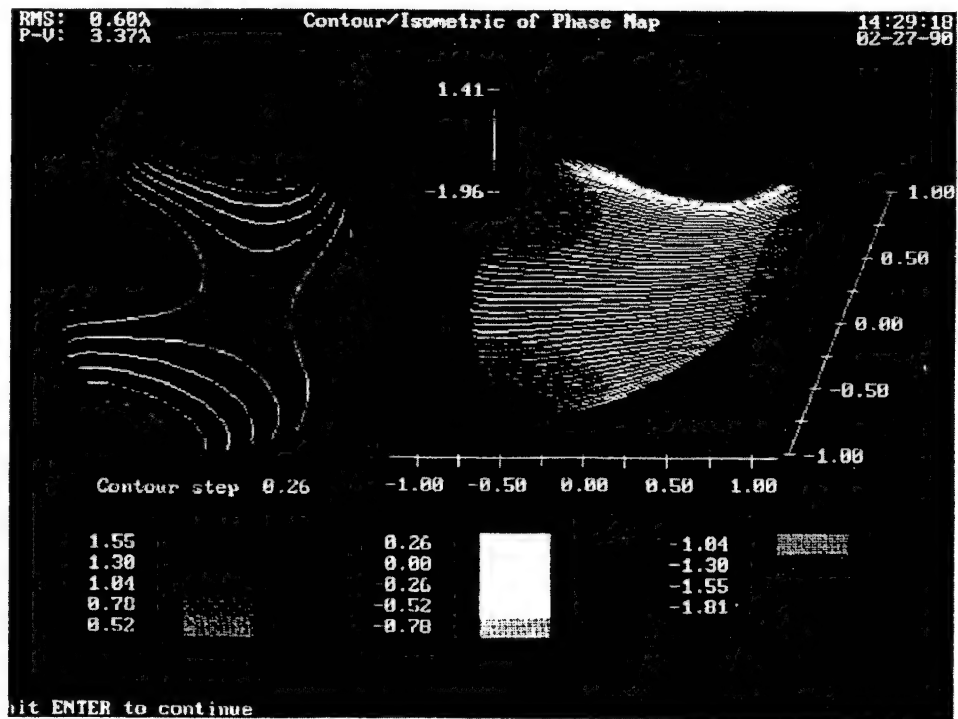
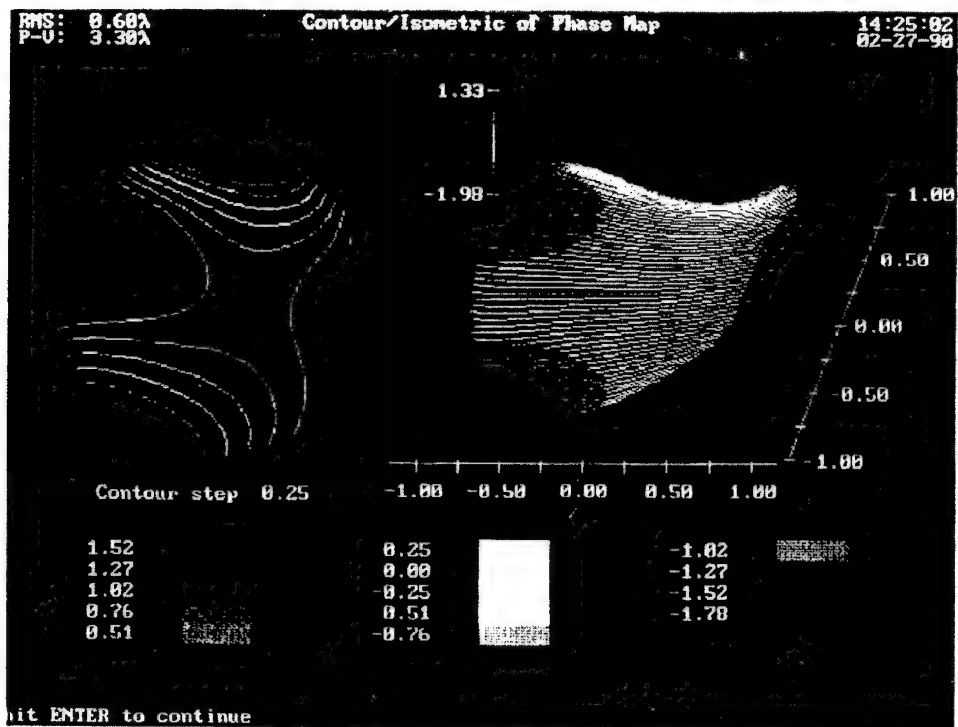


FIGURE 12. INTERFEROMETRY TEST AT 4000 Hz CAMERA RATE.

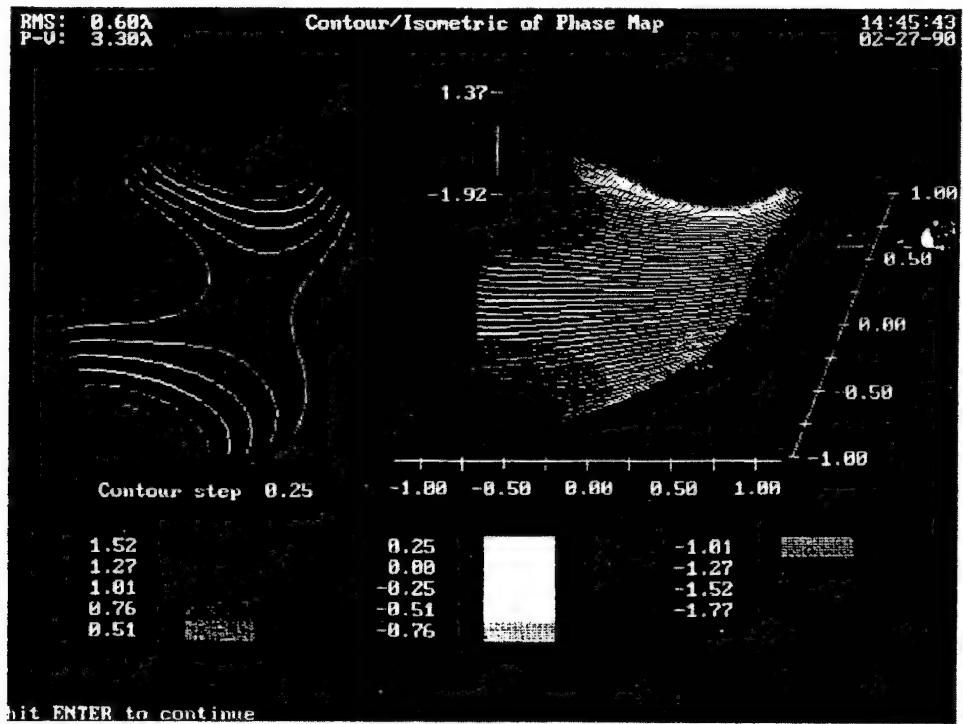
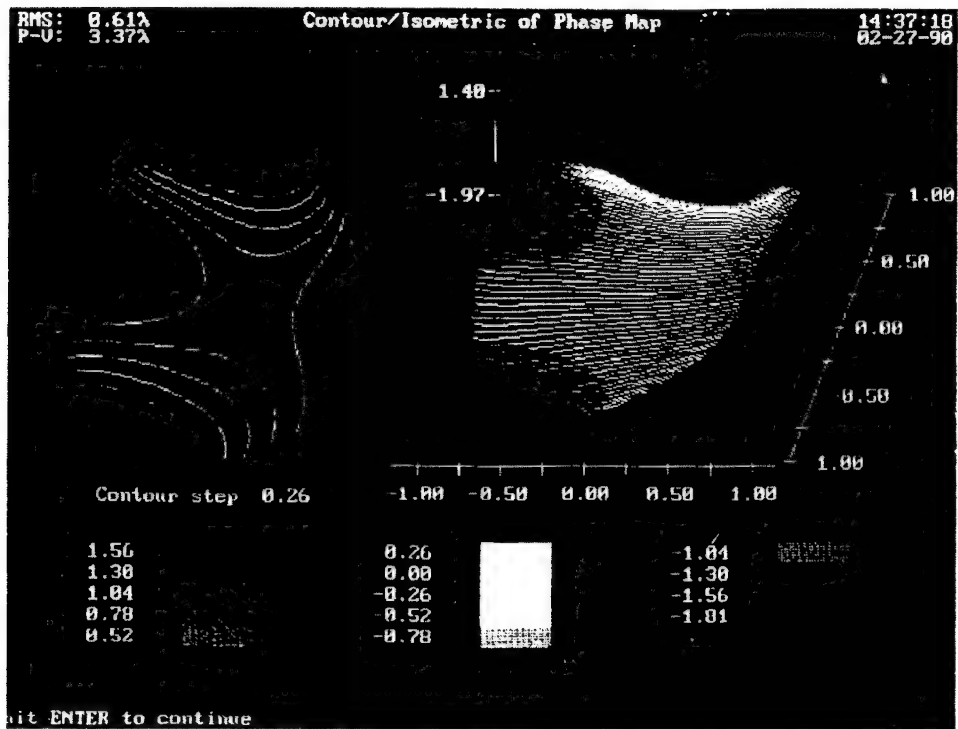


FIGURE 13. INTERFEROMETRY TEST AT 10,000 Hz CAMERA RATE. Interferograms (a) and (b) taken at approximately 10 minute intervals.

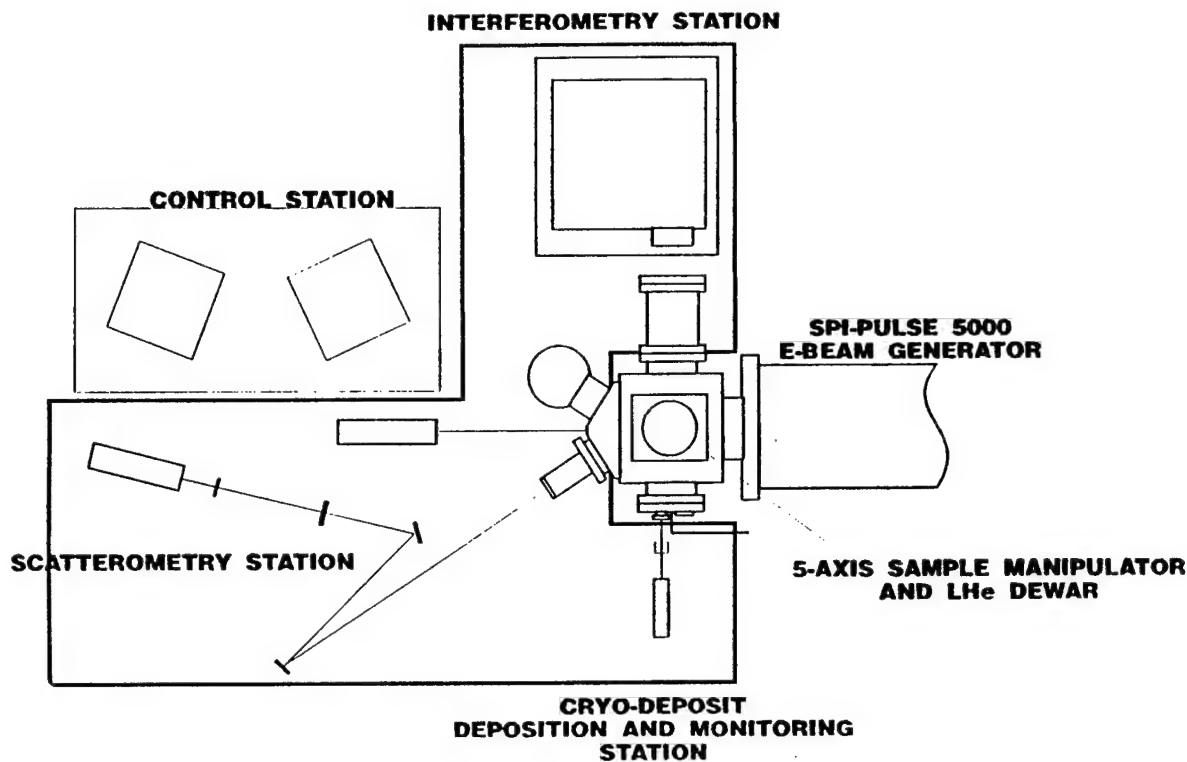


FIGURE 14. SKETCH OF INTERFEROMETER AND SCATTEROMETER OPTICAL TABLE.

inside a vacuum nipple. The interferometer was mounted on a tip-tilt stage that allows for precise alignment outside the vacuum chamber, eliminating vacuum feedthroughs which would degrade vacuum performance. The mount allows for sufficient movement for proper optical alignment; once aligned and locked, no further alignment is necessary unless the interferometer is removed from the mount. Separation is possible to perform separate interferometric studies; removing and returning the interferometer from the CRYOSCAT facility will not affect system performance.

The reference flat, supplied by the interferometer manufacturer, is rigidly mounted in a cylindrical vacuum nipple. This nipple connects to a large port on the main vacuum chamber with a wide aperture window for interferometer's six-inch diameter beam.

3.4 1 April 1990 Through 31 May 1990

- Scatterometer constructed and system profile tests begun

Scatterometer

A scatterometer utilizing reflective rather than refractive optics as a primary means of delivering the laser beam to the test sample was designed during the first few weeks of the

program. This system, shown schematically in Figure 6, was constructed during the months of March, April and May. There was considerable delay in completing this task due to procurement delays for critical mounting hardware and minor problems with the protective coating on the primary optics.

The system profile was measured while the scatterometer was detached from the main vacuum chamber and while the detector was in the "straight through" position without a test mirror. Initial tests performed at the end of May indicated that the system will operate at predicted performance levels.

A minor variation of the CO₂ laser beam dump was made to maximize performance near specular. The beam dump in use is a quartz plate with an oblong slit machined in its center. This slit is designed to provide a 1° field of view (FOV) for the detector in the plane of incidence and a 3° FOV perpendicular to the plane of incidence. Machining quartz to the dimensions required by this design was difficult, and the quality of the knife-edges was unsatisfactory. The modification utilized the 3° FOV built into the detector to maintain the perpendicular FOV and two quartz plates to define the in-plane FOV. Each plate has a straight, clean, knife-edge that sets to the desired 1° FOV when mounted on the detector. Machining and polishing quartz with this geometry is much easier and produced a high quality knife-edged beam dump.

Prior to performing system profile measurements on the scatterometer, tests were made to observe the laser beam characteristics. Computer modeling during design indicated that the system would produce a spot at the test mirror of approximately 4.5 mm in diameter. The calculations predicted a spot diameter in the plane of incidence for BRDF measurements of 4.48 mm at the $1/e^2$ point and a diameter perpendicular to the plane of incidence of 4.74 mm when the mirror surface normally is positioned 30° from the incident beam.

To compare computer predictions with system performance, a straightforward method of beam characterization was used. Thermal imaging, or "burn," paper was placed in the beam path at selected positions and exposed to the beam energy. The paper is capable of significant resolution and is a helpful tool in general IR alignment procedures. The high power density at the plane of the detector, where the beam focuses, required the use of ordinary paper to provide a "beam" footprint.

Figure 15 shows the beam shape immediately after collimation and at the plane of the test mirror. After collimation, the beam is circular and approximately 8 mm in diameter; at the test mirror, the spot is slightly elliptical, but sufficiently circular for accurate scatterometry. Its average diameter is less than 5 mm, as predicted.

The hole pattern shown in Figure 16 represents three series of burn hole measurements at the detector plane and at one inch on each side of the detector plane. The top row of holes was made with the paper located one inch in front of the detector plane and show a slightly oval shape in the vertical axis. The middle row of holes was made at the detector plane itself and appear circular. The lower row of holes was made one inch behind the detector plane and show an oval horizontal shape. This shift from oval vertical to circular to oval horizontal is due to the



FIGURE 15. CO_2 LASER SPOT IMAGES. Left: After collimation; Right: At test mirror.

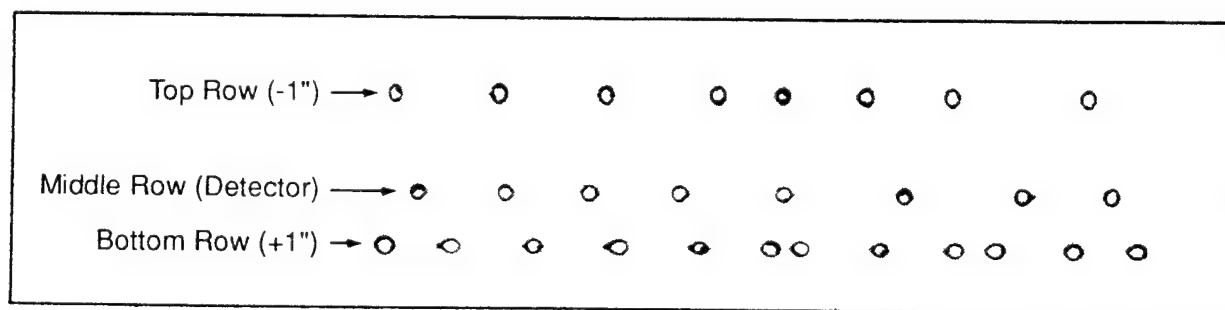


FIGURE 16. LASER BURN SPOTS NEAR DETECTOR PLANE.

small amount of astigmatism inherent in the system design and was predicted in the computer calculations. The middle row represents the "circle of least confusion," or focal point at the detector location during BRDF measurements.

3.5 1 June 1990 Through 31 July 1990

- Measurement of scatterometer optical system profile
- Scatterometer calibration
- Modification of final field stop aperture and review of optical system

3.5.1 Optical System Profile

The CRYOSCAT system, when fully functional, is restricted in many ways from performing as a typical scatterometer. The detector is rigidly connected to the high vacuum chamber by a flexible metal bellows, which not only limits scanning range to $\pm 10^\circ$ from a 30° specular angle but also does not allow for in-situ system profile measurements to be made.

System profile measurements are typically performed by scanning the laser beam directly without a sample in the beam. The CRYOSCAT scatterometer is unable to do this while connected to the vacuum chamber and must be disconnected entirely to perform such measurements. With the detector mounted directly in the path of the beam, system profile measurements were performed. The final field stop aperture was varied during several measurements to determine its optimum diameter. The optimum field stop should not intercept the laser beam while being small enough to block stray light produced by the system (especially the GaAs vacuum window). When the optimum geometry was determined, calibration of the system was performed, and the final system profile was measured.

Figure 17 shows a scatterometer scan of the laser beam without the GaAs window and without a final field stop. The first step was to optimize the field stop diameter to minimize the transmission of system produced stray light onto the test mirror. A range of aperture diameters was tested and the optimum selected. Figure 18 shows the BRDF of the laser beam with a 0.750-inch aperture in place as the final field stop. The scan of the beam itself (without an aperture) is overlaid for comparison.

The GaAs window was installed in addition to the 0.750-inch aperture. The field stop and baffle chamber, between the field stop and window, were designed to reduce stray light produced when the beam passes through the refractive window. The addition of the window to the system should not increase system profile if the field stop and baffle chamber are properly designed. A scan of the beam with the window and field stop in place produced the data presented in Figure 19 along with the profile of the beam without the window for comparison. This plot represents the optimized system profile for the CRYOSCAT optical scatterometer. The values shown on the vertical axis (BRDF) are not absolutely calibrated and should not be considered as accurate system noise equivalent BRDF (NEBRDF).

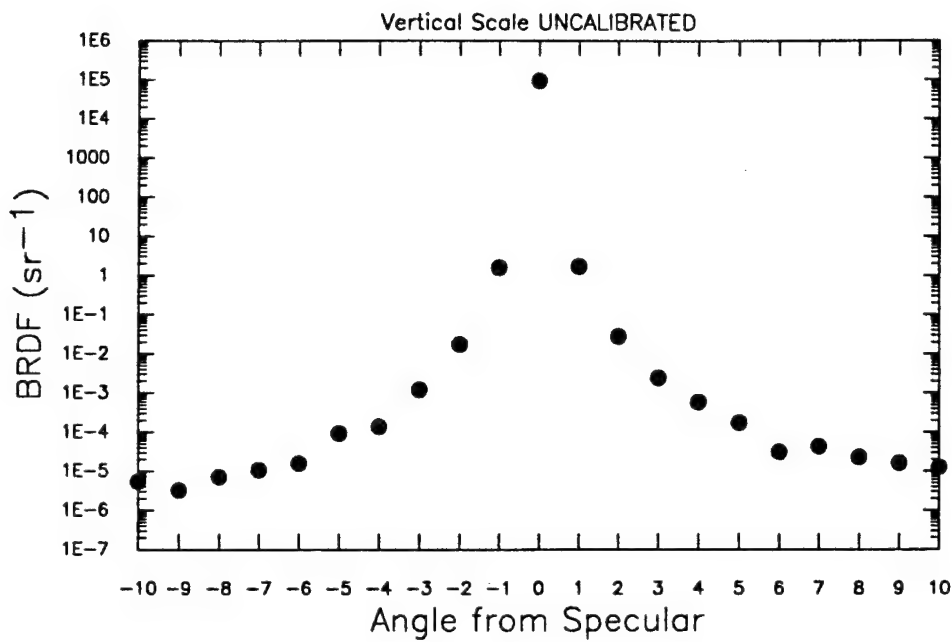


FIGURE 17. SYSTEM PROFILE WITHOUT FINAL FIELD STOP OR GaAs WINDOW.

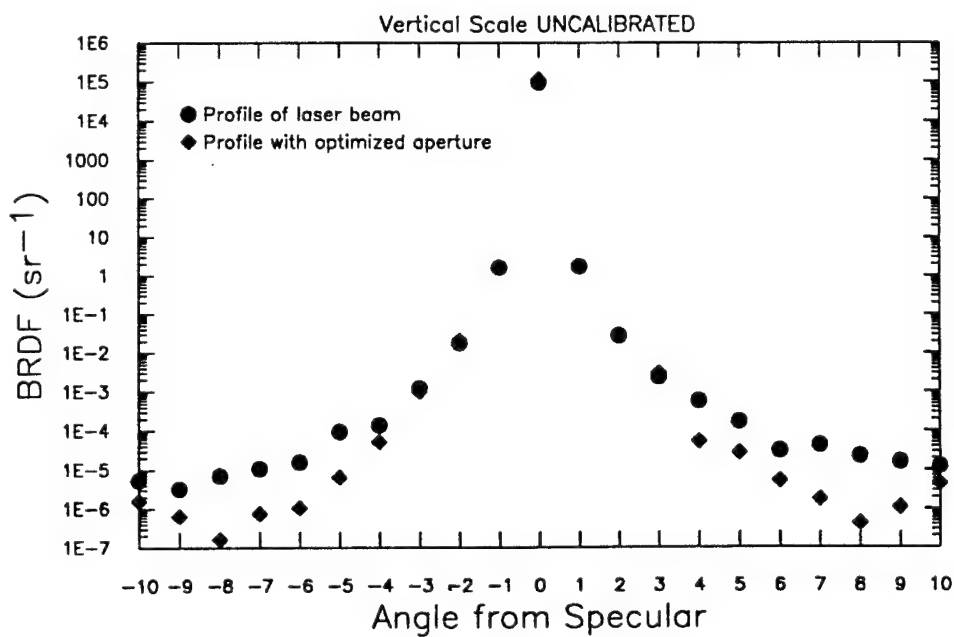


FIGURE 18. SYSTEM PROFILE WITH 0.75-INCH FIELD STOP (No GaAs Window).

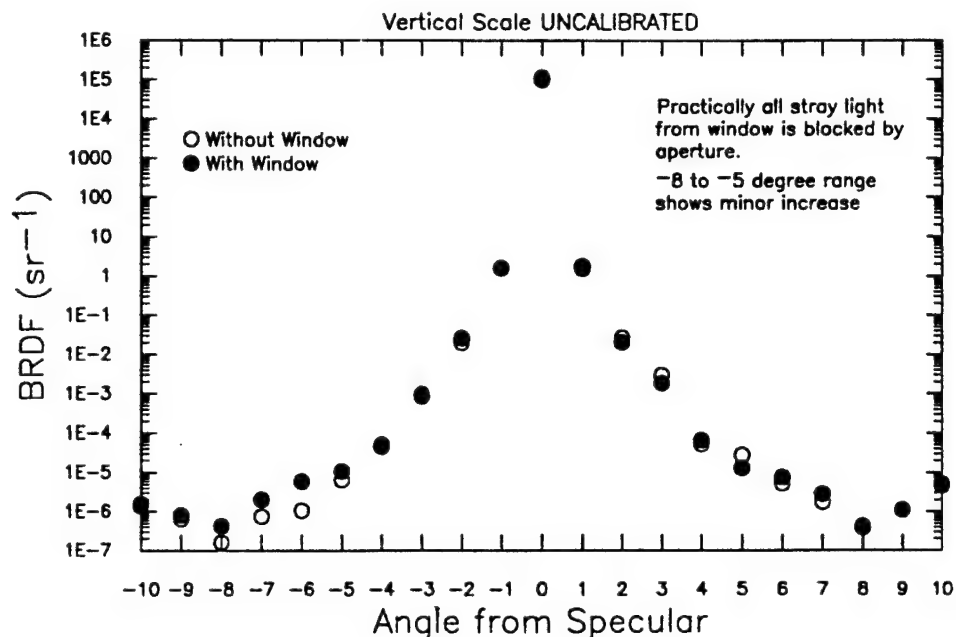


FIGURE 19. SYSTEM PROFILE WITH FINAL BEAM STOP AND GaAs WINDOW IN PLACE.

3.5.2 Optical System Calibration

There are at least two acceptable ways to calibrate a scatterometer; absolute and relative calibration. Due to the mechanical geometry of the CRYOSCAT vacuum system, the relative method is the only possible system calibration technique. This section presents details of the calibration procedure, which compares data from CRYOSCAT and from a second, independently calibrated scatterometer (FASCAT).

The relative calibration procedure involves the measurement of a known sample followed by calibration to match the known sample's BRDF value. The sample used for this procedure was an IR reflectance standard manufactured by Labsphere, Inc. (N. Sutton, NH). The sample appears to be Au-coated, coarse sandpaper but is a proprietary material with a measured average total hemispherical reflectance (THR) of 94% (six independent measurements). There are no known traceable standards for reflectance at 10.6 μm at the present time. The sample is placed in the scatterometer in the same orientation each time, set by fiducial marks on the back of the sample.

The sample should have a flat BRDF curve with a value of $2.99 \times 10^{-1} \text{ sr}^{-1}$ (total hemispherical reflectance divided by π). All measurements performed by CRYOSCAT on this sample have been calibrated to meet this theoretical value by multiplying all data by a calibration constant (CC). The calibration constant should not vary significantly over time. Previous long-term calibration checks showed a variation in the CC of less than 10%.

Figure 20 shows three uncalibrated BRDF measurements of the reference sample. These data sets include a first order regression curve fit which is used to determine RMS value and slope. RMS value is determined by the intersection of the first order regression line and the y-axis ($x=0$) which is the mid-point of the data. The uncalibrated scans show that the average RMS value of the reference is 0.354 sr^{-1} . The value specified above for the reference sample is 0.299 sr^{-1} , which results in a CC of 0.845 for the CRYOSCAT. Multiplying all data points by this CC yields calibrated plots which are presented in Figure 21 along with the recalculated average RMS mean BRDF value which matches the target value of 0.299 sr^{-1} .

BRDF measurements of the final system profile have been adjusted to incorporate the CC into the data acquisition algorithm. The calibrated system profile is presented in Figure 22 along with the BRDF value and standard deviation at each measurement angle from specular. BRDF measurements of mirrors during the course of this program will be compared to this profile unless further geometry changes are made to the optical system. For mirrors whose BRDF is in the 10^{-4} sr^{-1} range, data will be analyzed from ± 3.5 to 10 degrees from specular. Mirrors in the 10^{-5} sr^{-1} range will use data from ± 4.5 to 10 degrees from specular. Any mirrors found to be as low as the 10^{-6} sr^{-1} range will use data from ± 6.5 to 10 degrees from specular.

During the course of BRDF/radiation hardness testing of mirrors, mirror performance will be evaluated over the entire range described for mirrors of various qualities, or over more specific ranges within the usable range if required. The higher the quality of the mirror (lower BRDF) the smaller the angular range of usable scatter data. The ability to measure close to specular has improved considerably with the completion of the reflective optical system. Figure 23 compares the current system profile and that of the previous refractive system. The most significant improvement occurs in the $1^\circ - 7^\circ$ range, where profile levels have decreased by more than a decade at some angles. As a comparison, consider a mirror with a BRDF of $1 \times 10^{-5} \text{ sr}^{-1}$. The previous refractive system was capable of measuring data at this level within the 7 to 10 degree range, and even this was barely above noise floor. The new reflective system can measure data at this level from 5 to 10 degrees while remaining a decade above noise floor. This increase in range and sensitivity provides CRYOSCAT with the capability to test and evaluate mirrors of increasingly higher quality and to produce data with higher precision than previously possible.

The BRDF of the diffuse reference sample used to calibrate the CRYOSCAT was also measured on FASCAT. This machine has its own diffuse reflectance standard mounted within the system. It is measured before each run to establish its own CC. Measurements of the Labsphere reference by this instrument produced an average RMS BRDF of 0.389, which is well above the maximum value allowed by theory for a 100% reflective diffuse sample (0.318). These data are indicative of differences between the two scatterometers and the two reference samples.

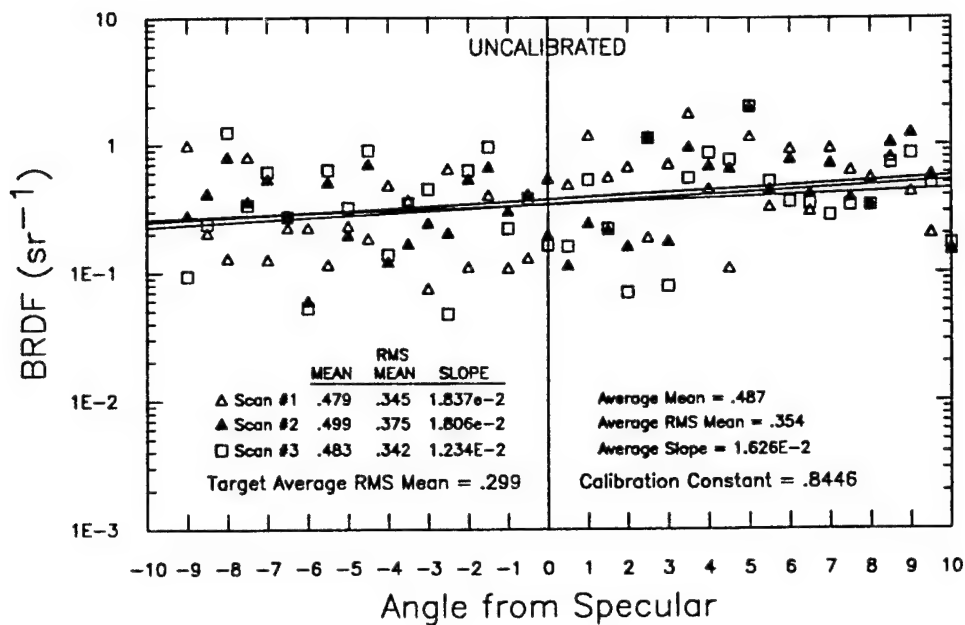


FIGURE 20. UNCALIBRATED BRDF MEASUREMENTS ON IR REFLECTANCE STANDARD.

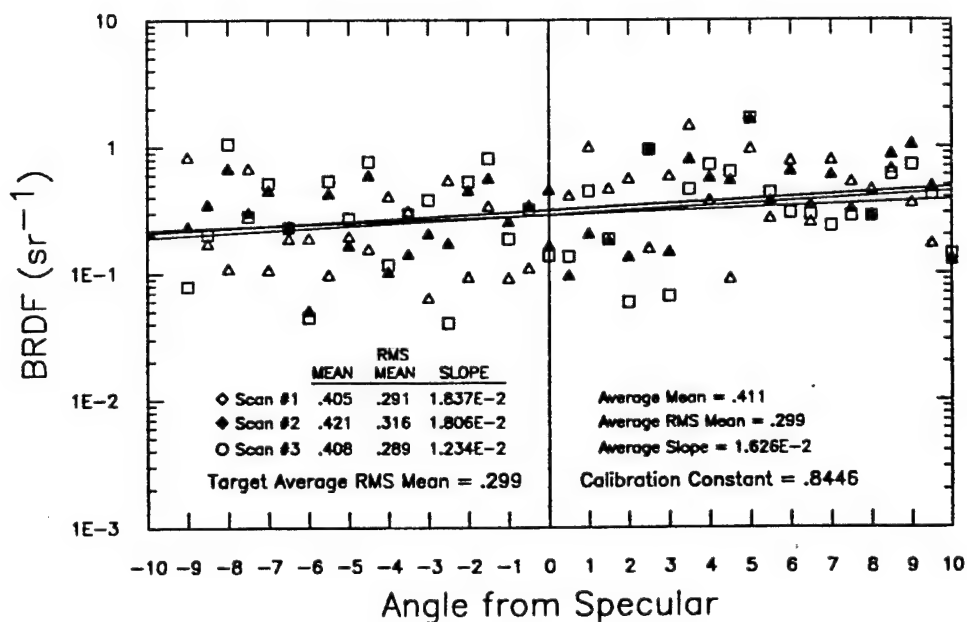


FIGURE 21. BRDF MEASUREMENTS CALIBRATED TO IR REFLECTANCE STANDARD.

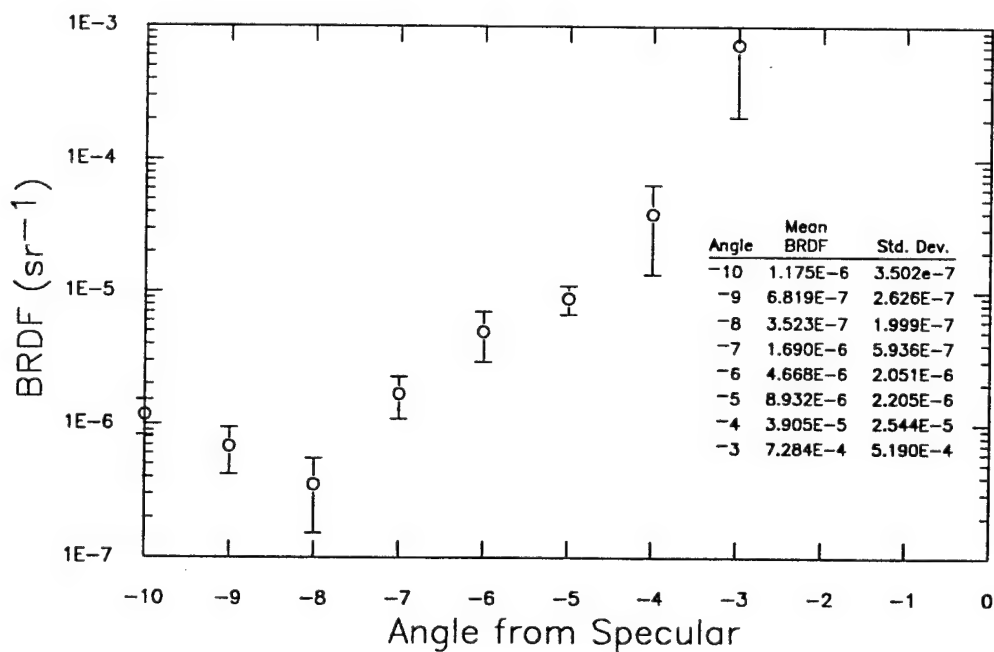
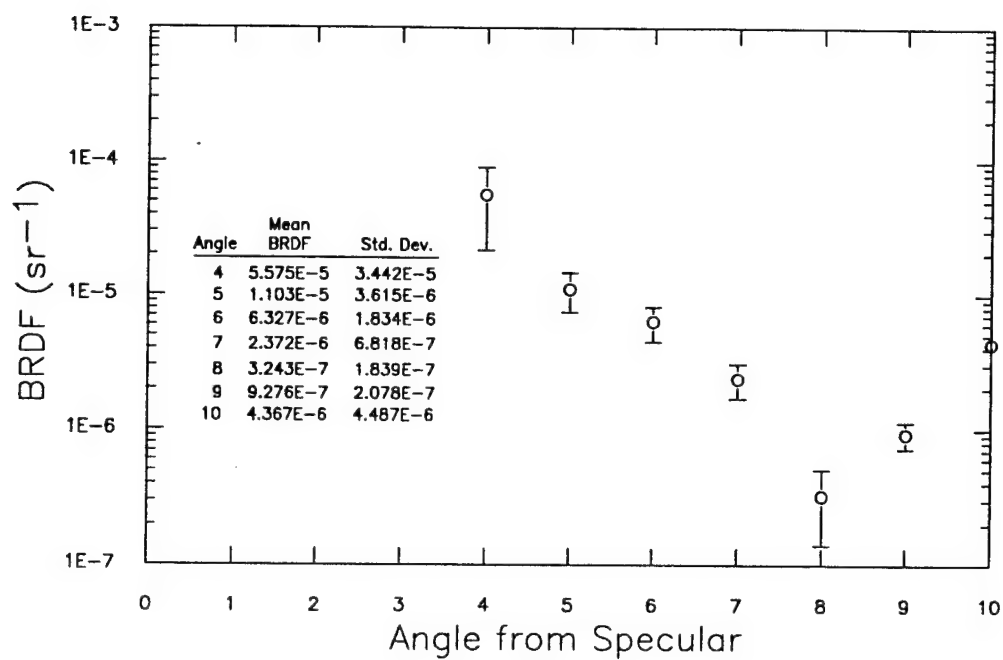


FIGURE 22. CALIBRATED CRYOSCAT SYSTEM PROFILE. (a) Forward scatter; (b) Backscatter.

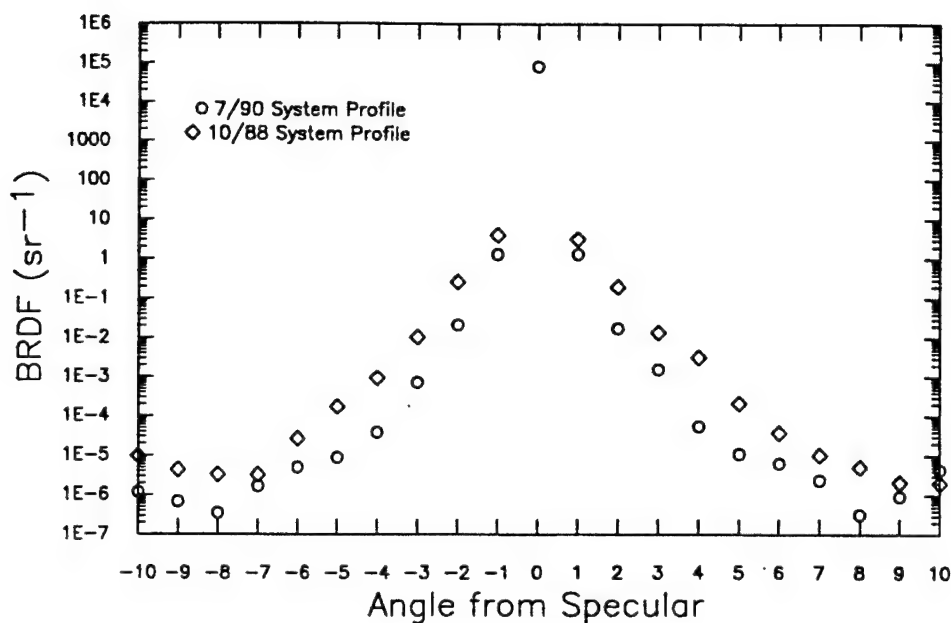


FIGURE 23. COMPARISON OF NEW REFLECTIVE SYSTEM PROFILE TO OLD REFRACTIVE OPTICAL SYSTEM.

Previous "round robin" measurements at $10.6\ \mu\text{m}$ on sets of diffuse and specular samples have shown that there can be extreme variations of BRDF on a particular sample when measured on different machines, while repeated measurement on a single machine can produce fairly repeatable results (within 10%). This phenomenon is subject to debate and there is considerable effort within the scientific community to standardize BRDF measurement techniques and equipment. Spire staff continues to assist in this effort and have maintained the operation of CRYOSCAT in accordance with accepted practice within the optical scatter measurement community. The same diffuse reflectance standard will be used for all calibration measurements during the course of this program to provide maximum repeatability of data.

3.5.3 Review of Final System

In review, the entire optical system for the CRYOSCAT scatterometer has been redesigned to achieve increased capability. The transition from a primarily refractive to a primarily reflective optical system reduced system profile by eliminating stray light produced by bulk scatter from refractive optics. The design also streamlined the beam to meet spot size requirements and minimize profile width.

In an effort to evaluate the performance of the CRYOSCAT scatterometer, a comparative set of measurements was performed using a previously measured beryllium mirror (Rockwell #94). First, BRDF was measured using the FASCAT scatterometer. These data are presented in Figure 24. A mean BRDF value was calculated for each scan over an angular range of ± 4 to 10 degrees from specular. Then an average of the three means was calculated and will be used to compare with CRYOSCAT measurements.

CRYOSCAT measurements were performed on the same spot measured by FASCAT. These data are presented in Figure 25 overlaid onto the FASCAT data. The average mean for the CRYOSCAT data was calculated in the same manner as the FASCAT data described above. The mean values of BRDF over the two angular intervals (forward scatter and backscatter) for the two instruments are presented for comparison. Data from both ranges agree to within a factor of two between the machines.

As a final test of system performance a comparison was made of current measurements of mirror RI94 and measurements taken by CRYOSCAT in 1988. Figure 26 shows that the new system has a considerably lower system profile for angles less than 7° from specular and, at the same time, closely reproduces the older system's data at larger angles.

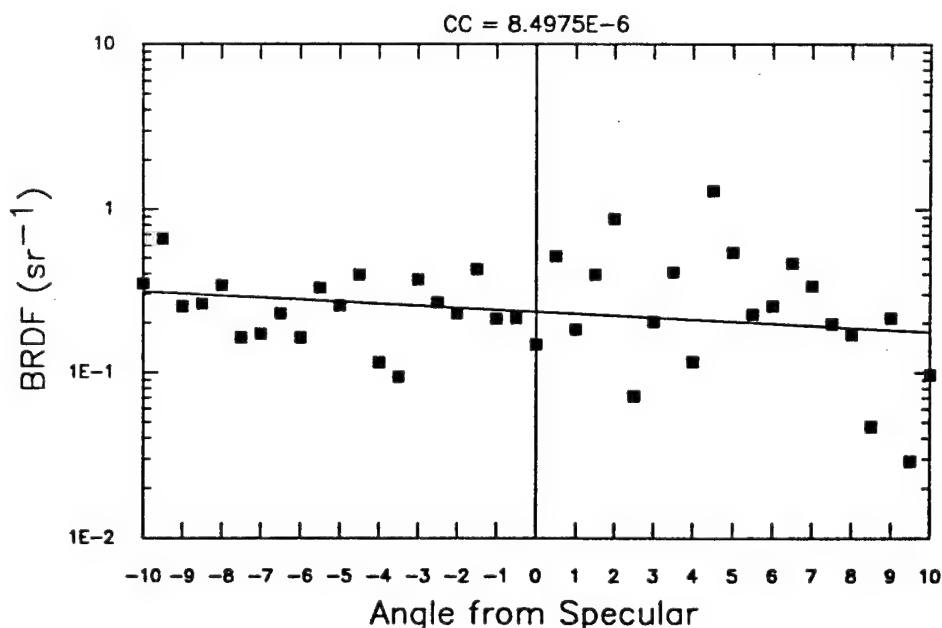


FIGURE 24. BRDF MEASUREMENT OF REFLECTANCE STANDARD ON FASCAT SCATTEROMETER.

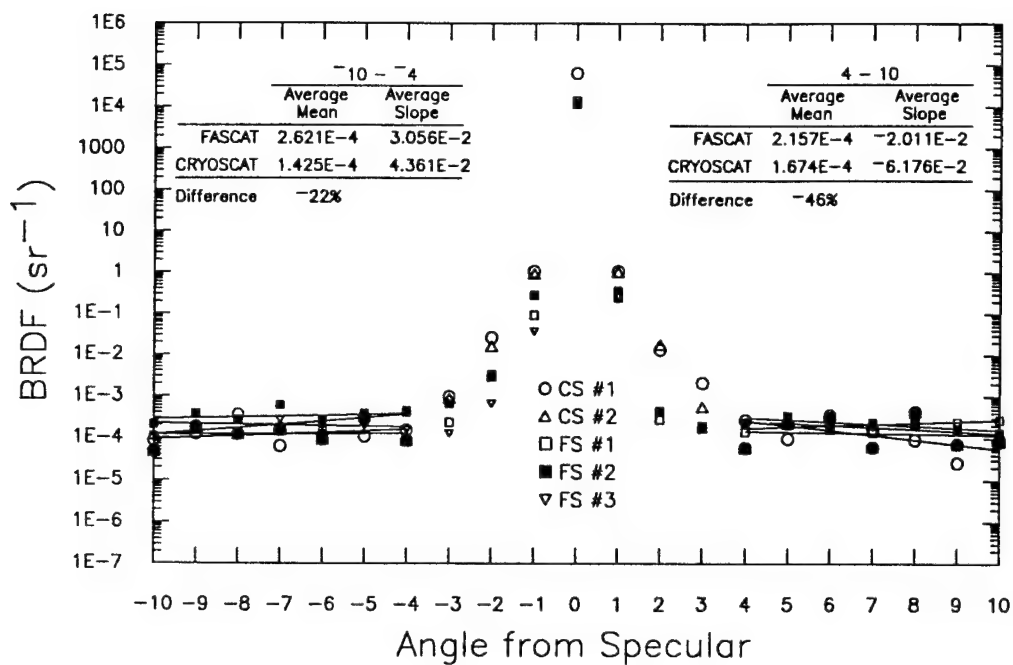


FIGURE 25. COMPARISON OF CRYOSCAT AND FASCAT BRDF MEASUREMENTS ON ROCKWELL RI 94 MIRROR.

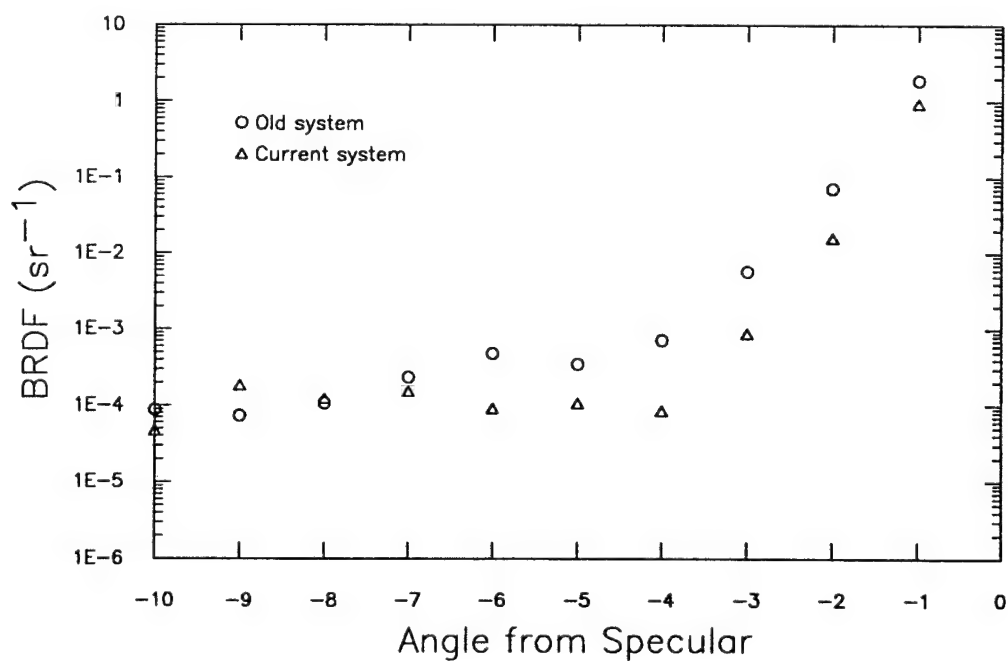


FIGURE 26. COMPARISON OF CURRENT AND OLD SYSTEM BRDF MEASUREMENTS ON RI 94 MIRROR.

3.6 1 August 1990 Through 31 August 1990

- E-beam calorimetry
- Final connection and testing of scatterometer after reconnection to vacuum chamber
- BRDF measurements on RI 94 and calibration reference
- Data acquisition and sample manipulator control software improvements

3.6.1 E-Beam Calibration

Fluence levels produced by the beam attenuation screens were measured using a graphite calorimeter. Voltage and current traces were monitored on a fast oscilloscope during these measurements to insure reproducible pulse width and amplitude. Several measurements were taken for each attenuation screen to check repeatability. The results of these measurements are listed in Table 2. These fluence levels will be used during full-scale mirror testing until different levels are required.

TABLE 2. ELECTRON BEAM ENERGY FLUENCE.

% Open Area of Screen	Fluence (Cal/cm ²)	Standard Deviation
32 %	0.20	0.01
50 %	0.30	0.02
67 %	0.45	0.03
100 %	0.80	0.03

91458

3.6.2 Scatterometer/Vacuum Chamber

Figure 27 is a photograph of the assembled CRYOSCAT system. All signal processing equipment and process control equipment has been arranged and signal lines routed to minimize electrical noise and to maintain optimum system performance. The addition of the interferometer and cryolayer system scheduled during the month of October 1990 are not shown in this figure.

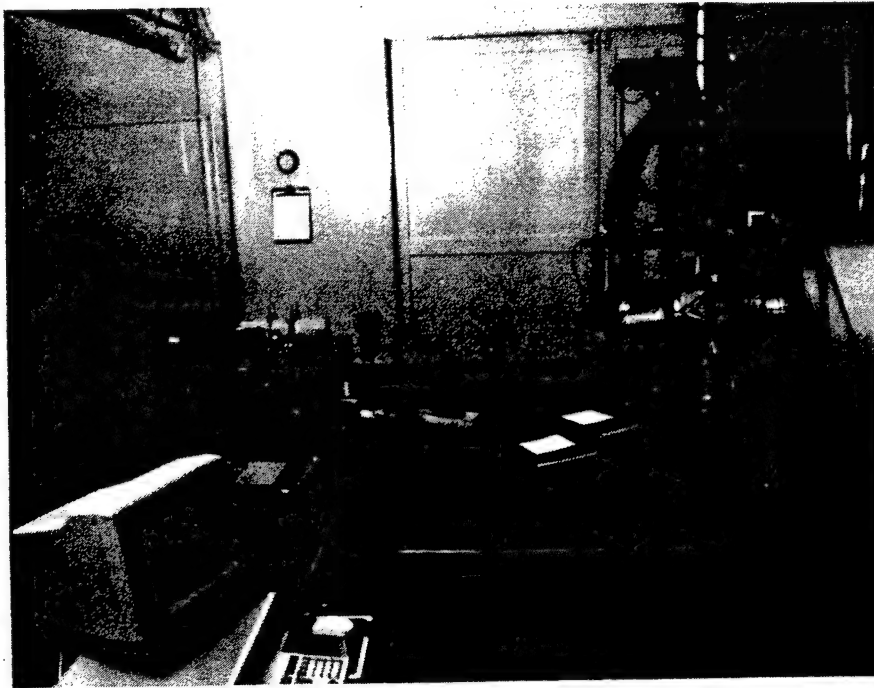


FIGURE 27. PHOTOGRAPH OF ASSEMBLED CRYOSCAT SYSTEM.

3.6.3 BRDF Data

BRDF measurements were performed in the fully-assembled CRYOSCAT on mirror RI 94 and on the calibration reference sample. RI 94 was measured repeatedly during qualification experiments as was the calibration reference. Measurements performed in the assembled system were used to test the repeatability of the scatterometer after reconnection and to insure that it was aligned properly.

Figure 28 presents data taken on RI 94 (center) before and after reconnecting CRYOSCAT to the vacuum chamber. A mean value is calculated and presented for each scan on both sides of specular. The range of data used for this calculation is ± 4 to 10 degrees. The lines drawn through the data plots represent the first order regression to determine the slope of the plots.

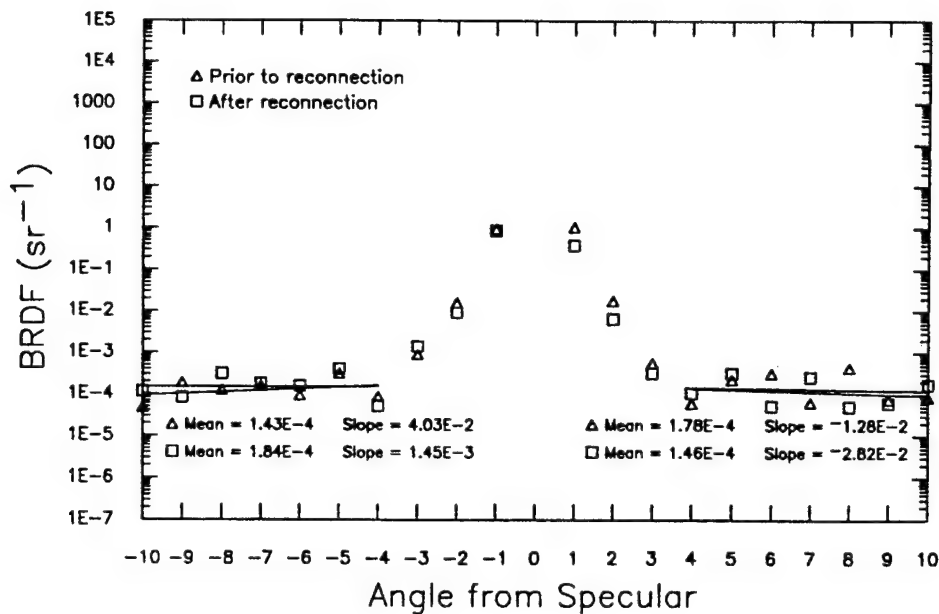


FIGURE 28. BRDF MEASUREMENTS ON MIRROR RI 94 FROM FULLY ASSEMBLED CRYOSCAT SYSTEM.

The repeatability demonstrated in this experiment provides a high level of confidence that the system profile measurements performed off-line are still accurate after the scatterometer was reconnected to the chamber; values produced by the two configurations agree to within 25%. The repeatability of this system is expected to be better than in the previous facility due to improvements in the optical train and data acquisition software. The previous system's repeatability was determined to be 50% from scan to scan. Further measurements are necessary to determine quantitatively the repeatability of the current system, but this measurement gives confidence that it is less than 50%.

3.6.4 BRDF Data Acquisition and Sample Manipulator Software

An updated version of the software routine that controls all system process was introduced and debugged. Data acquisition is now significantly faster, without sacrificing accuracy. More efficient process control routines allow for optimum communication between the computer and lock-in amplifier; typical BRDF scan time has been reduced from 25 minutes to 15 minutes.

Real-time input-power monitoring of the CO₂ laser beam has improved repeatability. This improvement has not yet been evaluated quantitatively but it is expected that a 10%

improvement has been achieved by eliminating the effects of slight power variations during the course of BRDF measurements.

The process control system for the sample manipulator has been incorporated into the control program, allowing access to the manipulator from a single computer keystroke.

Finally, the data output of the new program is now compatible with commercially available data analysis software which will reduce time required for data reduction. The overall result of the software modifications is that more time can be spent on performing useful measurements (both BRDF and interferometric) during the fixed cold-cycle period of eight to ten hours.

3.7 1 September 1990 Through 30 September 1990

- Cryogenic rad-hard testing of five (5) Be mirrors

3.7.1 Cryogenic Rad-Hard Testing

Three 2-inch diameter and two 1.5-inch diameter Be mirrors were tested. The mirrors tested were:

- Be O50-01 (1.5")
- Be O50-04 (1.5")
- POCT 56-W1-M1-1 (2")
- POCT 2V-A-67-A (2")
- POCT 56-W1-M1-2 (2")

The procedure used to test these mirrors follows:

1. The mirror is examined by eye under a focused halogen lamp for major defects or other anomalies. If found, they are described and mapped in reference to the fiducial markings.
2. If no fiducial markings exist, fiducial marks are set and documented before continuing.
3. The mirror is then cleaned according to the established procedure of:
 - Rinse with de-ionized water
 - Rinse with 1% solution of Triton-X in de-ionized water
 - Drag wipe with 1% solution of Triton-X in de-ionized water
 - using 100% cotton pads
 - Long rinse with de-ionized water
 - Rinse with electronic grade Propanol

- Allow mirror to dry under a beaker. Mirror is placed in a Class 10 flow-hood. It is placed on its edge on lint free paper, leaning against side of beaker. The evaporated propanol saturates the atmosphere within the beaker.
 - Mirror examined for residue from drying process
 - Recleaned if residue is found
4. The mirror is then photographed at each of the test sites (two sites for 1.5-inch mirrors and four sites for 2-inch mirrors) using Nomarski photomicroscopy at 50x and 200x. Polarized photomicrographs are also taken at 200x. Great care is taken to insure that the positions being photographed are the exact positions that will be tested. Figure 29 shows the size and location of the test sites.
 5. The scatterometer is calibrated to a diffuse reflecting standard.
 6. An ion implanted Si wafer is marked at its center and installed into the test chamber. This is used as an alignment device for the e-beam.
 7. The mirror is reinspected for contamination and recleaned if necessary. The mirror is then mounted onto the coldfinger and the chamber is sealed and brought under vacuum.
 8. BRDF measurements are taken at each of the test sites. The 10.6 μm laser beam is 5 mm in diameter and set at a 30° incident (specular) angle. Scatter is measured from $\pm 10^\circ$ from specular.
 9. The vacuum chamber is baked overnight to achieve a low 10^{-7} torr pressure.
 10. Residual gases are checked. If the atmosphere is acceptable the mirror is then cooled to 20 K with LHe.
 11. Once the mirror has reached thermal equilibrium, BRDF measurements are repeated at each of the test sites.
 12. The e-beam is located using the Si wafer which is positioned at a pre-determined, fixed distance from the mirror's center. Once the beam is located, the mirror can be manipulated so that the selected test sites can be irradiated. Up to four different fluences can be used during a single thermal cycle.
 13. Three of the four sites are irradiated on the 2-inch mirrors and both sites on the 1.5-inch mirrors are irradiated. Each test site receives a progressively higher fluence. A visual examination of the mirror before and after irradiation is performed and documented. The shape of the e-beam pulse

is recorded on the Si wafer and each pulse is monitored by recording the voltage/current traces.

14. After all sites are irradiated, BRDF measurements are repeated at each of the sites.
15. The mirror is warmed back up to room temperature overnight.
16. A visual inspection to observe damage is performed and documented. BRDF measurements are then repeated on each of the sites.
17. BRDF, e-beam fluence, and observed visual data are then tabulated and analyzed to evaluate performance and to determine the mirrors radiation response curve. A 1st-order linear regression curve fit is calculated for the BRDF data over a range of ± 5 to 10 degrees. The value of this curve fit at $\pm 7.5^\circ$ is used for comparison and this value is presented as the BRDF value for the test site at that stage of the test.
18. The mirror is removed from the test chamber and photomicrographs are taken at each of the test sites again.

Each of the mirrors tested in September underwent this procedure. The fluence levels used for each mirror were essentially the same. BRDF data was taken on both sides of specular and at each stage of the thermal cycle (Note: this is the first time such a complete set of data has been collected).

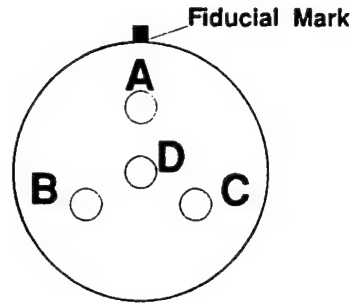
Data acquired for each mirror is presented in its own subsection below. A summary and discussion of results is presented at the end of this section.

3.7.1.1 Be O50-01: 1.5-inch Diameter Be Mirror

Be O50-01 was tested at two sites (A and B) as shown in Figure 29 for 1.5-inch diameter mirrors. Visual observation of this mirror prior to testing showed no unusual characteristics or defects in or around the test sites. The mirror was cleaned according to standard procedure and photographed prior to installation in the CRYOSCAT facility. Photomicrographs of the virgin surface are presented later along with comparison photomicrographs of the post irradiation surface.

BRDF measurements were performed at the two sites with the virgin sample at room temperature. The mirror was then cooled to 20 K and BRDF measurements were again taken. While still cold, the two sites were irradiated by pulsed e-beam. Site A received a fluence of 0.17 cal/cm^2 , and Site B received a fluence of 0.28 cal/cm^2 . BRDF measurements were repeated immediately following irradiation while the mirror was still cold. This measurement (20 K-post irradiation) was compared to the BRDF measurement taken immediately prior to irradiation (20 K-virgin surface) to determine the radiation response factor of the mirror at each fluence level. Finally, the mirror was returned to room temperature, and BRDF measurements were repeated

2.0-inch Diameter Mirror



1.5-inch Diameter Mirror

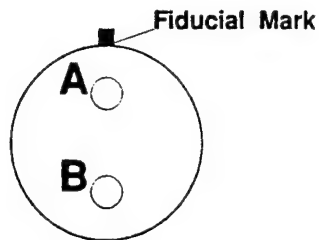


FIGURE 29. GEOMETRY OF e-BEAM TEST SITES ON Be MIRRORS.

a last time. This measurement (300 K-post irradiation) was compared with the original BRDF measurement (300 K-virgin surface) to find the overall response of the mirror to the e-beam irradiation and thermal cycle. All BRDF measurements were made as described above. The raw data of each scan was used to produce BRDF plots and first order regression of the data between $\pm 5^\circ$ and 10° was used to determine BRDF at a specific angle from specular.

Figure 30 shows BRDF plots for Site A (0.17 cal/cm^2) at each of the four measurements stages of the experiment for both sides of specular. The vertical lines at $\pm 7.5^\circ$ represent the point at which the BRDF plot comparison has been done. The value of the BRDF plots at this angle are tabulated in Table 3. The e-beam response, which was evaluated at $\pm 7.5^\circ$, is defined as the difference of two BRDF measurements divided by the original (virgin) value.

The mirror's response to 0.17 cal/cm^2 , while cold, was measured to be 0.63 (backscatter) and 0.99 (forward scatter). The overall response of the mirror due to 0.17 cal/cm^2 and thermal cycling was measured to be 2.50 (backscatter) and 0.33 (forward scatter).

Site B was irradiated by a higher fluence of 0.28 cal/cm^2 . Figure 31 presents the BRDF plots; data at $\pm 7.5^\circ$ scattering angle is presented in Table 3. This fluence produced similar response as at 0.17 cal/cm^2 , while the mirror remained cold. Backscatter response was 0.50, while forward scatter response was 0.38. After warming to room temperature, there is an overall response of 2.18 on the backscatter side of specular and an overall response of 0.13 on the forward scatter side.

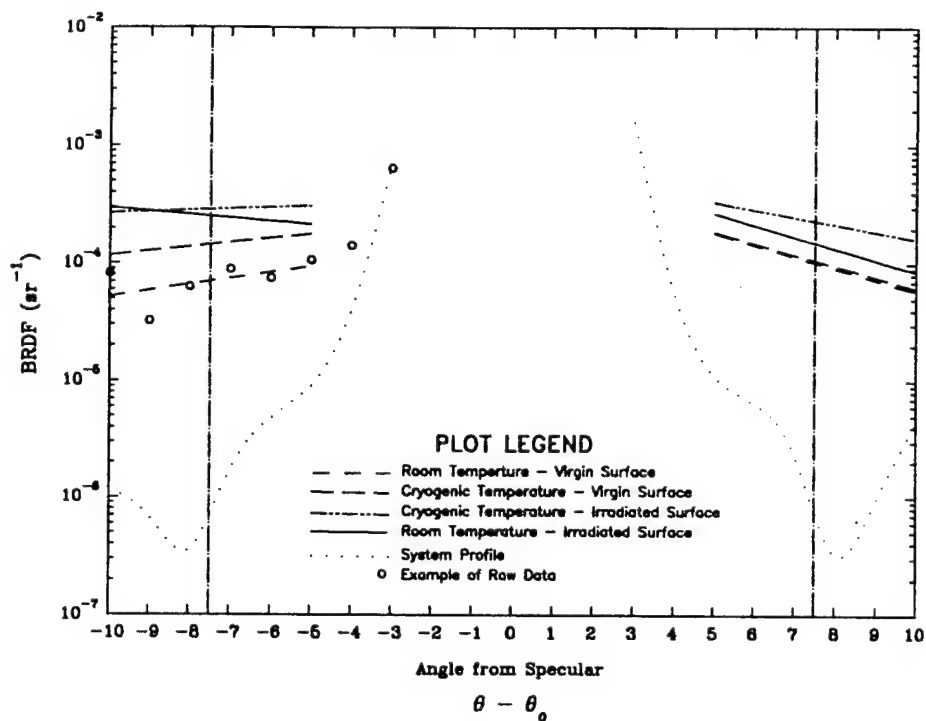


FIGURE 30. BRDF MEASUREMENTS ON MIRROR Be O50-01 AT SITE A (0.17 cal/cm² e-BEAM IRRADIATION).

TABLE 3. BRDF DATA AT $\pm 7.5^\circ$ FOR MIRROR Be O50-01.

BACKSCATTER BRDF at -7.5	STATUS OF MIRROR	FORWARDSCATTER BRDF at 7.5
7.45E-05	300 K - Virgin Surface	1.27E-04
1.84E-04	20 K - Virgin Surface	1.23E-04
MIRROR IRRADIATED WITH A FLUENCE LEVEL = 0.17 Cal/cm ²		
3E-04	20 K - Post Irradiation	2.45E-04
2.61E-04	300 K - Post Irradiation	1.69E-04
RESPONSE TO e-BEAM		
0.63	20 K Post vs. 20 K Virgin	0.99
2.50	300 K Post vs. 300 K Virgin	0.33

BACKSCATTER BRDF at -7.5	STATUS OF MIRROR	FORWARDSCATTER BRDF at 7.5
1.02E-04	300 K - Virgin Surface	1.35E-04
1.27E-04	20 K - Virgin Surface	1.86E-04
MIRROR IRRADIATED WITH A FLUENCE LEVEL = 0.28 Cal/cm ²		
1.9E-04	20 K - Post Irradiation	2.56E-04
3.24E-04	300 K - Post Irradiation	1.52E-04
RESPONSE TO e-BEAM		
0.50	20 K Post vs. 20 K Virgin	0.38
2.18	300 K Post vs. 300 K Virgin	0.13

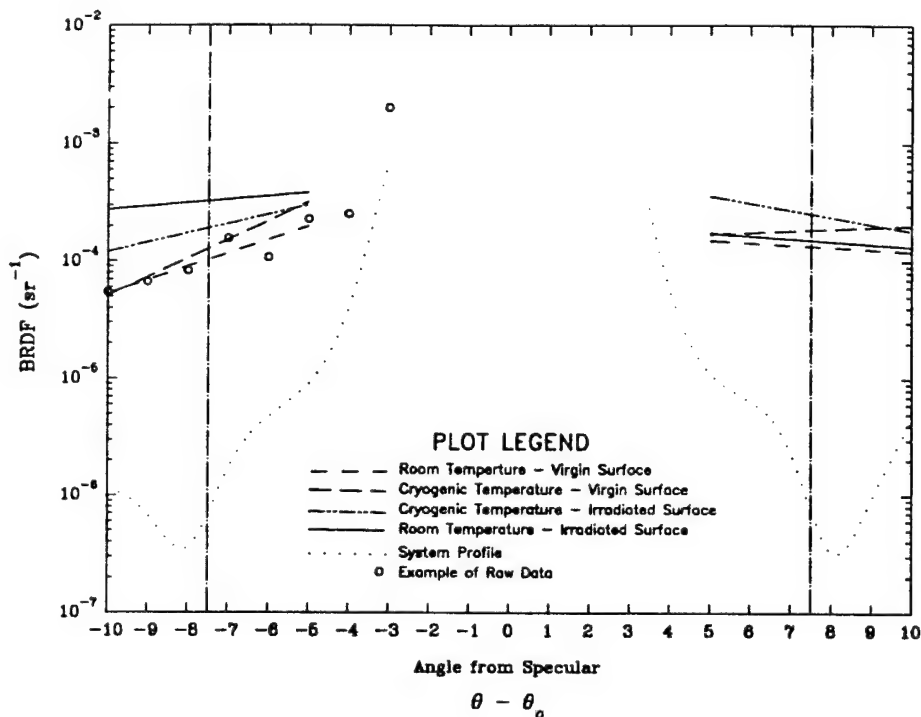


FIGURE 31. BRDF MEASUREMENTS OF MIRROR Be O50-01 AT SITE B (0.28 cal/cm² e-BEAM IRRADIATION).

This mirror responded very similarly to both fluence levels. The response of the mirror, while cold, to both fluence levels was a small increase in scatter on both sides of specular. After warming, however, a marked increase in scatter on the backscatter side of specular was observed for both fluence levels, while forward scatter remained virtually unchanged after irradiation and thermal cycling.

After the test was completed, the mirror was removed from the test chamber and Nomarski photomicrographs were taken of the two test sites again. These photomicrographs are presented along side the virgin surface photomicrographs in Figures 32 and 33. The observed physical change in the surface of the mirror appears to be roughly proportional to the fluence

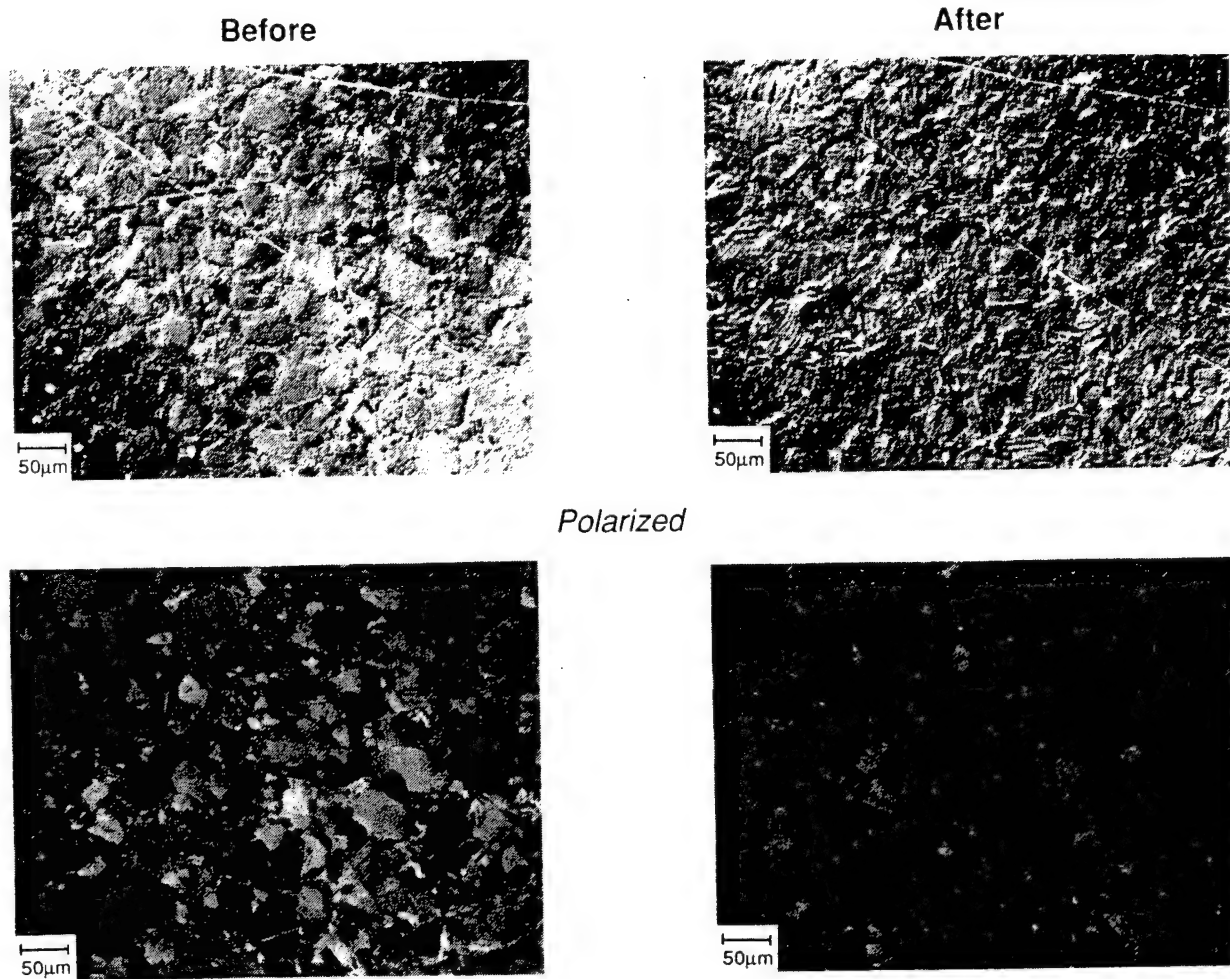


FIGURE 32. NOMARSKI PHOTOMICROGRAPHS OF MIRROR Be O50-01 AT SITE A (0.17 cal/cm^2 e-BEAM FLUENCE).

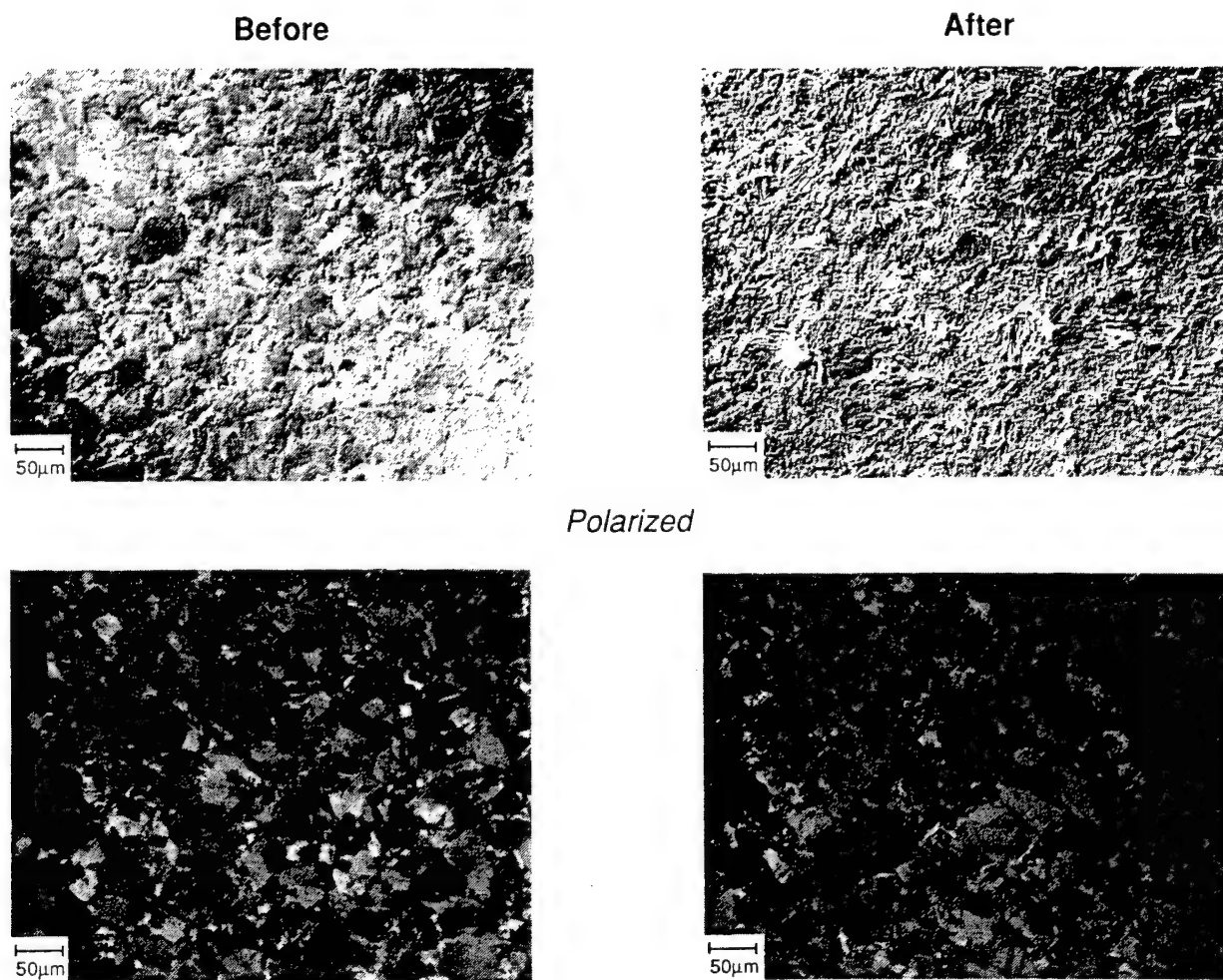


FIGURE 33. NOMARSKI PHOTOMICROGRAPHS OF MIRROR Be O50-01 AT SITE B (0.28 cal/cm^2 e-BEAM FLUENCE).

3.7.1.2 Be O50-04: 1.5-inch Diameter Be Mirror

Be O50-04 was tested at two sites (A and B) as described above for 1.5-inch diameter mirrors. Visual observation of this mirror prior to testing showed no unusual characteristics or defects in or around the test sites. The mirror was cleaned according to standard procedure and photographed prior to installation into the CRYOSCAT facility. The photomicrographs of the virgin surface are presented later along with comparison photomicrographs of the post irradiation surface.

BRDF measurements were performed at the two sites while the virgin sample was at room temperature. The mirror was then cooled to 20 K and BRDF measurements were taken again at this temperature. While still cold, the two sites were irradiated by pulsed e-beam. Site A received a fluence of 0.28 cal/cm^2 and Site B received a fluence of 0.45 cal/cm^2 . (These fluences are higher than those used to irradiate Be O50-01. Both mirrors are from the same manufacturing series and the higher fluences used on the second coupon determine the radiation response for this series over a wider range of fluences.) BRDF measurements were repeated immediately following irradiation while the mirror was still cold. This measurement (20 K-post irradiation) was compared to the BRDF measurements taken immediately prior to irradiation (20 K-virgin surface) to calculate the radiation response factor of the mirror to each fluence level. Finally, the mirror was warmed back to room temperature and BRDF measurements were repeated for a last time. This measurement (300 K-post irradiation) was compared with the original BRDF measurement (300 K-virgin surface) to calculate the overall response of the mirror to the e-beam irradiation and thermal cycle. All BRDF measurements were made in the manner described above. The raw data of each scan was used to produce BRDF plots. A first order regression of the data between $\pm 5^\circ$ and 10° is used to determine the BRDF at a specific angle ($\pm 7.5^\circ$) from specular.

Figure 34 shows the BRDF plots for Site A at each of the four measurements stages of the experiment for both sides of specular. The vertical lines at $\pm 7.5^\circ$ represent the angle at which the BRDF comparisons were made. BRDF values at this angle are tabulated in Table 4. The response to e-beam is evaluated at $\pm 7.5^\circ$ and is defined as the difference of two BRDF measurements, divided by the original (virgin) value.

The mirror's response to 0.28 cal/cm^2 , while cold, was found to be 0.75 (backscatter) and 0.56 (forward scatter). The overall response of the mirror due to 0.28 cal/cm^2 and thermal cycling was measured to be 2.24 (backscatter) and 1.02 (forward scatter). While the mirror remained cold, the response due to e-beam alone produced a small increase in scatter on both sides of specular. After warming the mirror to room temperature, there was an overall increase in scatter of 2.24 on the backscatter side of specular, and forward scatter showed an increase of 1.02. This compares well to the response observed on Be O50-01 - Site B, which was irradiated by the same fluence level. This time there was a noted overall increase in forward scatter which was not observed previously.

Site B was irradiated by a higher fluence of 0.45 cal/cm^2 . Figure 35 presents BRDF plots and the data are presented in Table 4. This fluence produced slightly higher response levels while the mirror remained cold. Backscatter response was 1.81 while forward scatter response

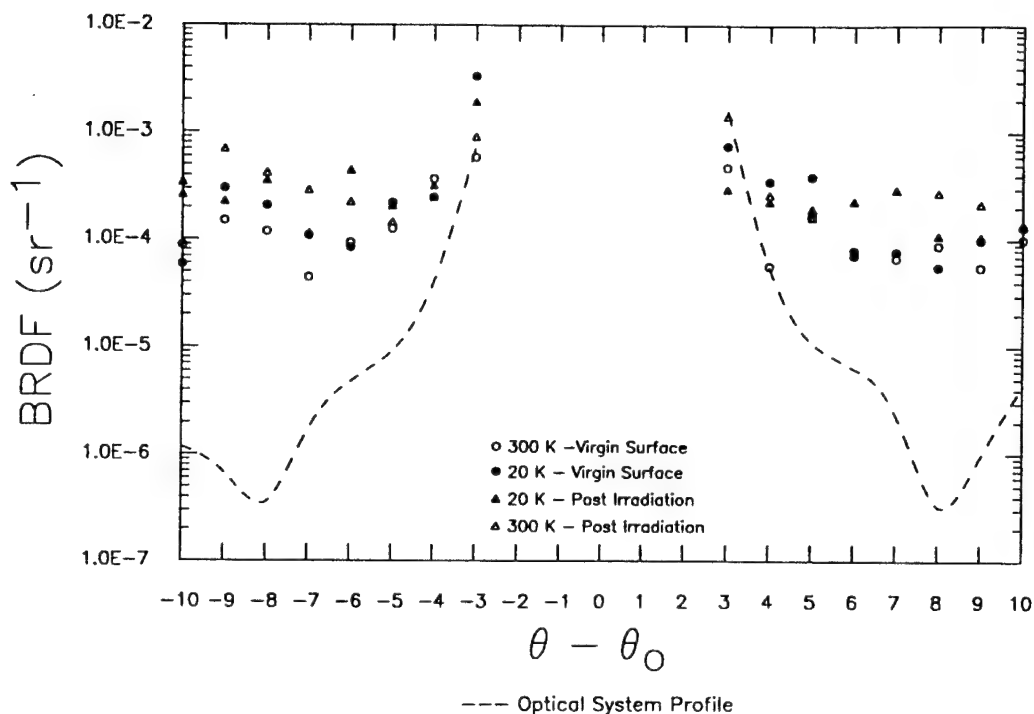


FIGURE 34. BRDF MEASUREMENTS OF MIRROR Be O50-04 AT SITE A (0.28 cal/cm² e-BEAM FLUENCE).

TABLE 4. BRDF DATA AT $\pm 7.5^\circ$ FOR MIRROR Be O50-04.

BACKSCATTER BRDF at -7.5	STATUS OF MIRROR	FORWARDSCATTER BRDF at 7.5
9.68E-05	300 K - Virgin Surface	8.73E-05
1.4E-04	20 K - Virgin Surface	1.07E-04
MIRROR IRRADIATED WITH A FLUENCE LEVEL = 0.28 Cal/cm ²		
2.45E-04	20 K - Post Irradiation	1.67E-04
3.14E-04	300 K - Post Irradiation	1.76E-04
RESPONSE TO e-BEAM		
0.75	20 K Post vs. 20 K Virgin	0.56
2.24	300 K Post vs. 300 K Virgin	1.02

A.

BACKSCATTER BRDF at -7.5	STATUS OF MIRROR	FORWARDSCATTER BRDF at 7.5
7.51E-05	300 K - Virgin Surface	1.57E-04
1.35E-04	20 K - Virgin Surface	2.29E-04
MIRROR IRRADIATED WITH A FLUENCE LEVEL = 0.45 Cal/cm ²		
3.8E-04	20 K - Post Irradiation	3.53E-04
2.49E-04	300 K - Post Irradiation	3.41E-04
RESPONSE TO e-BEAM		
1.81	20 K Post vs. 20 K Virgin	0.54
2.32	300 K Post vs. 300 K Virgin	1.17

B.

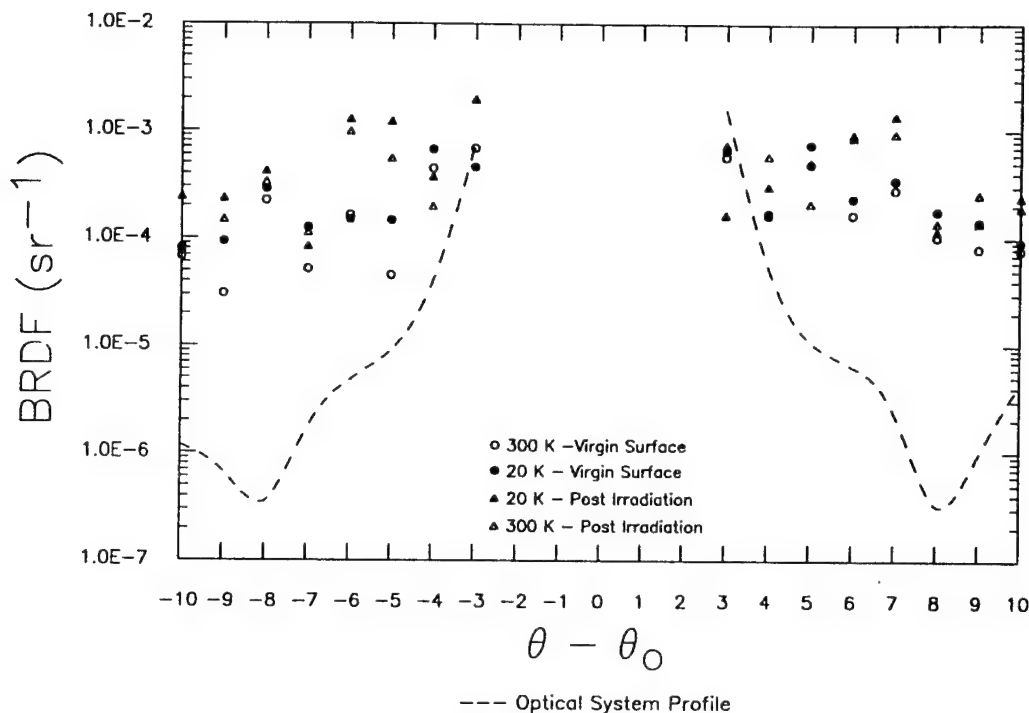


FIGURE 35. BRDF MEASUREMENTS OF MIRROR Be O50-04 AT SITE B (0.45 cal/cm² e-BEAM FLUENCE).

was 0.54. After warming the mirror to room temperature, there was an overall response of 2.32 on the backscatter side of specular and an overall response of 1.17 on the forward scatter side.

This mirror responded similarly to both fluence levels, although the higher 0.45 cal/cm² fluence produced a greater cold response in the backscatter direction. The response of the mirror, while cold, to 0.28 cal/cm² was a small increase in scatter on both sides of specular, which compares well to the results of Be O50-01 - Site B. After warming, however, a marked increase in scatter on the backscatter side of specular was observed for both fluence levels, while forward scatter was only slightly increased as a result of irradiation and thermal cycling.

After the test was completed, the mirror was removed from the test facility and Nomarski photomicrographs were taken of the two test sites. These photomicrographs are presented along with the virgin surface photomicrographs in Figures 36 and 37. The observed physical change in the surface of the mirror appears to be about the same for both fluence levels with a slightly greater response to the higher 0.45 cal/cm² irradiation.

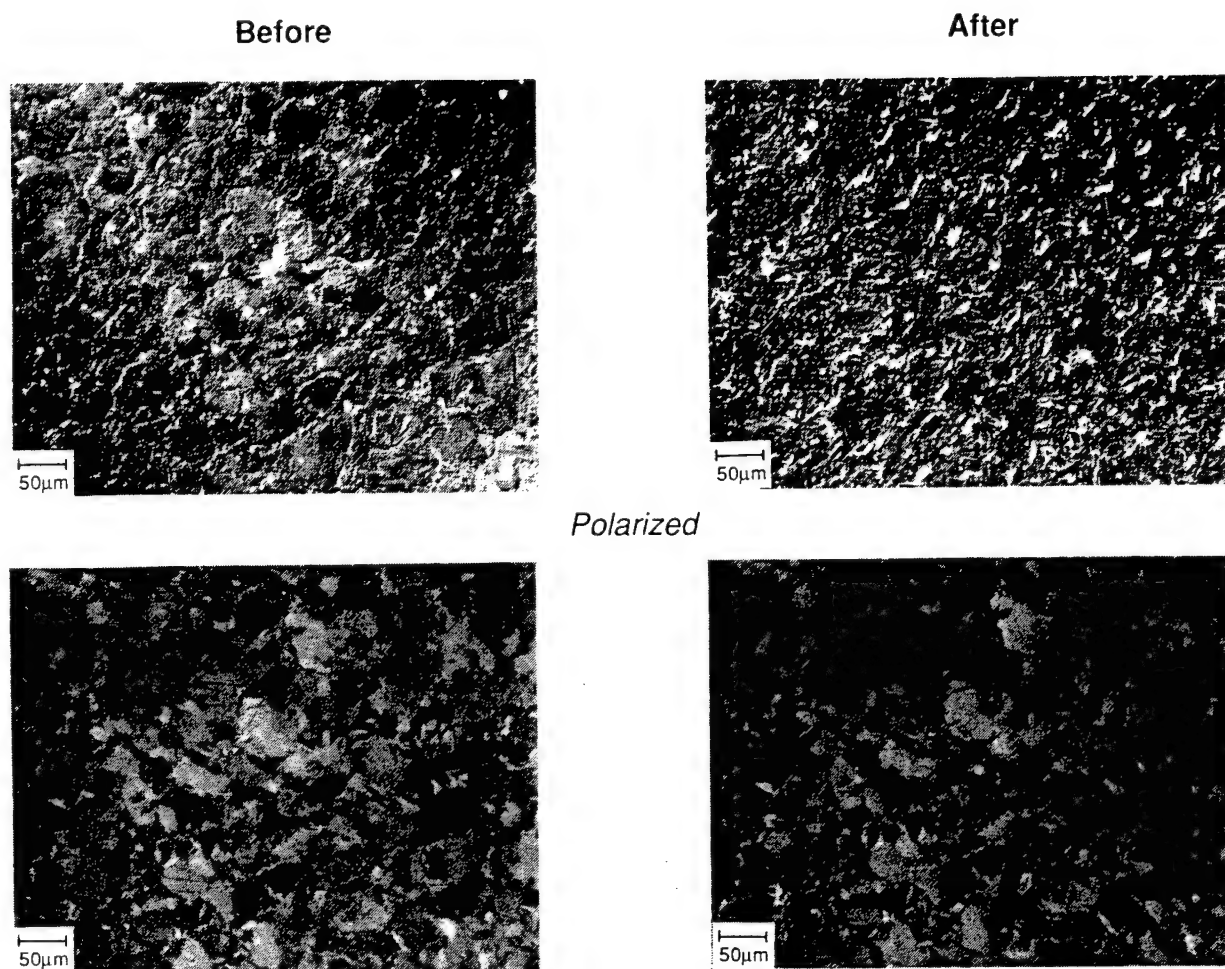


FIGURE 36. NOMARSKI PHOTOMICROGRAPHS OF MIRROR Be O50-04 AT SITE A (0.28 cal/cm^2).

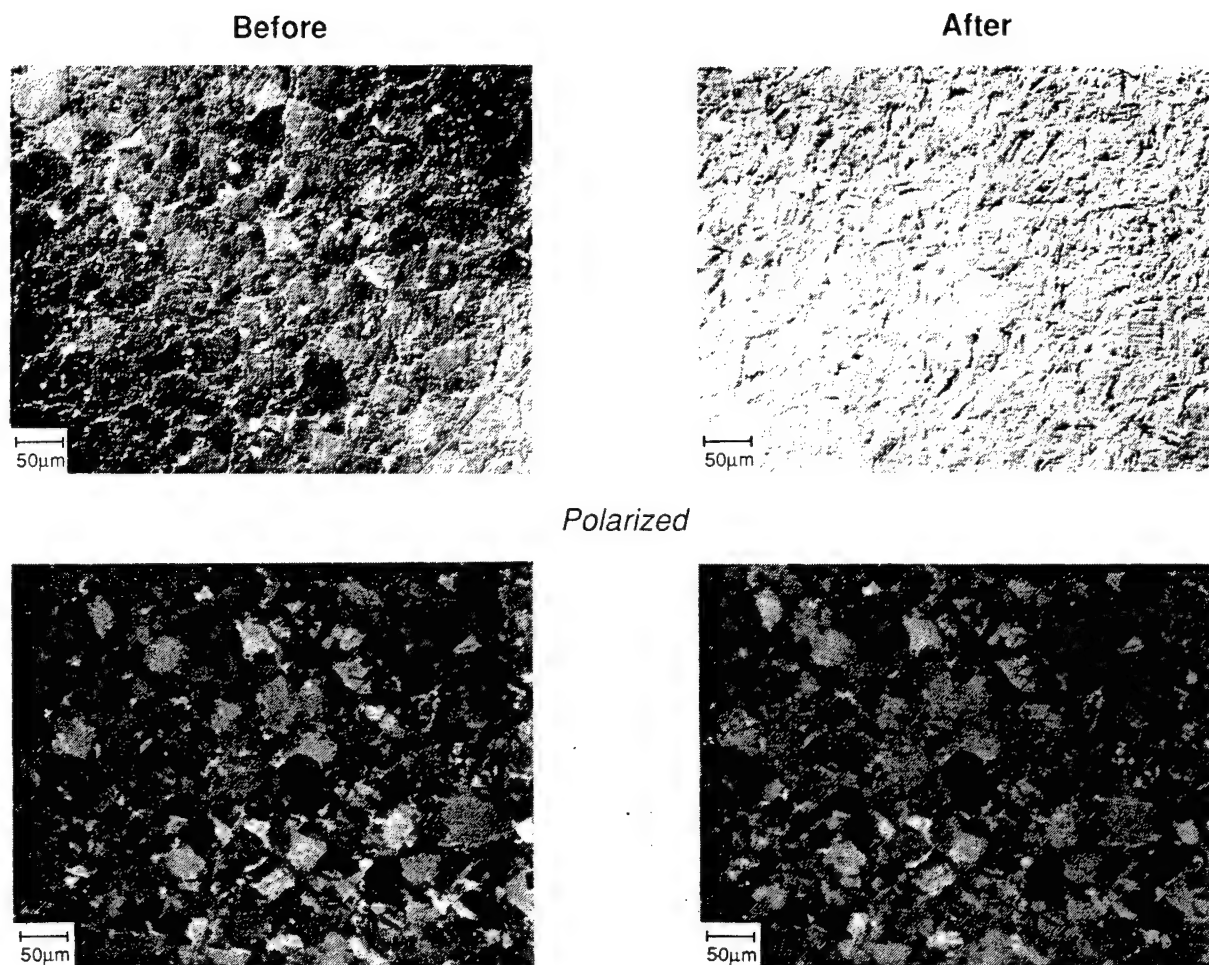


FIGURE 37. NOMARSKI PHOTOMICROGRAPHS OF MIRROR Be O50-04 AT SITE B (0.45 cal/cm^2).

3.7.1.3 POCT 56-W1-M1-1: Two-inch Diameter Be Mirror

POCT 56-W1-M1-1 was tested at four sites (A, B, C, and D) for two-inch diameter mirrors. Visual observation of this mirror prior to testing showed no unusual characteristics or defects in or around the test sites. The mirror was cleaned according to standard procedure and photographed prior to installation into the CRYOSCAT facility. Photomicrographs of the virgin surface are presented later along with comparison photomicrographs of the post-irradiation surface.

BRDF measurements were performed at the four sites while the virgin sample was at room temperature. The mirror was then cooled to 20 K and BRDF measurements were taken again at this temperature. While still cold, three of the four sites were irradiated by pulsed e-beam. Site A received a fluence of 0.27 cal/cm^2 , Site B received a fluence of 0.33 cal/cm^2 , and Site C received a fluence of 0.45 cal/cm^2 . Site D (center) was not irradiated. BRDF measurements were repeated immediately following irradiation while the mirror was still cold. This measurement (20 K-post irradiation) was compared to the BRDF measurement taken immediately prior to irradiation (20 K-virgin surface) to calculate the radiation response factor of the mirror to each fluence level. Finally, the mirror was warmed to room temperature and BRDF measurements were repeated for a last time. This measurement (300 K-post irradiation) was compared to the original BRDF measurement (300 K-virgin surface) to calculate the overall response of the mirror to the e-beam irradiation and thermal cycle. All BRDF measurements were made in the manner described earlier. The raw data of each scan was used to produce BRDF plots. A first order regression of the data between $\pm 5^\circ$ and 10° was used to determine the BRDF value at a specific angle (0.75°) from specular.

Figure 38 shows BRDF plots for Site A (0.27 cal/cm^2) at each of the four measurements stages of the experiment for both sides of specular. The vertical lines at $\pm 7.5^\circ$ represents the angle at which BRDF comparisons were made. The BRDF values at this angle are tabulated in Table 5. The response to e-beam values were evaluated at $\pm 7.5^\circ$ and calculated as before.

The mirror's response to 0.27 cal/cm^2 , while cold, was measured to be 0.65 (backscatter) and 2.00 (forward scatter). The overall response of the mirror to 0.27 cal/cm^2 and thermal cycling was found to be 0.39 (backscatter) and 0.77 (forward scatter). While the mirror remained cold, the response due to e-beam alone produced a small increase in scatter in the backscatter direction while producing a considerable increase in the forward scatter direction. After warming the mirror back to room temperature, the overall increase in scatter was small on both sides of specular. Site B was irradiated by a higher fluence of 0.33 cal/cm^2 . Figure 39 presents the BRDF plots and response data is presented in Table 5. This fluence produced significantly higher response levels while the mirror remained cold. Backscatter response was 1.25, while forward scatter response was 5.05. After warming the mirror to room temperature, there was an overall response of 1.02 on the backscatter side of specular and an overall response of 4.45 on the forward scatter side.

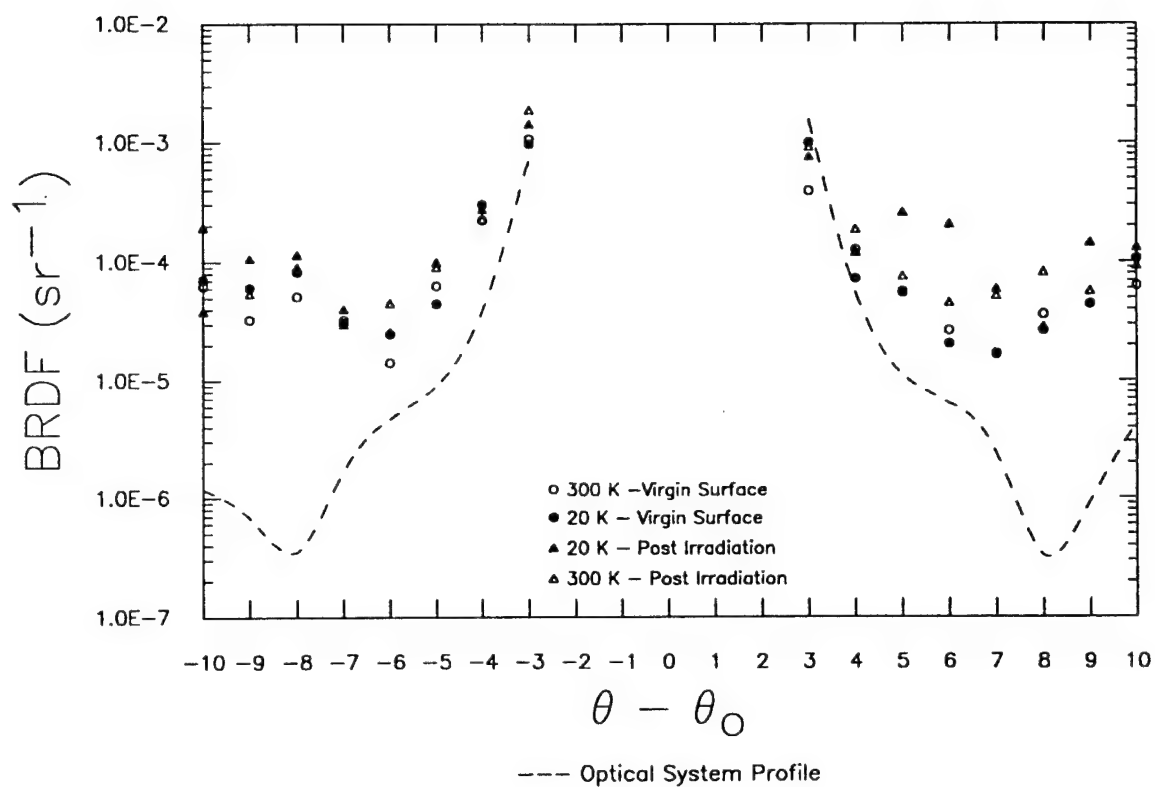


FIGURE 38. BRDF MEASUREMENTS OF MIRROR POCT 56-W1-M1-1 AT SITE A (0.27 cal/cm²).

TABLE 5. BRDF DATA AT $\pm 7.5^\circ$ FOR MIRROR POCT 56-W1-M1-1.

BACKSCATTER BRDF at -7.5	STATUS OF MIRROR	FORWARDSCATTER BRDF at 7.5
3.84E-05	300 K - Virgin Surface	3.69E-05
4.81E-05	20 K - Virgin Surface	3.67E-05
MIRROR IRRADIATED WITH A FLUENCE LEVEL = 0.27 Cal/cm ²		
7.93E-05	20 K - Post Irradiation	1.1E-04
5.35E-05	300 K - Post Irradiation	6.54E-05
RESPONSE TO e-BEAM		
0.65	20 K Post vs. 20 K Virgin	2.00
0.39	300 K Post vs. 300 K Virgin	0.77

A.

BACKSCATTER BRDF at -7.5	STATUS OF MIRROR	FORWARDSCATTER BRDF at 7.5
3.31E-05	300 K - Virgin Surface	1.89E-05
3.9E-05	20 K - Virgin Surface	2.94E-05
MIRROR IRRADIATED WITH A FLUENCE LEVEL = 0.33 Cal/cm ²		
8.78E-05	20 K - Post Irradiation	1.78E-04
6.67E-05	300 K - Post Irradiation	1.03E-04
RESPONSE TO e-BEAM		
1.25	20 K Post vs. 20 K Virgin	5.05
1.02	300 K Post vs. 300 K Virgin	4.45

B.

BACKSCATTER BRDF at -7.5	STATUS OF MIRROR	FORWARDSCATTER BRDF at 7.5
3.71E-05	300 K - Virgin Surface	2.79E-05
2.98E-05	20 K - Virgin Surface	4.49E-05
MIRROR IRRADIATED WITH A FLUENCE LEVEL = 0.45 Cal/cm ²		
1.88E-04	20 K - Post Irradiation	1.23E-04
1.18E-04	300 K - Post Irradiation	1.02E-04
RESPONSE TO e-BEAM		
5.31	20 K Post vs. 20 K Virgin	1.74
2.18	300 K Post vs. 300 K Virgin	2.66

C.

BACKSCATTER BRDF at -7.5	STATUS OF MIRROR	FORWARDSCATTER BRDF at 7.5
4.53E-05	300 K - Virgin Surface	3.44E-05
5.94E-05	20 K - Virgin Surface	3.94E-05
MIRROR IRRADIATED WITH A FLUENCE LEVEL = 0.00 Cal/cm ²		
1.69E-04	20 K - Post Irradiation	1.78E-04
1.49E-04	300 K - Post Irradiation	1.97E-04
RESPONSE TO e-BEAM		
1.85	20 K Post vs. 20 K Virgin	3.52
2.29	300 K Post vs. 300 K Virgin	4.73

D.

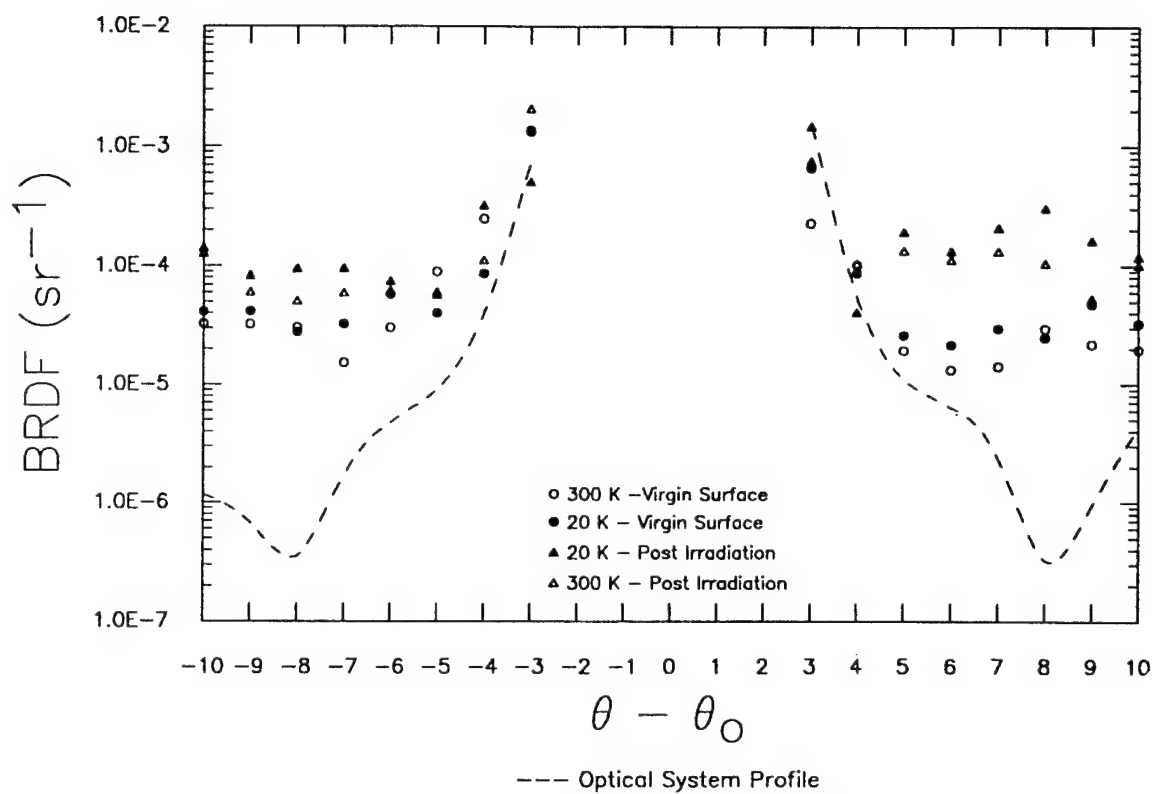


FIGURE 39. BRDF MEASUREMENTS OF MIRROR POCT 56-W1-M1-1 AT SITE B (0.33 cal/cm²).

Site C was irradiated by a higher fluence of 0.45 cal/cm^2 . Figure 40 presents the BRDF plots and the data is presented in Table 5. While the mirror remained cold, backscatter response was 5.31 while forward scatter response was 1.74. After warming the mirror back to room temperature, there is an overall response of 2.18 on the backscatter side of specular and an overall response of 2.66 on the forward scatter side.

The overall and cold backscatter response increased with increased fluence. The forward scatter response (cold and overall) also increased with fluence up to 0.33 cal/cm^2 . After that, the response dropped as fluence increased to 0.45 cal/cm^2 , showing an overall increase favoring backscatter, as observed with the other mirrors tested and described above.

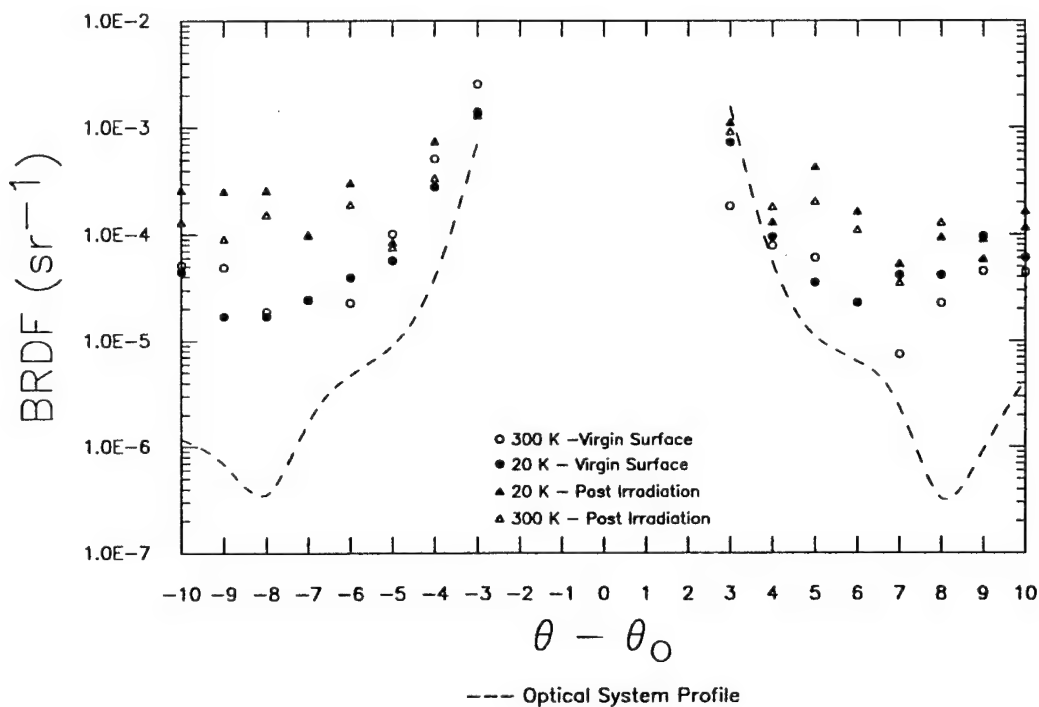


FIGURE 40. BRDF MEASUREMENTS OF MIRROR POCT 56-W1-M1-1 AT SITE C (0.45 cal/cm^2).

Site D (center) was not irradiated but was measured at each stage of the experiment. The close proximity of Site D to the other three sites suggests that residual effects may be observed as a result of the irradiation of those sites. Figure 41 shows the BRDF plots measured at Site D and Table 5 presents response data. Cold response to the indirect irradiation of the center of the mirror was 1.85 (backscatter) and 3.52 (forward scatter). Overall response was 2.29 (backscatter) and 4.73 (forward scatter). The center position of the mirror shows a significant increase in cold and overall scatter on both sides of specular. Forward scatter is greater than backscatter in this case. The type(s) of damage effecting scatter at this site are the result of three irradiations within close proximity of the site, rather than direct irradiation of a specific fluence.

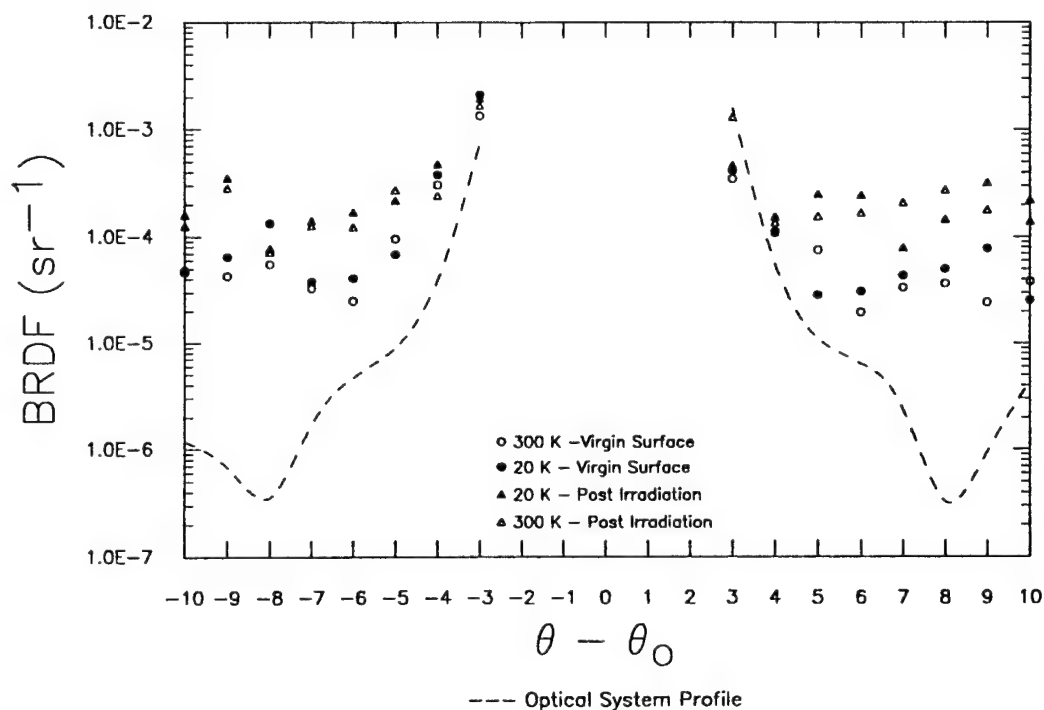


FIGURE 41. BRDF MEASUREMENTS OF MIRROR POCT 56-W1-M1-1 AT SITE D (central position receiving only indirect e-beam irradiation).

After the test was completed, the mirror was removed from the test chamber and Nomarski photomicrographs were taken of all test sites. These photomicrographs are presented alongside the virgin surface photomicrographs in Figures 42 through 45. The observed physical change on the mirror surface appears to be proportional to the e-beam irradiation fluence levels. The center position (Site D) shows little or no visible damage in the photomicrographs.

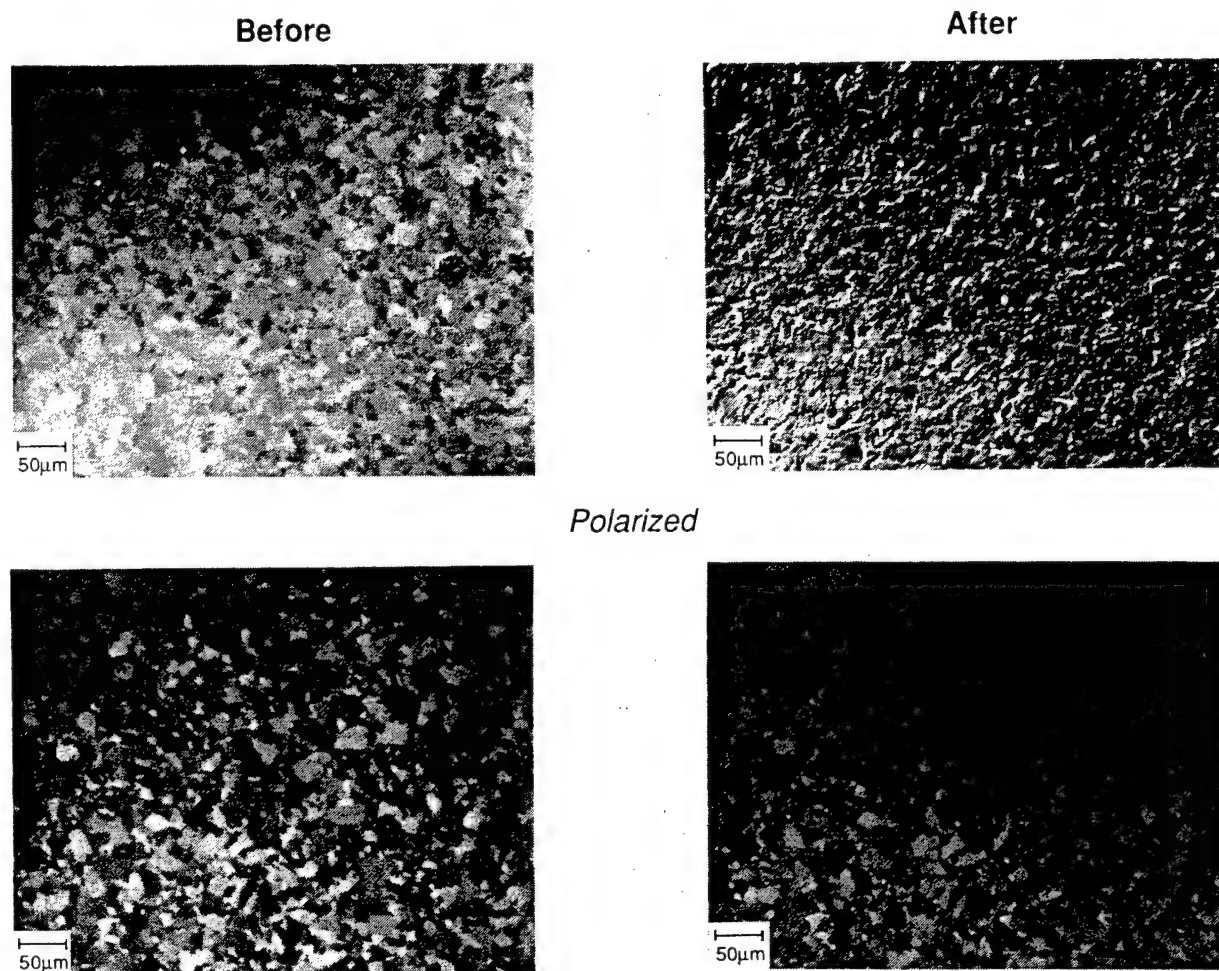


FIGURE 42. NOMARSKI PHOTOMICROGRAPH OF MIRROR POCT 56-W1-M1-1 AT SITE A (0.27 cal/cm^2).

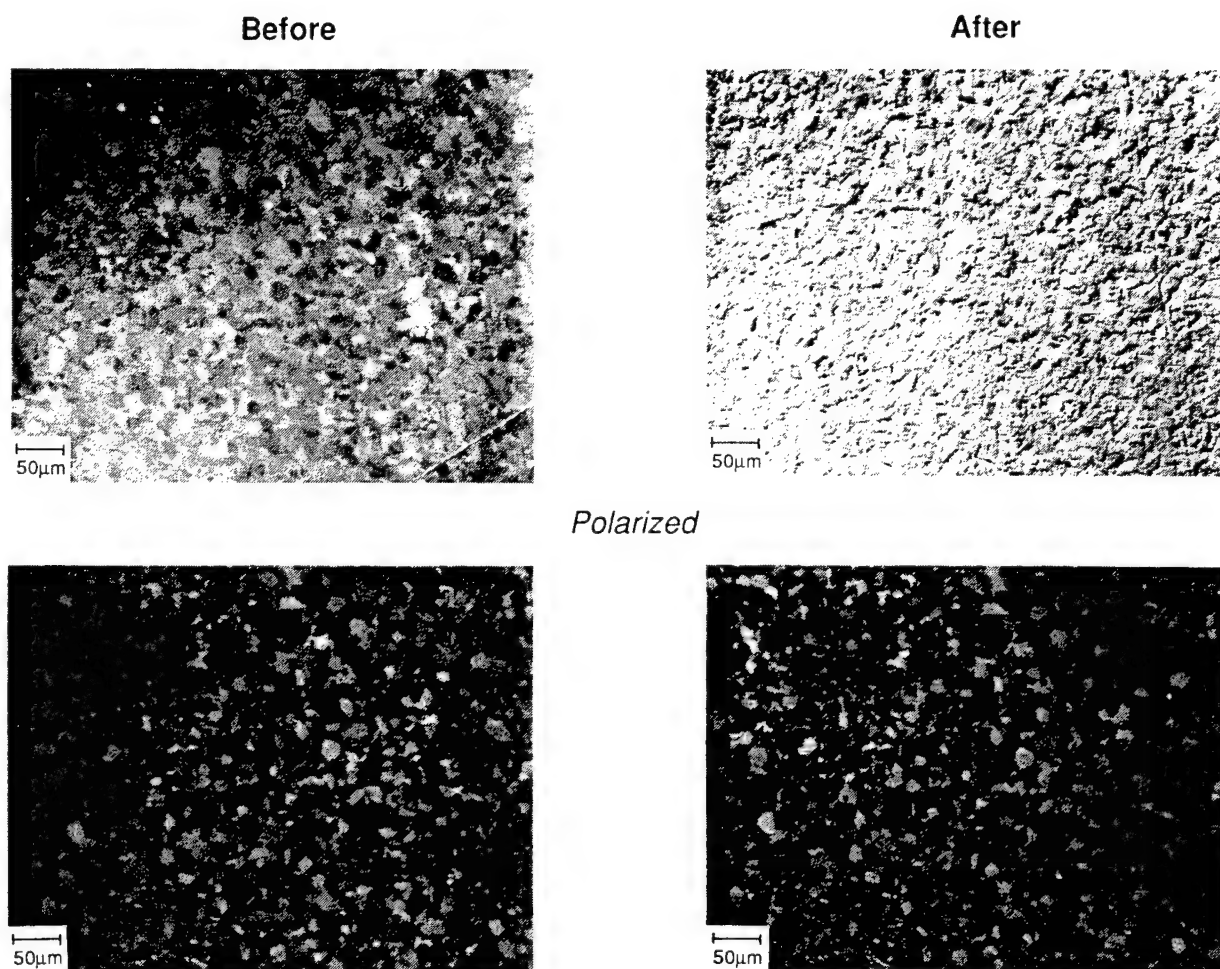


FIGURE 43. NOMARSKI PHOTOMICROGRAPH OF MIRROR POCT 56-W1-M1-1 AT SITE B (0.33 cal/cm^2).

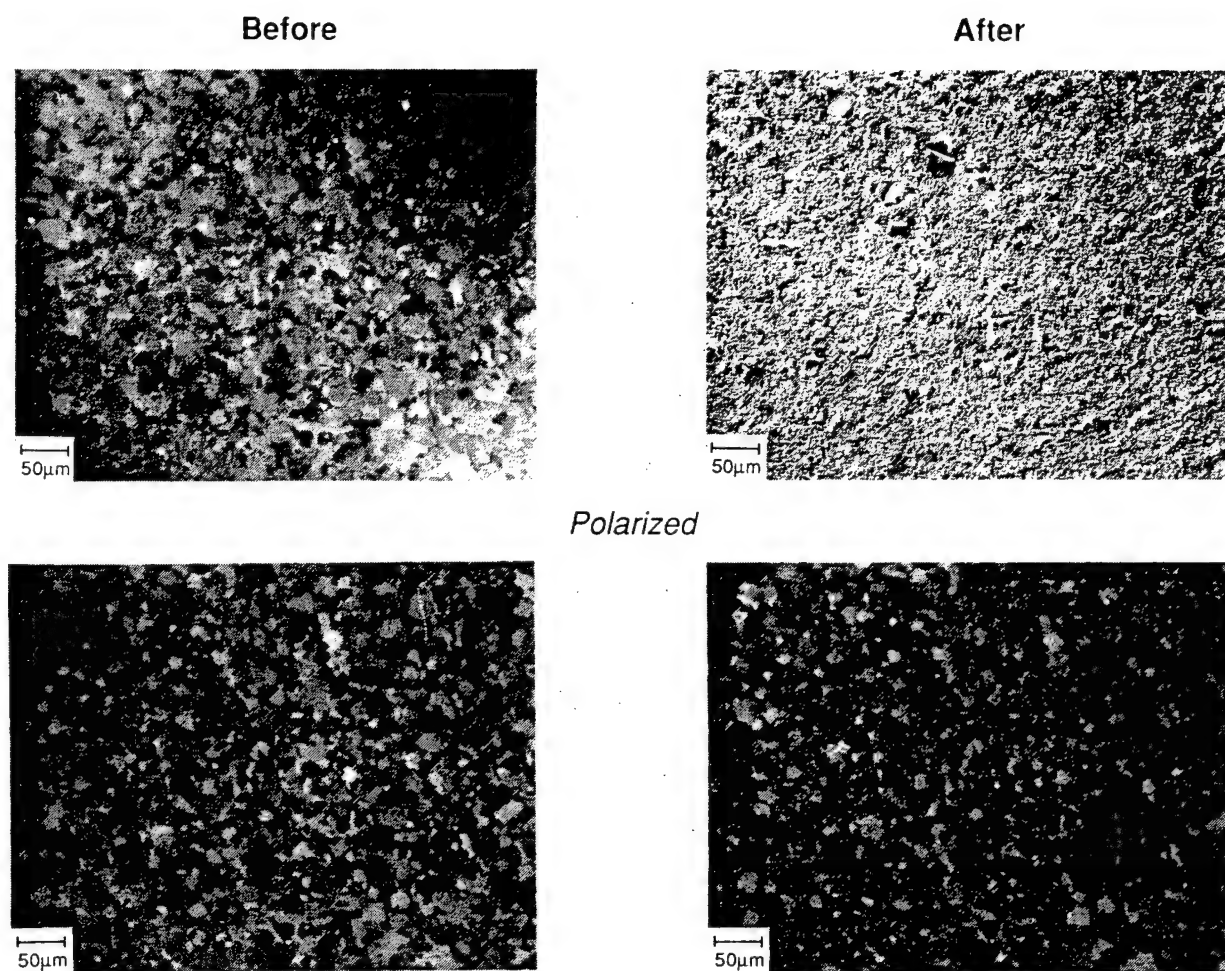


FIGURE 44. NOMARSKI PHOTOMICROGRAPH OF MIRROR POCT 56-W1-M1-1 AT SITE C (0.45 cal/cm^2).

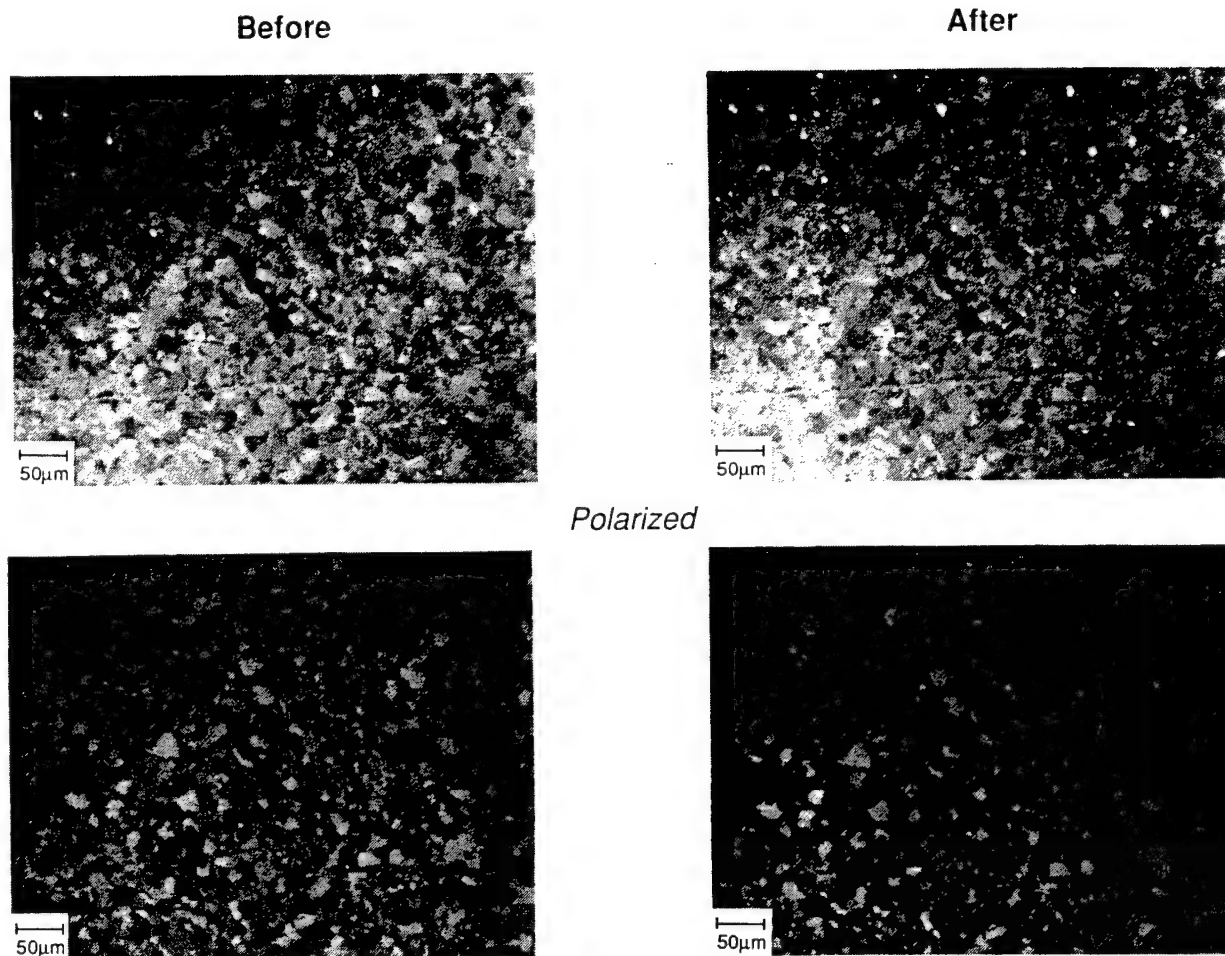


FIGURE 45. NOMARSKI PHOTOMICROGRAPH OF MIRROR POCT 56-W1-M1-1 AT SITE D (central position, no direct e-beam irradiation).

3.7.1.4 POCT 2V-A-67-A: Two-inch Diameter Be Mirror

POCT 2V-A-67-A was tested at four sites (A, B, C, and D) as described above for two-inch diameter mirrors. Visual observation of this mirror prior to testing showed no unusual characteristics or defects in or around the test sites. The mirror was cleaned according to standard procedure and photographed prior to installation into the CRYOSCAT facility. The photomicrographs of the virgin surface are presented later along with comparison photomicrographs of the post-irradiation surface.

BRDF measurements were performed at all four sites with the virgin sample at room temperature. The mirror was then cooled to 20 K and BRDF measurements were taken again at this temperature. While still cold, three of the four sites were irradiated by pulsed e-beam. Site A received a fluence of 0.27 cal/cm^2 , Site B received a fluence of 0.37 cal/cm^2 , and Site C received a fluence of 0.45 cal/cm^2 . Site D (center) was not irradiated. BRDF measurements were repeated immediately following irradiation while the mirror was still cold. This measurement (20 K-post irradiation) was compared to the BRDF measurement taken immediately prior to irradiation (20 K-virgin surface) to calculate the radiation response of the mirror to each fluence level. Finally, the mirror was warmed to room temperature, and BRDF measurements were repeated. This measurement (300 K-post irradiation) was compared to the original BRDF measurement (300 K-virgin surface) to calculate the overall response of the mirror to e-beam irradiation and thermal cycling. All BRDF measurements were made as described earlier. The raw data of each scan was used to produce BRDF plots. A first order regression of the data between $\pm 5^\circ$ and 10° was used to determine BRDF at a specific angle (± 7.5) from specular.

Figure 46 shows BRDF plots for Site A (0.25 cal/cm^2) at each of the four measurements stages of the experiment for both sides of specular. The vertical lines at $\pm 7.5^\circ$ represent the point at which BRDF comparison were done. The BRDF values at this angle are tabulated in Table 6. The response to e-beam values were evaluated at $\pm 7.5^\circ$ and were calculated as before.

The mirror's response to 0.27 cal/cm^2 , while cold, was measured to be 0.88 (backscatter) and 0.20 (forward scatter). The overall response of the mirror due to 0.27 cal/cm^2 and the thermal cycle was measured to be 2.15 (backscatter) and 0.11 (forward scatter). While the mirror remained cold, the response due to e-beam alone produced a small increase in scatter in the backscatter direction while producing relatively no increase in the forward scatter direction. After warming the mirror back to room temperature, the overall increase in scatter was small on the forward side of specular and large on the backscatter side as observed with the first two mirrors tested and described above.

Site B was irradiated by a higher fluence of 0.37 cal/cm^2 . Figure 47 shows BRDF plots and response data is presented in Table 6. This fluence produced significantly higher response levels while the mirror remained cold. Backscatter response was 1.19 while forward scatter response was 3.09. After warming the mirror to room temperature, there was an overall response of 2.63 on the backscatter side of specular and an overall response of 1.74 on the forward scatter side.

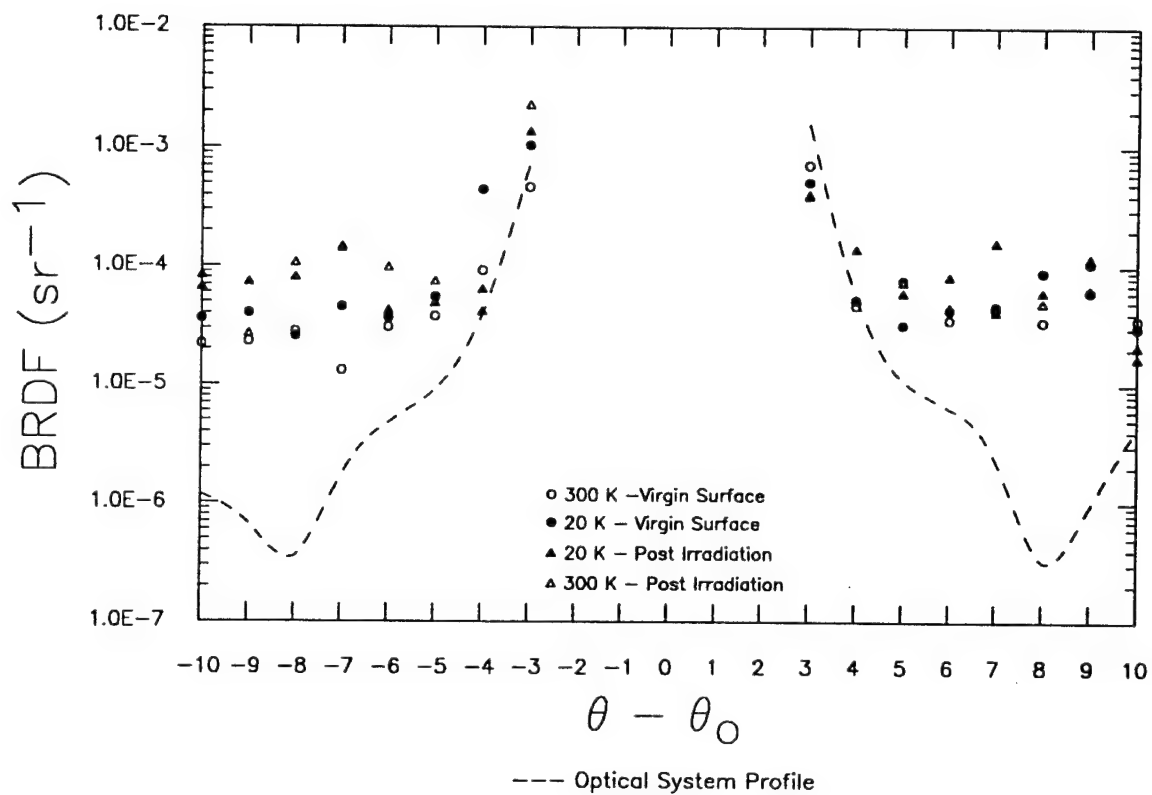


FIGURE 46. BRDF MEASUREMENTS ON MIRROR POCT 2V-A-67-A AT SITE A (0.27 cal/cm^2).

TABLE 6. BRDF DATA AT $\pm 7.5^\circ$ FOR MIRROR POCT 2V-A-67-A.

BACKSCATTER BRDF at -7.5	STATUS OF MIRROR	FORWARDSCATTER BRDF at 7.5
2.45E-05	300 K - Virgin Surface	4.62E-05
3.88E-05	20 K - Virgin Surface	5.12E-05
MIRROR IRRADIATED WITH A FLUENCE LEVEL = 0.27 Cal/cm ²		
7.28E-05	20 K - Post Irradiation	6.13E-05
7.71E-05	300 K - Post Irradiation	5.11E-05
RESPONSE TO e-BEAM		
0.88	20 K Post vs. 20 K Virgin	0.20
2.15	300 K Post vs. 300 K Virgin	0.11

A.

BACKSCATTER BRDF at -7.5	STATUS OF MIRROR	FORWARDSCATTER BRDF at 7.5
1.64E-05	300 K - Virgin Surface	2.46E-05
2.12E-05	20 K - Virgin Surface	2.47E-05
MIRROR IRRADIATED WITH A FLUENCE LEVEL = 0.37 Cal/cm ²		
4.65E-05	20 K - Post Irradiation	1.01E-04
5.95E-05	300 K - Post Irradiation	6.75E-05
RESPONSE TO e-BEAM		
1.19	20 K Post vs. 20 K Virgin	3.09
2.63	300 K Post vs. 300 K Virgin	1.74

B.

BACKSCATTER BRDF at -7.5	STATUS OF MIRROR	FORWARDSCATTER BRDF at 7.5
4.29E-05	300 K - Virgin Surface	3.54E-05
5.99E-05	20 K - Virgin Surface	4.8E-05
MIRROR IRRADIATED WITH A FLUENCE LEVEL = 0.45 Cal/cm ²		
1.02E-04	20 K - Post Irradiation	6.37E-05
6.55E-05	300 K - Post Irradiation	4.77E-05
RESPONSE TO e-BEAM		
0.70	20 K Post vs. 20 K Virgin	0.33
0.53	300 K Post vs. 300 K Virgin	0.35

C.

BACKSCATTER BRDF at -7.5	STATUS OF MIRROR	FORWARDSCATTER BRDF at 7.5
3.5E-05	300 K - Virgin Surface	2.59E-05
4.04E-05	20 K - Virgin Surface	2.83E-05
MIRROR IRRADIATED WITH A FLUENCE LEVEL = 0.00 Cal/cm ²		
8.37E-05	20 K - Post Irradiation	5.88E-05
7.26E-05	300 K - Post Irradiation	5.16E-05
RESPONSE TO e-BEAM		
1.07	20 K Post vs. 20 K Virgin	1.08
1.07	300 K Post vs. 300 K Virgin	0.99

D.

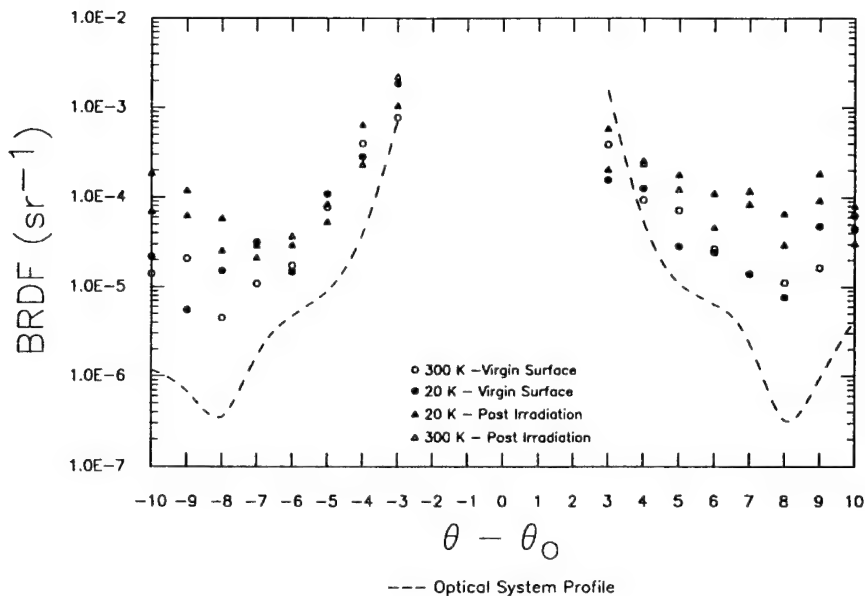


FIGURE 47. BRDF MEASUREMENTS ON MIRROR POCT 2V-A-67-A AT SITE B (0.37 cal/cm²).

Site C was irradiated by a still higher fluence of 0.45 cal/cm². Figure 48 presents the BRDF plots and response data is presented in Table 6. While the mirror remained cold, backscatter response was 0.70 while forward scatter response was 0.33. After warming the mirror to room temperature, there was an overall response of 0.53 on the backscatter side of specular and an overall response of 0.35 on the forward scatter side.

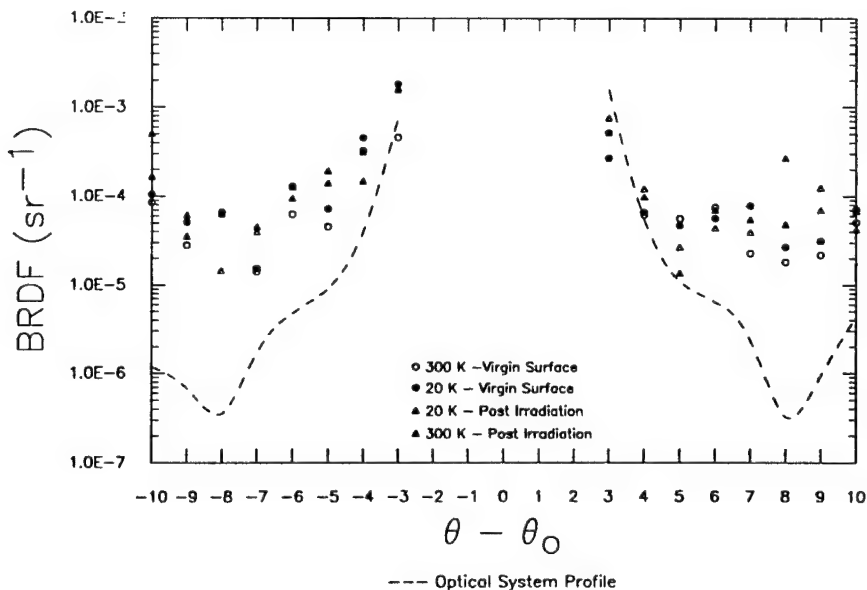


FIGURE 48. BRDF MEASUREMENTS ON MIRROR POCT 2V-A-67-A AT SITE C (0.45 cal/cm²).

Site D (center) was not irradiated but was measured at each stage of the experiment. Figure 49 shows BRDF plots measured at Site D and Table 6 presents response data. Cold response to indirect irradiation at the center of the mirror was 1.07 (backscatter) and 1.08 (forward scatter). Overall response was 1.07 (backscatter) and 0.99 (forward scatter). The center position of the mirror shows a minor increase in scatter on both sides of specular both while cold and overall. Neither forward scatter nor backscatter is favored in this case.

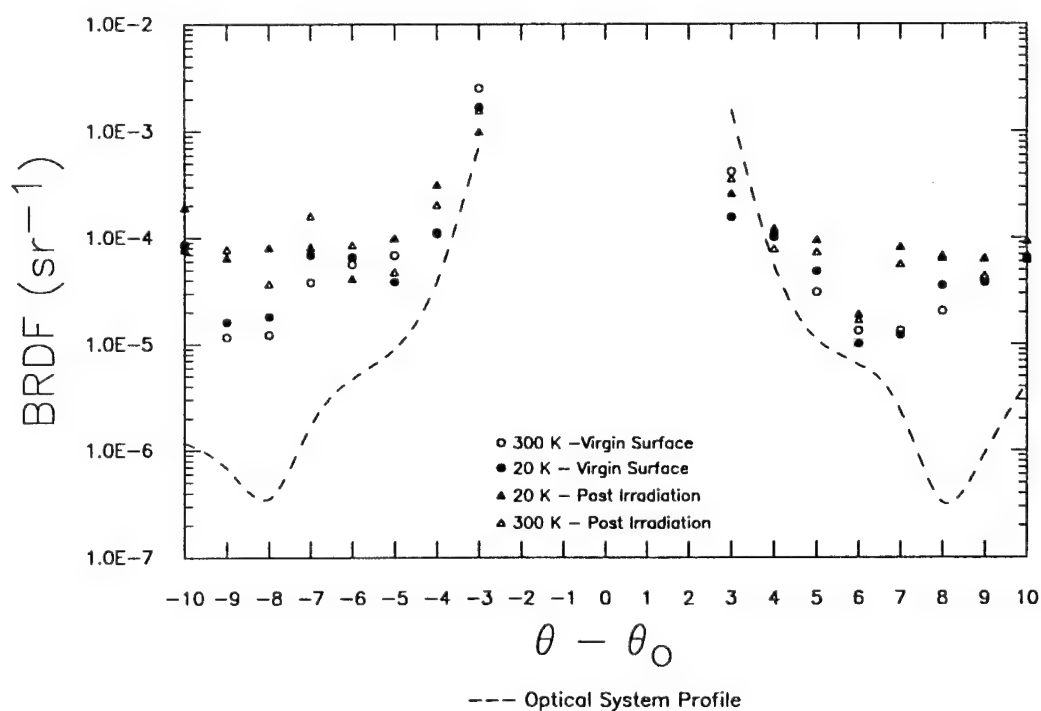


FIGURE 49. BRDF MEASUREMENTS ON MIRROR POCT 2V-A-67-A AT SITE D (central position, no direct irradiation).

After the test was completed, the mirror was removed from the test chamber and Nomarski photomicrographs were taken of two test sites. These photomicrographs are presented along side the virgin surface photomicrographs in Figures 50 through 53. The observed physical change in the surface of the mirror appears to be proportional to the fluence levels used to irradiate it. The center position (Site D) shows some damage in the photomicrographs.

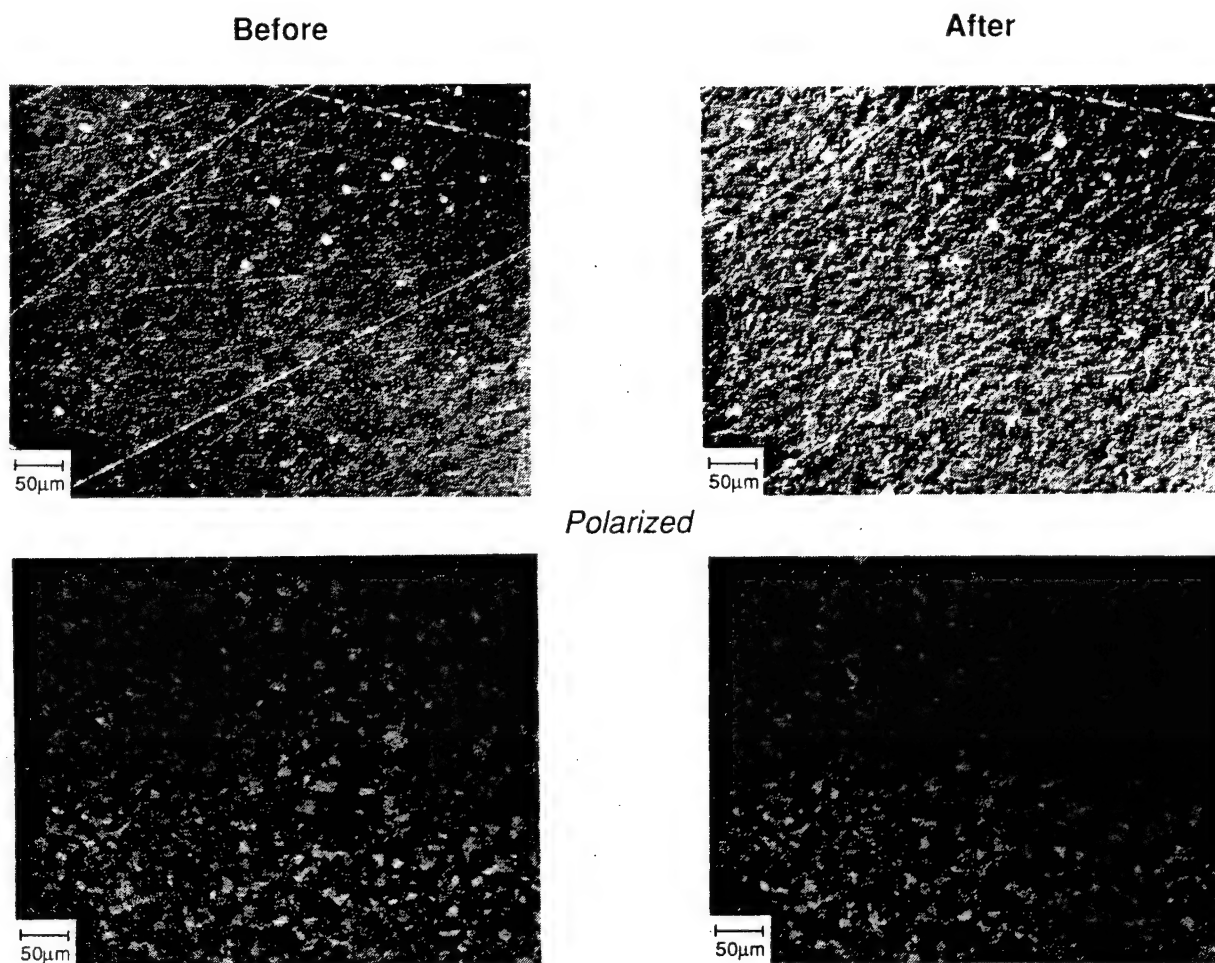


FIGURE 50. NOMARSKI PHOTOMICROGRAPHS OF MIRROR POCT 2V-A-67-A AT SITE A (0.27 cal/cm^2).

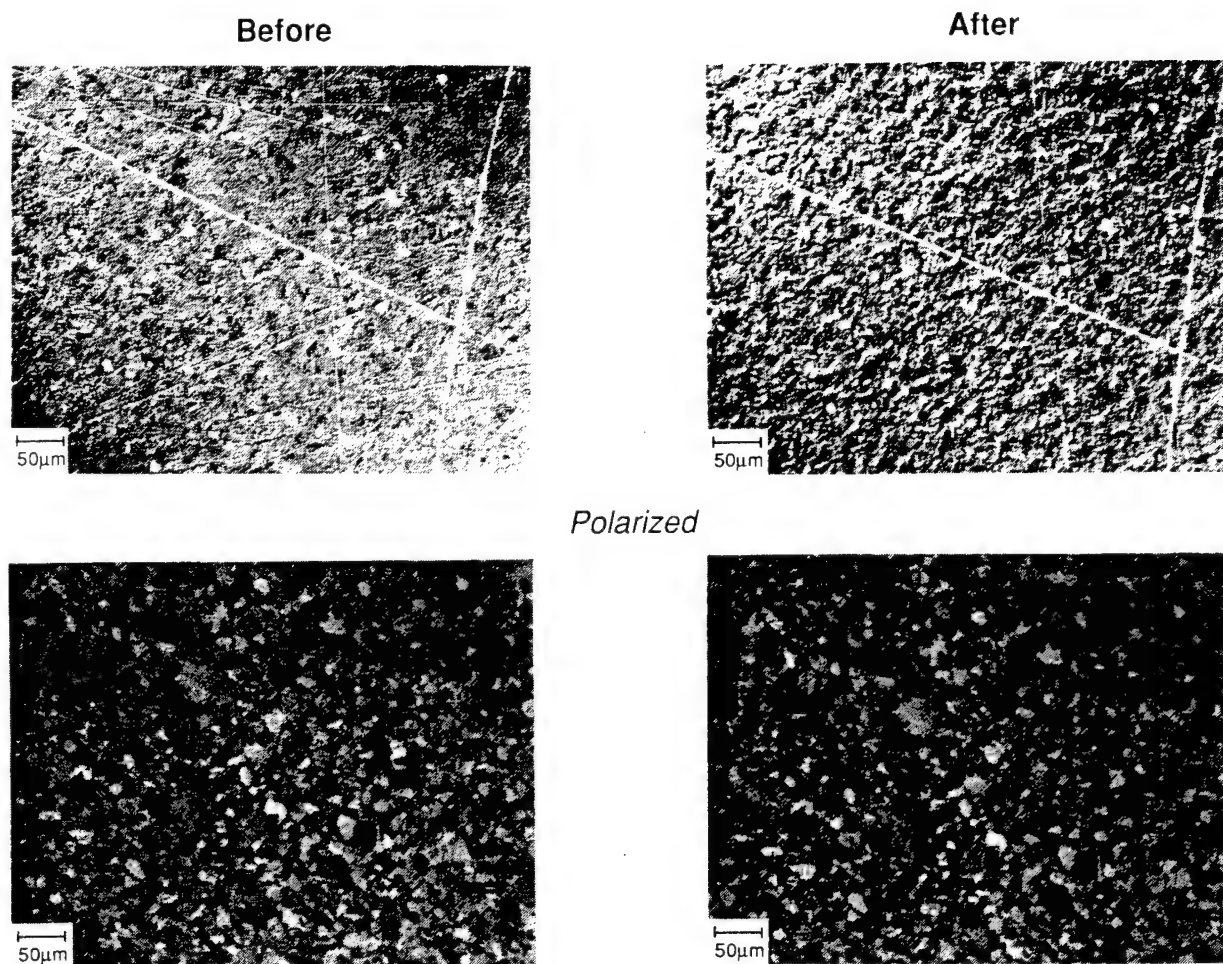


FIGURE 51. NOMARSKI PHOTOMICROGRAPHS OF MIRROR POCT 2V-A-67-A AT SITE B (0.33 cal/cm²).

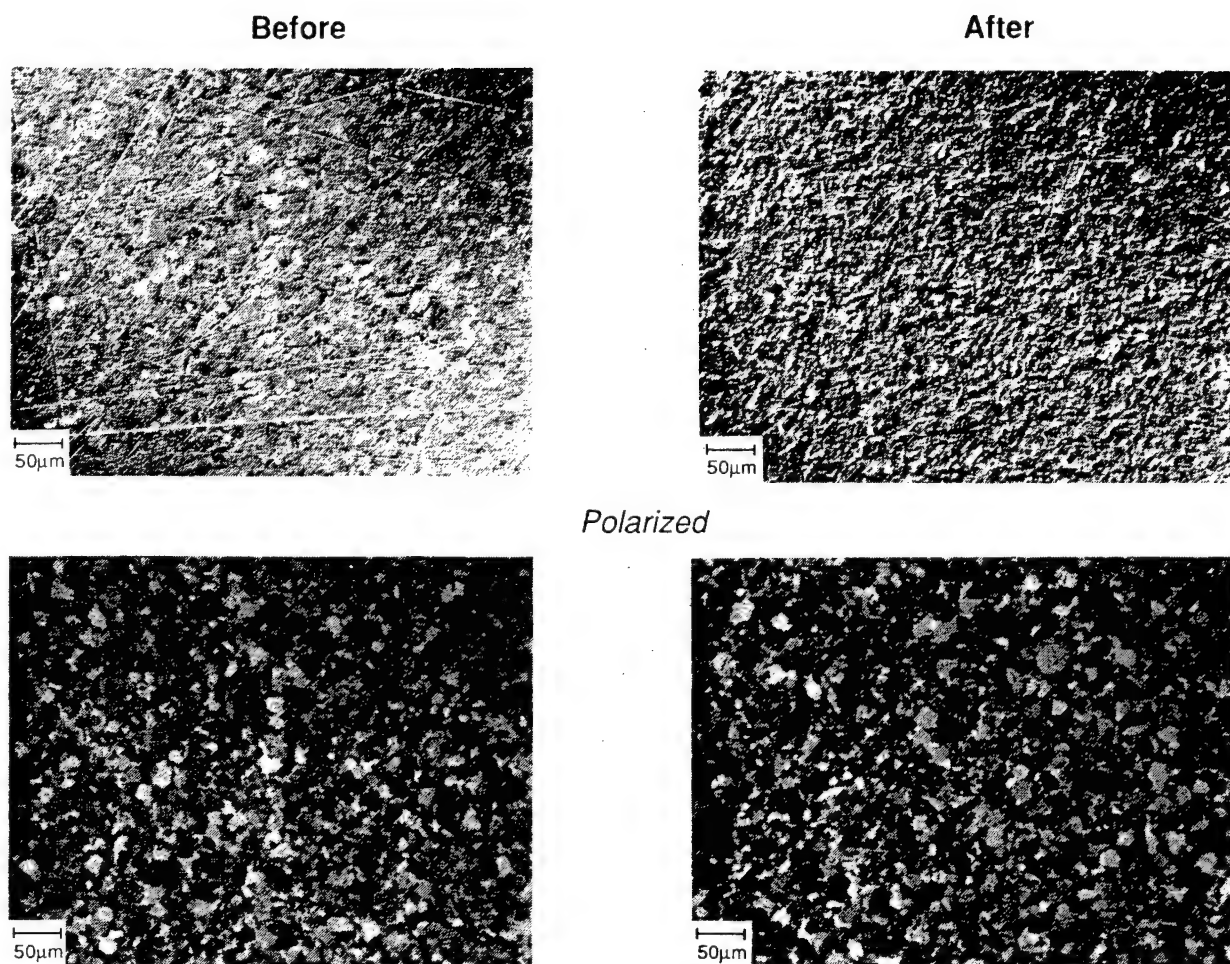
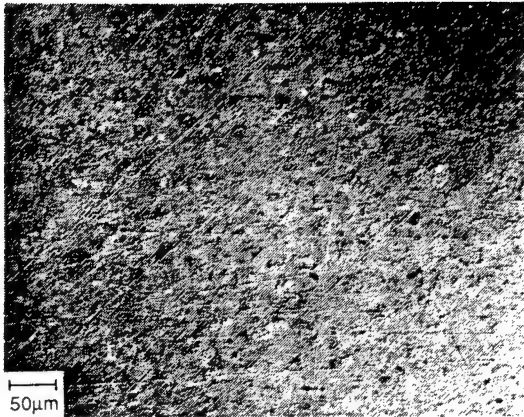
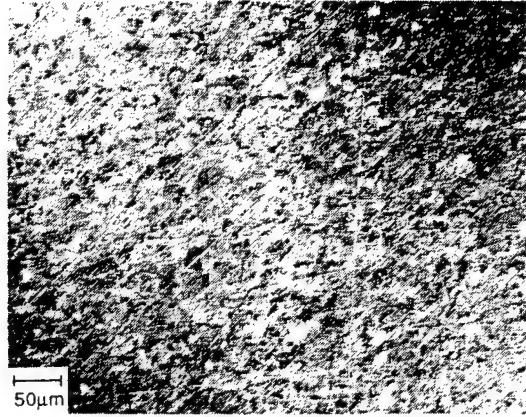


FIGURE 52. NOMARSKI PHOTOMICROGRAPHS OF MIRROR POCT 2V-A-67-A AT SITE C (0.45 cal/cm^2).

Before



After



Polarized

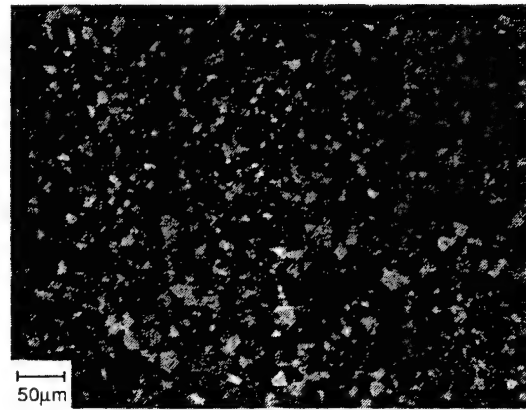
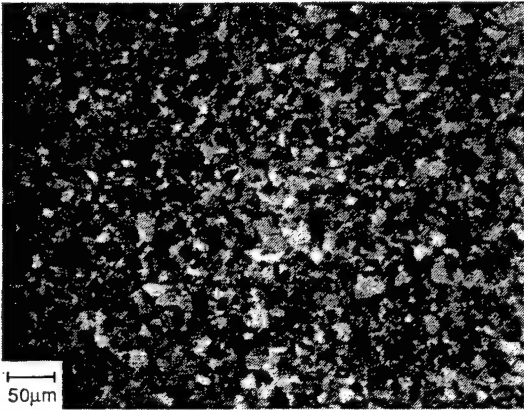


FIGURE 53. NOMARSKI PHOTOMICROGRAPHS OF MIRROR POCT 2V-A-67-A AT SITE D (mirror center, no direct irradiation).

3.7.1.5 POCT 56-W1-M1-2: Two-inch Diameter Be Mirror

POCT 56-W1-M1-1 was tested at four sites (A, B, C, and D) as described above for two-inch diameter mirrors. Visual observation of this mirror prior to testing showed no unusual characteristics or defects in or around the test sites. The mirror was cleaned according to standard procedure and photographed prior to installation into the CRYOSCAT facility. The photomicrographs of the virgin surface are presented later along with the photomicrographs of the post irradiation surface for comparison.

BRDF measurements were performed at the four sites while the virgin sample was at room temperature. The mirror was then cooled to 20 K and BRDF measurements were taken again at this temperature. While still cold, three of the four sites were irradiated by pulsed e-beam. On this particular test, the e-beam was not perfectly aligned with the mirror and the actual irradiation sites were approximately 3 mm below target. The size of the e-beam footprint is about 5 mm in diameter. BRDF measurements were taken at both the target sites and the actual irradiation sites and produced nearly the same results.

Site A received a fluence of 0.27 cal/cm^2 , Site B received a fluence of 0.37 cal/cm^2 , and Site C received a fluence of 0.45 cal/cm^2 . Site D (center) was not irradiated. BRDF measurements were repeated immediately following irradiation while the mirror was still cold. This measurement (20 K-post irradiation) was compared to the BRDF measurement taken immediately prior to irradiation (20 K-virgin surface) to calculate the radiation response of the mirror at each fluence level. Finally, the mirror was warmed to room temperature and BRDF measurements were repeated. This measurement (300 K-post irradiation) was compared to the original BRDF measurement (300 K-virgin surface) to calculate the overall response of the mirror to the e-beam irradiation and thermal cycling. All BRDF measurements were made as described earlier. The raw data of each scan was used to produce BRDF plots. A first order regression of the data between $\pm 5^\circ$ and 10° was used to determine the BRDF value at 7.5° from specular.

Figure 54 shows the BRDF plots for Site A at each of the four measurements stages of the experiment for both sides of specular. The vertical lines at $\pm 7.5^\circ$ represents the point at which the BRDD comparison was done. The value of the BRDF plots at this angle are tabulated in Table 7. The response to e-beam values are evaluated at $\pm 7.5^\circ$ and are calculated as before.

The mirror's response to 0.27 cal/cm^2 , while cold, was measured to be 0.01 (backscatter) and 0.06 (forward scatter). The overall response of the mirror due to 0.27 cal/cm^2 and thermal cycling was measured to be 0.12 (backscatter) and -0.11 (forward scatter). The response due to e-beam irradiation alone and the overall response produced negligible change scatter for both directions. These small numbers (± 0.30) are considered to be within the reproducibility of the system and are considered to represent no measurable change.

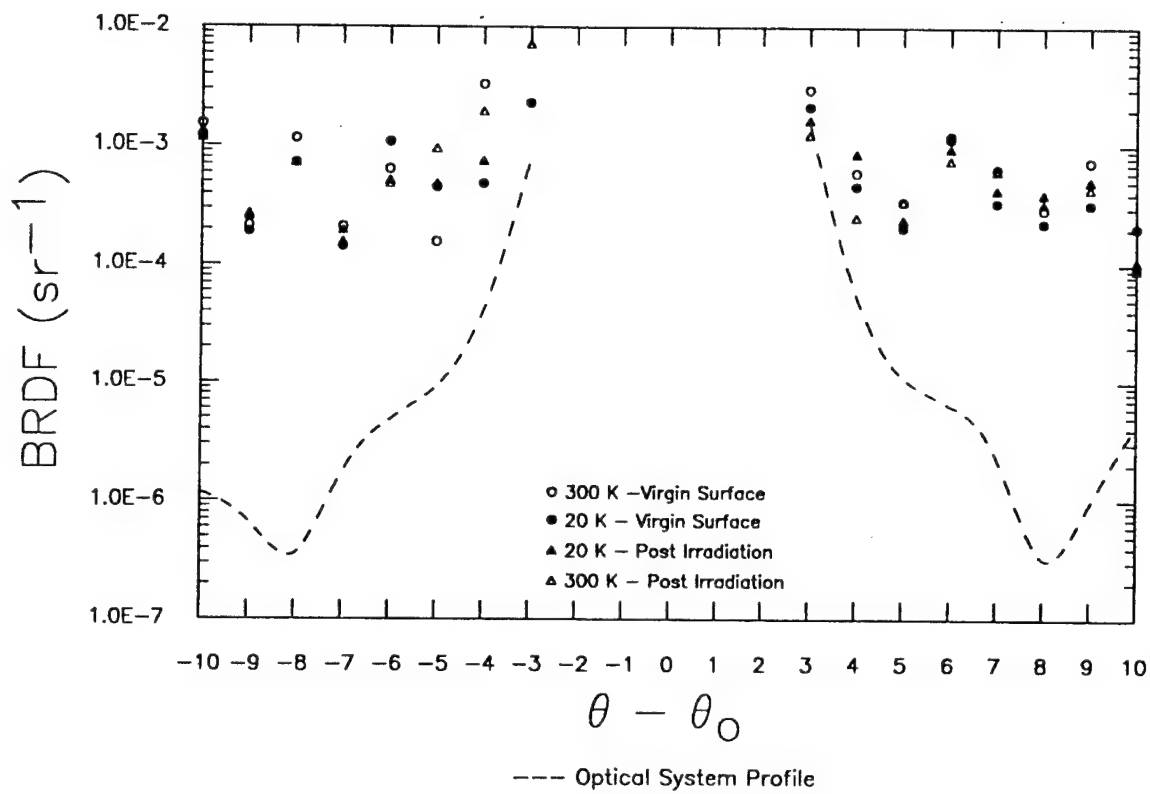


FIGURE 54. BRDF MEASUREMENTS ON MIRROR POCT 56-W1-M1-2 AT SITE A (0.27 cal/cm²).

TABLE 7. BRDF DATA AT $\pm 7.5^\circ$ FOR MIRROR POCT 56-W1-M1-2.

BACKSCATTER BRDF at -7.5	STATUS OF MIRROR	FORWARDSCATTER BRDF at 7.5
4.46E-04	300 K - Virgin Surface	4.14E-04
4.74E-04	20 K - Virgin Surface	3.3E-04
MIRROR IRRADIATED WITH A FLUENCE LEVEL = 0.27 Cal/cm ²		
4.81E-04	20 K - Post Irradiation	3.49E-04
4.99E-04	300 K - Post Irradiation	3.7E-04
RESPONSE TO e-BEAM		
0.01	20 K Post vs. 20 K Virgin	0.06
0.12	300 K Post vs. 300 K Virgin	-0.11

A.

BACKSCATTER BRDF at -7.5	STATUS OF MIRROR	FORWARDSCATTER BRDF at 7.5
8.31E-05	300 K - Virgin Surface	1.1E-04
1.29E-04	20 K - Virgin Surface	9.86E-05
MIRROR IRRADIATED WITH A FLUENCE LEVEL = 0.37 Cal/cm ²		
1.76E-04	20 K - Post Irradiation	2.11E-04
1.2E-04	300 K - Post Irradiation	1.37E-04
RESPONSE TO e-BEAM		
0.36	20 K Post vs. 20 K Virgin	1.14
0.44	300 K Post vs. 300 K Virgin	0.25

B.

BACKSCATTER BRDF at -7.5	STATUS OF MIRROR	FORWARDSCATTER BRDF at 7.5
9.9E-05	300 K - Virgin Surface	6.31E-05
1.13E-04	20 K - Virgin Surface	9.11E-05
MIRROR IRRADIATED WITH A FLUENCE LEVEL = 0.45 Cal/cm ²		
5.2E-04	20 K - Post Irradiation	2.45E-04
3.41E-04	300 K - Post Irradiation	1.35E-04
RESPONSE TO e-BEAM		
3.60	20 K Post vs. 20 K Virgin	1.69
2.44	300 K Post vs. 300 K Virgin	1.14

C.

BACKSCATTER BRDF at -7.5	STATUS OF MIRROR	FORWARDSCATTER BRDF at 7.5
7.19E-05	300 K - Virgin Surface	1.28E-04
1.8E-04	20 K - Virgin Surface	1.04E-04
MIRROR IRRADIATED WITH A FLUENCE LEVEL = 0.00 Cal/cm ²		
1.76E-04	20 K - Post Irradiation	1.67E-04
1.93E-04	300 K - Post Irradiation	1.52E-04
RESPONSE TO e-BEAM		
-0.02	20 K Post vs. 20 K Virgin	0.61
1.68	300 K Post vs. 300 K Virgin	0.19

D.

Site B was irradiated by a higher fluence of 0.37 cal/cm^2 . Figure 55 presents the BRDF plots and response data is presented in Table 7. This fluence produced noticeably higher response in the forward scatter direction while the mirror remained cold. Cold backscatter response was 0.36 while forward scatter response was 1.14. After warming the mirror to room temperature, there was an overall response of 0.44 on the backscatter side of specular and an overall response of 0.25 on the forward scatter side.

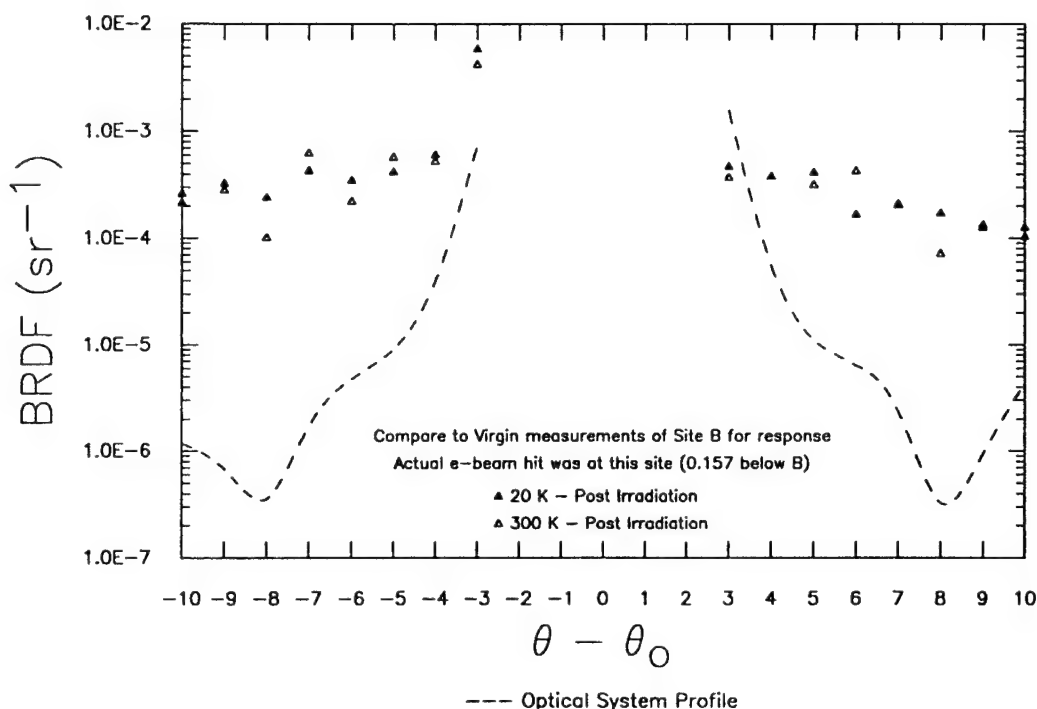


FIGURE 55. BRDF MEASUREMENTS ON MIRROR POCT 56-W1-M1-2 AT SITE B (0.37 cal/cm^2).

Site C was irradiated by a higher fluence of 0.45 cal/cm^2 . Figure 56 shows BRDF plots and response data is presented in Table 7. While the mirror remained cold, backscatter response was 3.60 and forward scatter response was 1.69. After warming the mirror to room temperature, there was an overall response of 2.44 on the backscatter side of specular and an overall response of 1.14 on the forward scatter side.

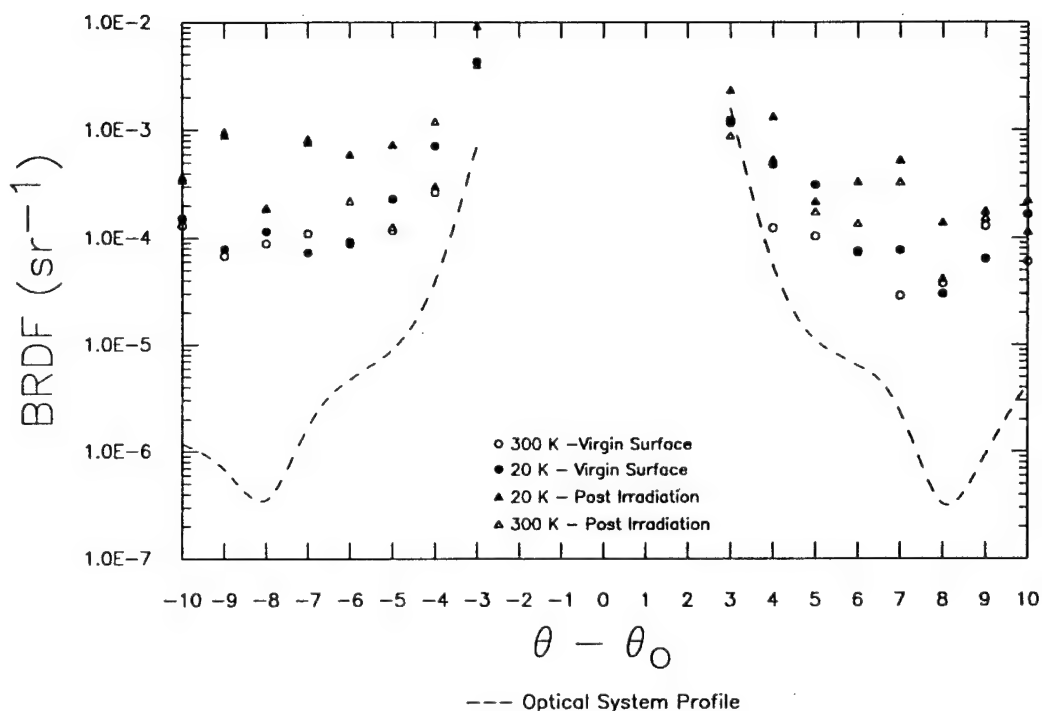


FIGURE 56. BRDF MEASUREMENTS ON MIRROR POCT 56-W1-M1-2 AT SITE C (0.45 cal/cm²).

Site D (center) was not irradiated but was measured at each stage of the experiment. The close proximity of Site D to the other three sites means that there will be residual effects observed as a result of the irradiation of those sites. Figure 57 shows the BRDF plots measured at Site D and Table 7 presents response data. Cold response to the indirect irradiation of the center of the mirror was -0.02 (backscatter) and 0.61 (forward scatter). Overall response was 1.68 (backscatter) and 0.19 (forward scatter). The center position of the mirror showed negligible change in scatter on both sides of specular both while cold and overall for forward scatter. Overall backscatter increased by a notable amount. The damage affecting scatter at this site is the result of three irradiations within close proximity of the site, rather than direct e-beam irradiation.

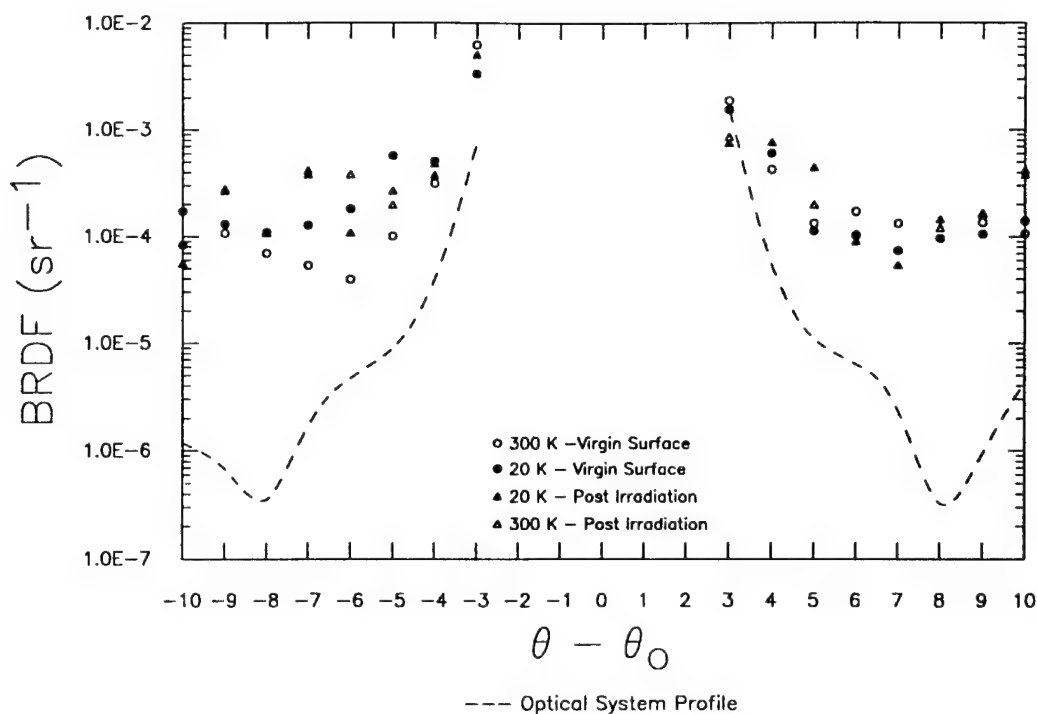


FIGURE 57. BRDF MEASUREMENTS ON MIRROR POCT 56-W1-M1-2 AT SITE D (center of mirror, no direct irradiation).

After the test was completed, the mirror was removed from the test chamber and Nomarski photomicrographs were taken of all test sites. These photomicrographs are presented alongside the virgin surface photomicrographs in Figures 58 through 61. The observed physical change in the surface of the mirror appears to be roughly proportional to the fluence levels for Sites A and B. Site C response appears about the same, if not less than Site B. The center position (Site D) shows little or no visible damage in the photomicrographs.

3.7.2 Summary and Discussion of Results

For the first time, beryllium mirrors have been measured for BRDF on both sides of specular at four locations at each stage of a single thermal cycle. The five mirrors discussed above represent the first complete data set on mirror response to e-beam irradiation. Each mirror's behavior was somewhat different from that of other mirrors, but some interesting trends were observed.

There tended to be a marked difference between backscatter and forward scatter response; backscatter response was usually greater than forward scatter. Also, scatter increased with e-beam fluence to a certain level and then decreased at the highest fluence levels on some mirrors.

The results of cool-down and warm-up were not tabulated, but all except two were in the ± 0.50 range in which ($\Delta\text{BRDF}/\text{BRDF}$) is considered to be within system repeatability. It should be noted that these tests were done without the benefit of the 10-inch vacuum pump. The lower pressure expected with the larger pump should further reduce cryogenic contamination effects.

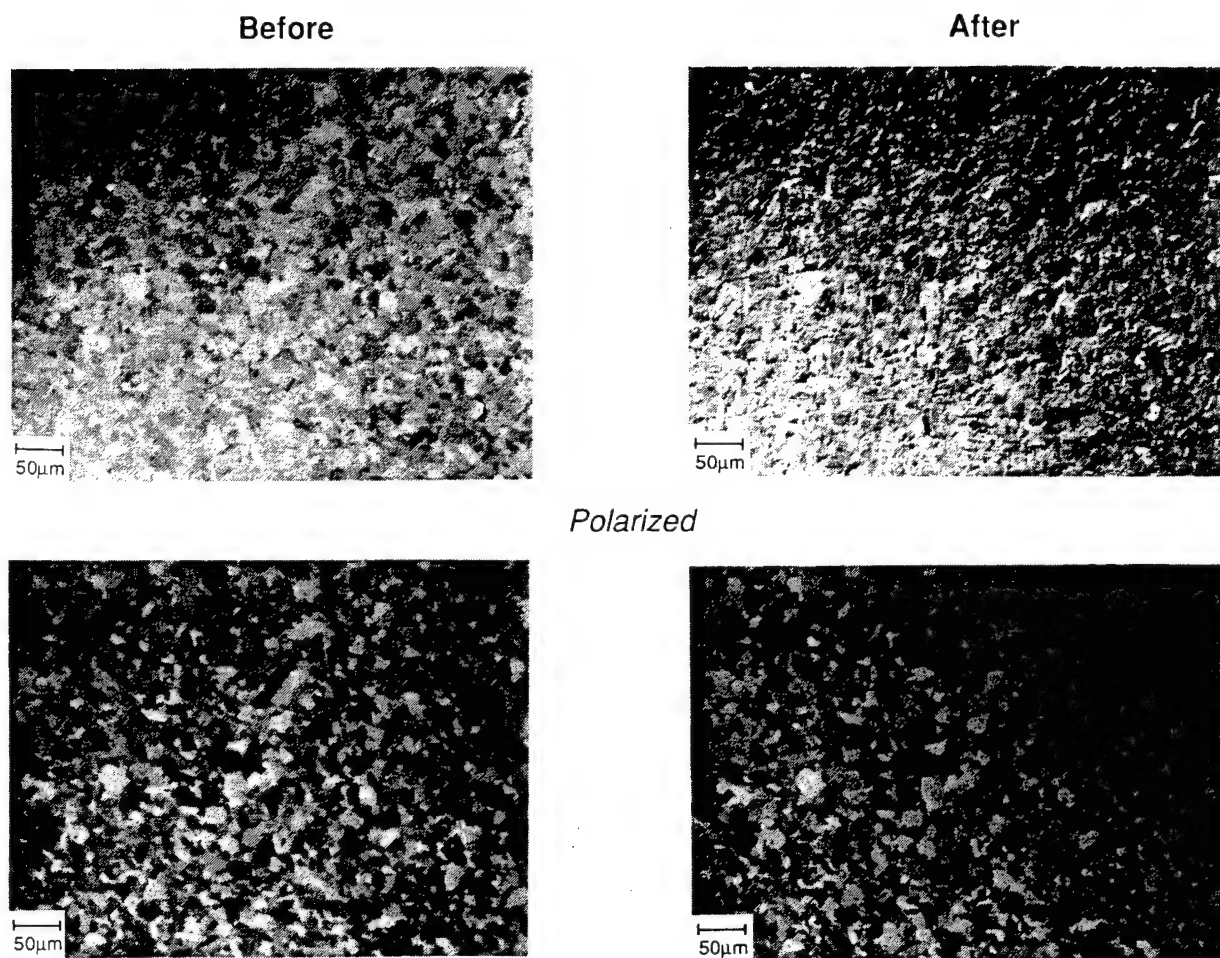


FIGURE 58. NOMARSKI PHOTOMICROGRAPHS OF MIRROR POCT 2V-A-67-A AT SITE A (0.27 cal/cm^2).

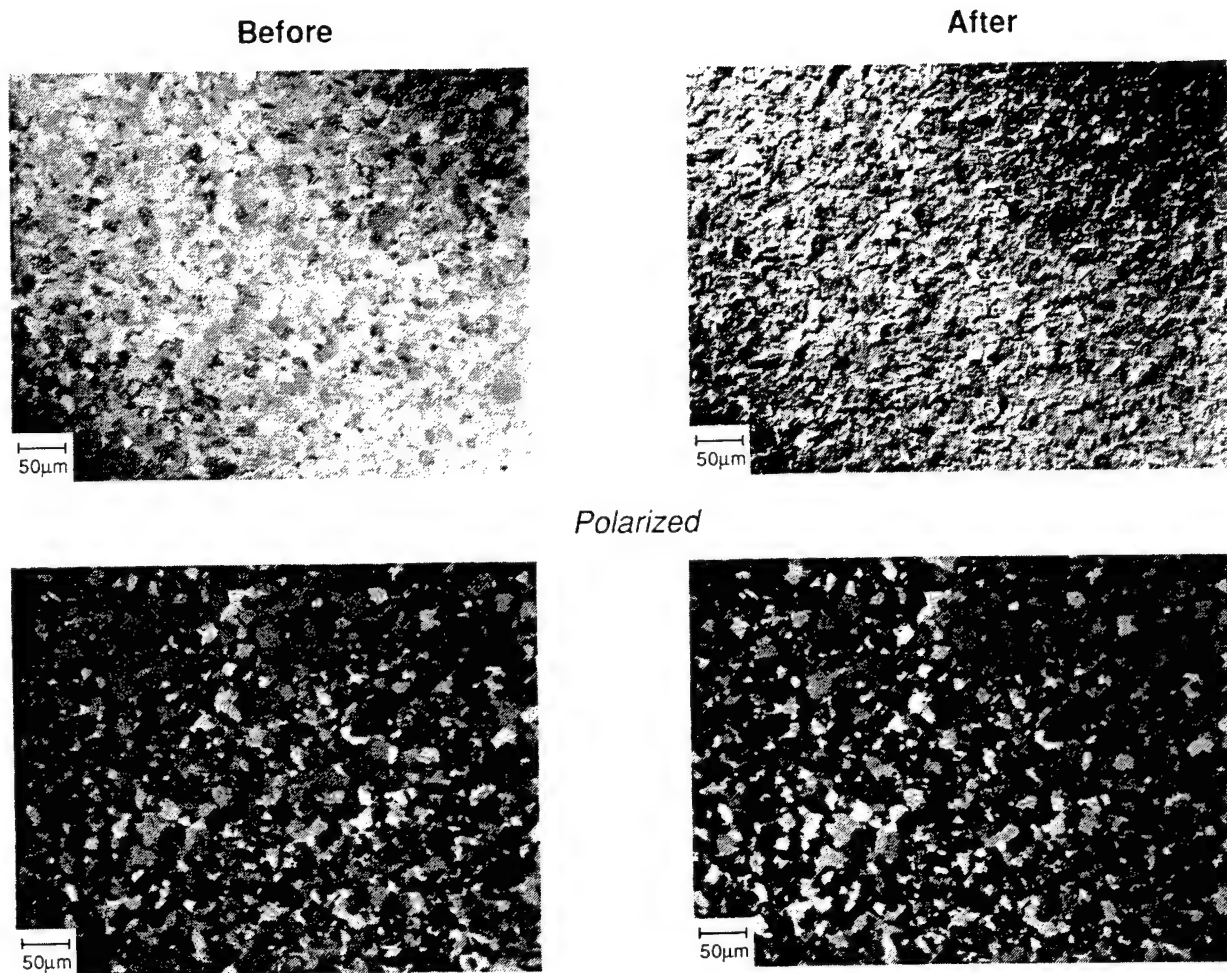


FIGURE 59. NOMARSKI PHOTOMICROGRAPHS OF MIRROR POCT 2V-A-67-A AT SITE B (0.37 cal/cm^2).

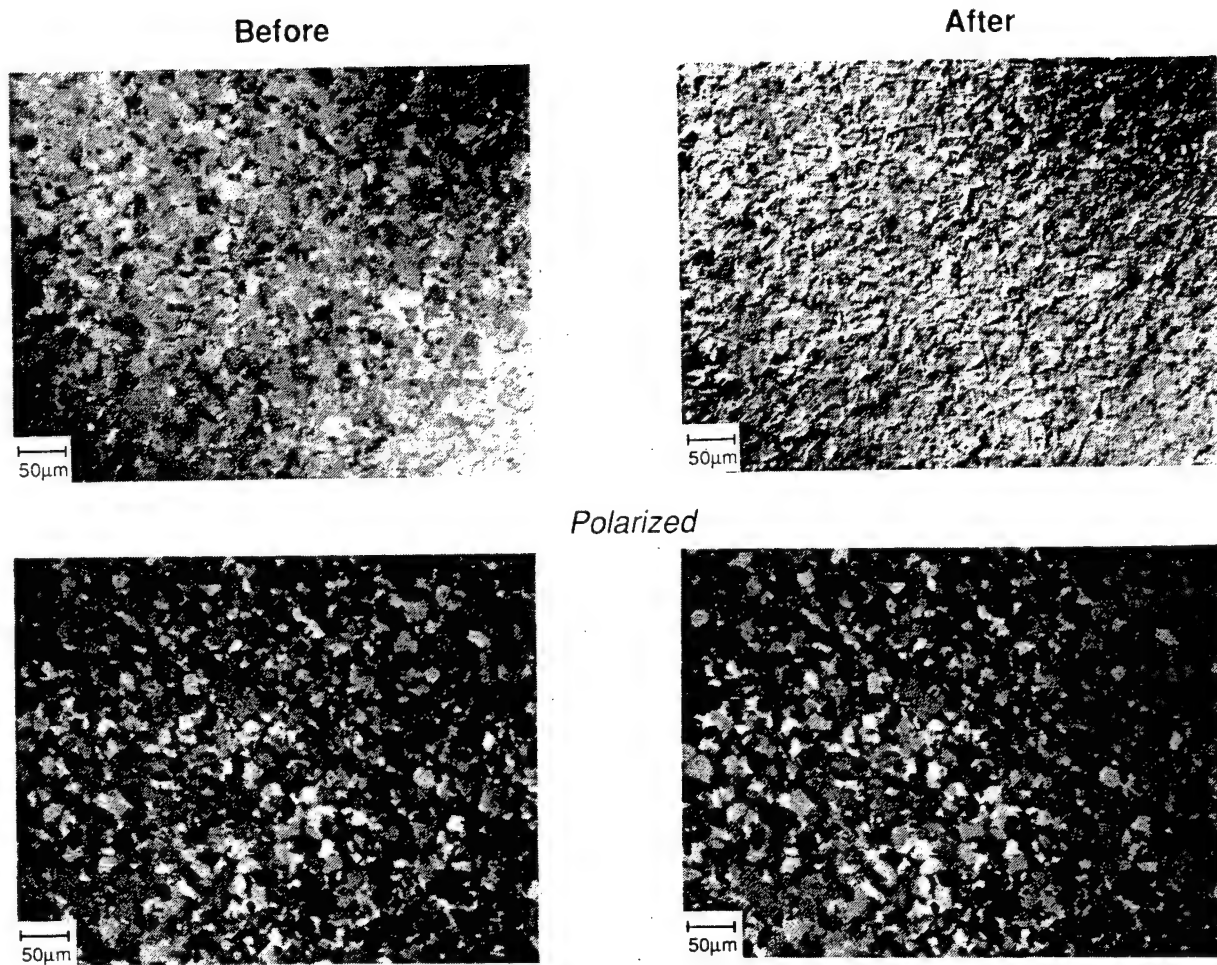


FIGURE 60. NOMARSKI PHOTOMICROGRAPHS OF MIRROR POCT 2V-A-67-A AT SITE C (0.45 cal/cm^2).

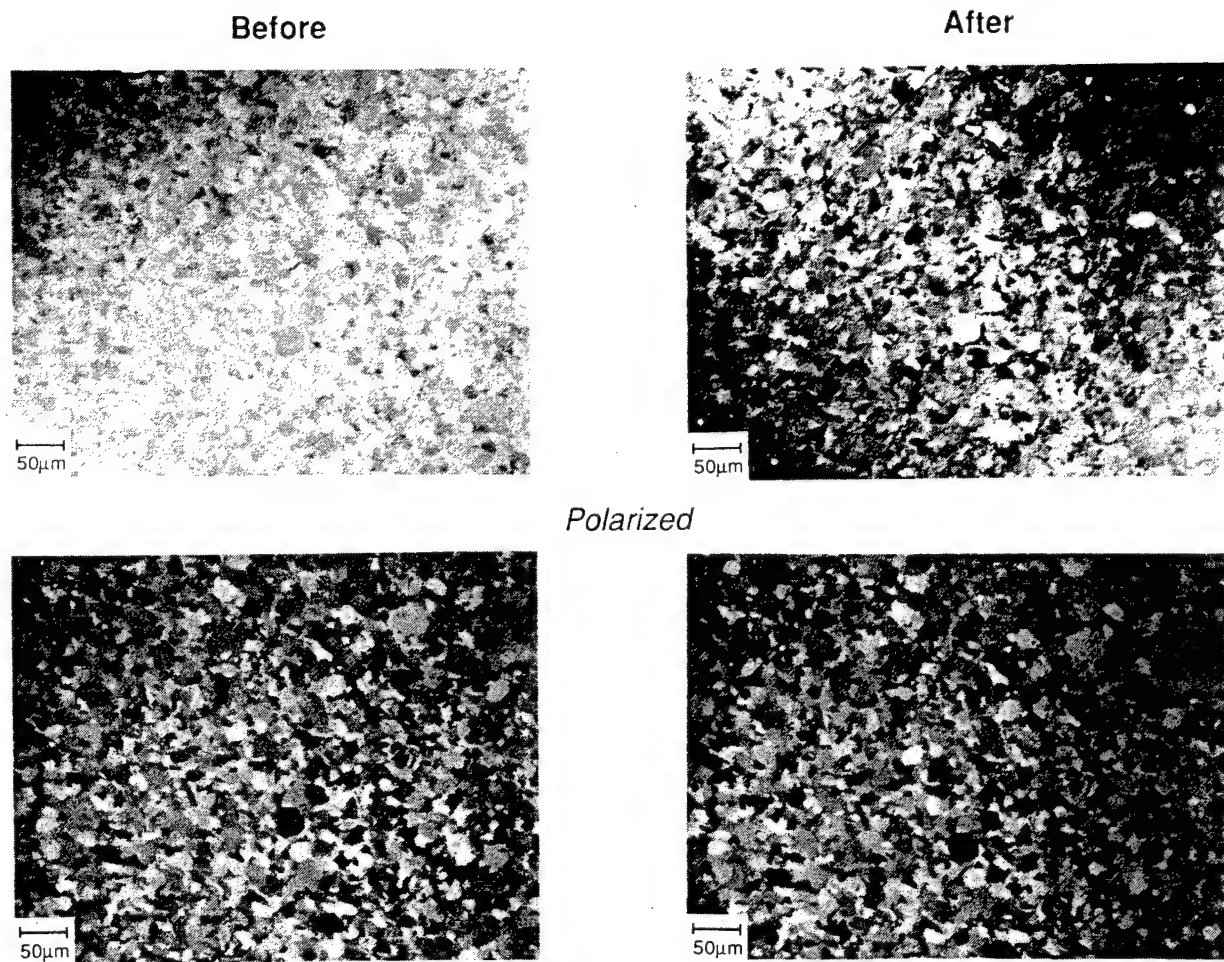


FIGURE 61. NOMARSKI PHOTOMICROGRAPHS OF MIRROR POCT 2V-A-67-A AT SITE D (center of mirror, no direct irradiation).

3.8 1 October 1990 Through 30 November 1990

- New systems installed: vacuum, vibration isolation, interferometry, and cryo-deposits
- First annual technical review meeting

3.8.1 New Systems

The final months of Year 1 were devoted to installation of new and modified systems. Designing and planning for these tasks began several months previously and were completed on schedule. A major reason for the relatively quick retrofit was the modular design of the facility which was incorporated early in the contract period. Figure 62 shows the modularity of all major sections of the apparatus, which are free-standing and independent of each other. This simplifies service and maintenance and also allows for easy modification/addition of subsystems without affecting other systems.

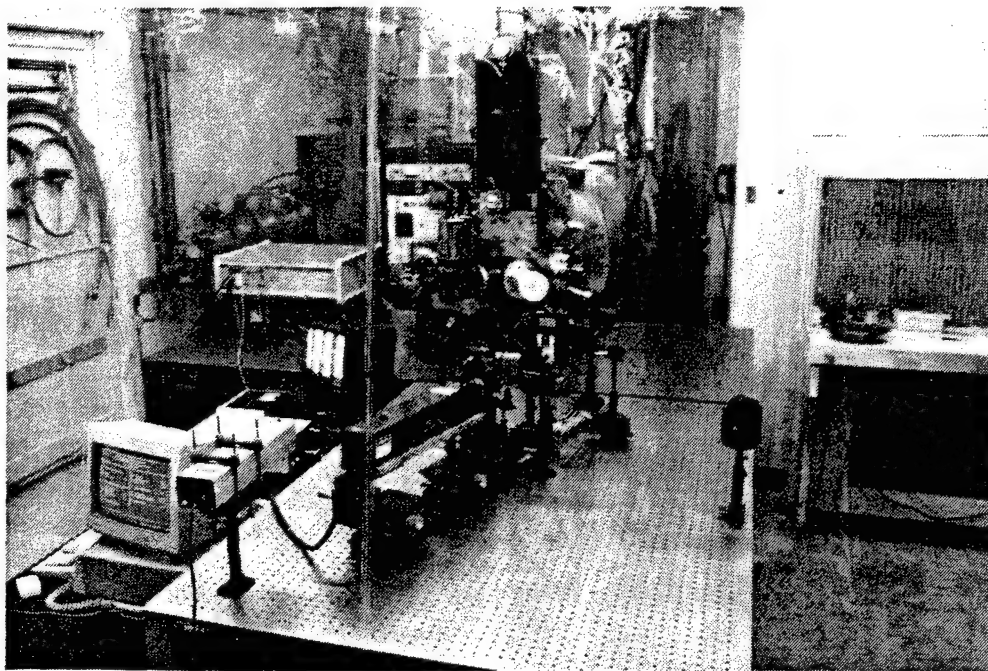


FIGURE 62. NEW SYSTEM COMPONENTS.

The first system installed was the 10-inch cryopump/gate valve vacuum system. This system was attached to the vacuum chamber without disassembling the manipulator system. Once connected, vacuum integrity was checked and the entire vacuum chamber superstructure was reconnected to the SPI-PULSE™ 5000.

The second stage of the refit involved the delivery and assembly of the optical table onto which the scatterometer, interferometer, and cryo-deposit deposition/monitoring systems are mounted. Aside from requiring more table space for the additional systems, a major consideration in the design of the optical table was providing a large mass for vibration damping.

After the table was assembled and in place, the interferometer and scatterometer systems were assembled onto it. All systems are now functional but require final fine-tuning and alignment before mirror tests can resume. Initial tests on the interferometer systems went well. The vacuum window in front of the internally mounted reference flat required an anti-reflection coating as it produced significant interference in the interferometer.

3.8.2 Technical Review Meeting

On October 23, 1990, Spire hosted the first annual contract technical review meeting. The status of the program and the overall program objectives are reviewed and discussed. The meeting lasted one full day and covered all technical activities since the contract's beginning. All major milestones have been reached on schedule and 5 Be mirrors have been tested. The meeting was held one month ahead of the original schedule and all tasks were pushed up and completed in time for the meeting, essentially putting the entire program one month ahead of schedule.

4. STATUS OF PROGRAM MILESTONES

There are a total of nine specific milestones to be reached during the performance of this contract.

- Milestone 1: **Submit Program Plan - REACHED**
- Milestone 2: **Technical "Kickoff" Meeting - REACHED**
- Milestone 3: **Begin e-Beam Testing - REACHED**
- Milestone 4: **Interferometer/Cryolayer System Installed - Installation complete - qualification delayed**
- Milestone 5: **Begin Cryolayer Testing - Full-scale testing of two-inch diameter mirrors will commence 30 to 60 days after completion of Milestone 4**
- Milestone 6: **Begin seven-inch Mirror Testing - Full-scale testing of seven-inch diameter mirrors will commence 30 to 60 days after completion of Milestone 4**
- Milestone 7: **AGT Mirror Set Complete - To be scheduled by program management**

Milestone 8: **Mirror Testing Completed** - Completion of all test scheduled for month 35 of contract (21 October 1992)

Milestone 9: **Final Report Submitted** - Schedule for submission on 21 November 1992

5.0 INVENTORY OF MIRRORS AT SPIRE

Appendix B lists all mirrors in stock at Spire Corporation as of the writing of 30 November 1990.

APPENDIX A
DRAFT PROCEDURAL CHECKLISTS

AU-REFERENCE CALIBRATION

DATE: _____

OPERATOR: _____

CHECKED BY: _____

- ____ 1. System must be set to specular by a mirror
- ____ 2. Mirror used thickness _____
 Au-Reference and mount thickness _____
 Difference (Au+Mount - Mirror) _____
- ____ 3. Translate X by above amount
- ____ 4. Set Home
- ____ 5. Remove mirror and install Au-Reference
- ____ 6. Send Home
- ____ 7. Scan from 20 to 40 degrees by 0.5 degree increments
- ____ 8. Average all points: _____
 Should be 3.0×10^{-1}

- ____ 9. Calculate new Calibration Constant
 Old Calibration Constant = _____ = OC
 Average of data take today = _____ = A
 Theoretical BRDF = 3.0×10^{-1}
 New Calibration Constant = CC = $OC(a/3.0 \times 10^{-1}) =$ _____

DAILY SET-UP PROCEDURE

DATE: _____
SAMPLE: _____
OPERATOR: _____
CHECKED BY: _____

- ____ 1. Line filter on
- ____ 2. Rough Pump on, 1st valve open
- ____ 3. Remove dust covers and attenuator wheel closed
- ____ 4. Laser power on, open shutter: note time _____
- ____ 5. Control panel on (if under vacuum): IG, RGA, Temp, Chart
- ____ 6. Disk technician computer
- ____ 7. Warning lights on
- ____ 8. Rough pump 2nd valve open when pressure < 5 microns
- ____ 9. Check supplies:
 - LHe _____ liters
 - He _____ pounds
 - Ar _____ pounds
 - LN₂ _____ tank
- ____ 10. E-Beam on if it is going to be used
- ____ 11. Indexers on (if not on already)
- ____ 12. Detector at 30 degrees and drive belt attached
- ____ 13. Battery power check + _____ Volts and - _____ Volts
If less than +, - 12 Volts, trickle charge
- ____ 14. Open Detector valve and pump at least 5 minutes _____
- ____ 15. HeNe back reflection O.K.
- ____ 16. Check Aperture sizes
 - Transmission
 - .65" ==> 60.7%
 - .60" ==> 59.0%
 - .55" ==> 51.8%
 - .50" ==> 45.8%
- ____ 17. Power meter aligned properly
- ____ 18. All equipment operating and connected
- ____ 19. Vac-Sorb pump: if was baking, unplug and insert stopper
if to be used today, fill with LN₂
if recently used start bakeout
- ____ 20. Check laser stability (after 30 min.) Power _____
- ____ 21. TEM₀₀ Mode operation
- ____ 22. Chopper stable at 41 Hz
- ____ 23. Top off Detector
- ____ 24. File Disk Technician Reports

DAILY SHUT-DOWN PROCEDURE

DATE: _____

SAMPLE: _____

OPERATOR: _____

CHECKED BY: _____

- _____ 1. Attenuator wheel closed
- _____ 2. Laser off, shutter closed
- _____ 3. Power off detector, disconnect
- _____ 4. Dust covers on
- _____ 5. Mirror in safe position
- _____ 6. Indexer #5 off (all if testing is complete)
- _____ 7. Controls off: IG, RGA, Temp, Chart
- _____ 8. Back-up files to floppy
- _____ 9. Back-up hard disk to tape
- _____ 10. Warning lights out
- _____ 11. Tally up bellows motions
- _____ 12. Bake Vac-Sorb pump if used today
- _____ 13. Line filter off when computer is finished
- _____ 14. Lock-up, lights-out

OVERALL TESTING SCHEDULE

DATE: _____

SAMPLE: _____

OPERATOR: _____

CHECKED BY: _____

____ 1. Cleaning:

- DI water rinse
- Triton-X soap wash
- Triton-X soap swab
- Long DI water rinse
- Isopropyl Alcohol rinse
- Dry under glass
- Visually examine surface with halogen lamp
 - if clean, continue
 - if filmy or otherwise dirty, repeat alcohol rinse

____ 2. Photomicroscopy:

- A: _____x50 _____x200
B: _____x50 _____x200
C: _____x50 _____x200
D: _____x50 _____x200

____ 3. Profilometry (WYKO)

Shipped _____
Returned _____

____ 4. FASCAT:

- ____ Infrared at A, B, C and D
____ Visible at A, B, C and D

____ 5. Reclean as necessary

____ 6. Install into CRYOSCAT

____ 7. Calibration Constant from last calibration run _____

____ 8. Room Temperature Virgin BRDF

____ 9. Bake Out

____ 10. Cold Run

____ 11. Warm up

____ 12. Room Temperature Virgin #2 Brdf

____ 13. Cold Run with e-Beam irradiations

____ 14. Warm up

____ 15. Room Temperature post irradiation BRDF

____ 16. Vent chamber and remove sample

____ 17. Au-Reference Calibration: new constant _____

____18. FASCAT

____ Infrared at A, B, C and D

____ Visible at A, B, C and D

____19. Photomicroscopy

A: ____x50 ____x200

B: ____x50 ____x200

C: ____x50 ____x200

D: ____x50 ____x200

____20. Profilometry (if necessary)

Shipped _____

Returned _____

____21. Data Collection and documentation

SAMPLE INSTALLATION/PUMP-DOWN

DATE: _____

SAMPLE: _____

OPERATOR: _____

CHECKED BY: _____

SEE OVERALL MIRROR TEST CHECKLIST BEFORE PROCEEDING

- ____ 1. Sample Diameter: _____
Mount's inner diameter: _____
difference: _____
- ____ 2. Cold finger facing port. If chamber is under vacuum,
vent with argon and open after relief valve opens
- ____ 3. Insert marked I.I. Si wafer in mount and secure
- ____ 4. "A" fiducial mark on the mirror is lined up with the closed
hole in the mounting ring and is held in place by
tightening the set-screw.
- ____ 5. Mirror is flush with mounting ring surface. If not, repeat
- ____ 6. Place assemble onto lower two bolts on mounting block
- ____ 7. Tighten all three until resistance is felt then back off
turn
- ____ 8. Slowly tighten each one with equally distributed torque.
- ____ 9. Rotate to HeNe to observe back-reflection:
If on normal plane, continue
If off normal plane, remove assembly and repeat 3 to 8
- ____ 10. Vent off
- ____ 11. Close port
- ____ 12. Rough to less than 1000 microns
- ____ 13. Vac-sorb to at least 50 microns
- ____ 14. High-vacuum on.

ALIGNMENT PROCEDURE

DATE: _____

SAMPLE: _____

OPERATOR: _____

CHECKED BY: _____

- ____ 1. Adjust tilt to bring HeNe back-reflection into plane
- ____ 2. Adjust rotation to retro-reflect HeNe
- ____ 3. Translate Z "-" until HeNe is on Bottom of mount ring
- ____ 4. Translate Y until vertical line is in center of HeNe
- ____ 5. Translate Z until HeNe is on inner edge of ring

Note Z = _____ mm.

Translate Z "+" until HeNe is on opposite inner edge

Note Z = _____ mm.

Add the absolute value of these and divide by 2, then
translate Z this distance in the "-" direction

- ____ 6. Set Home
- ____ 7. Translate X "+" and "-" until signal is found, then zero
in on this signal until peak is found.
- ____ 8. Adjust detector height until peaked
- ____ 9. Adjust detector rotation until peaked
- ____ 10. Repeat 7 to 10 until satisfied
- ____ 11. Set Home
- ____ 12. Move to center of Si wafer: note Y = _____

Z = _____

Return Home and re-do note Y = _____

Z = _____

Averages Y = _____

Z = _____

Use these for e-beam alignment

ROOM TEMPERATURE RUN

DATE: _____

SAMPLE: _____

OPERATOR: _____

CHECKED BY: _____

- _____ 1. Before continuing, use checklist for start-up and alignment
- _____ 2. Pressure readings: IG _____ torr
RGA _____ mb
- _____ 3. Temperature reading: _____ °K
- _____ 4. RGA scan, slow scan, chart at 1cm/min
- _____ 5. Visual inspection with Halogen lamp: Comments;

- _____ 6. Scan as required:

When changing sample positions:

- _____ SLOSTEP to new position
 - _____ Detector at 30°
 - _____ Visually check HeNe position
 - _____ Adjust X-motion at 100 steps to peak signal
 - _____ Adjust height of detector to peak signal
 - _____ Adjust rotation of detector to peak signal
 - _____ Repeat until satisfied
- _____ 7. At end of measurements return to home position
- _____ 8. List drive: \Directory\Subdirectory for files: _____

Filename: 1 2 3 4 5 6 7 8 . 9 10 11

A B C D E F

A = sample name code

B = sample position

C = final angle of scan

D = sample temperature

E = sample status (virgin or post)

F = scan number for this situation

<hr/>	<hr/>	<hr/>
<hr/>	<hr/>	<hr/>
<hr/>	<hr/>	<hr/>
<hr/>	<hr/>	<hr/>

BAKE OUT PROCEDURE

DATE: _____

SAMPLE: _____

OPERATOR: _____

CHECKED BY: _____

- _____ 1. RGA scan
- _____ 2. Mirror in safe position
- _____ 3. Quartz lamp on 30% of maximum overnight
- _____ 4. Heating tape on dewar set at 200 degrees
- _____ 5. Wrap detector with tape and set at 150 degrees
- _____ 6. Secure temperature monitors and switch tapes on
- _____ 7. Sun lamp on low directed at mirror surface

COLD TEMPERATURE RUN

DATE: _____

SAMPLE: _____

OPERATOR: _____

CHECKED BY: _____

- ```

____ 1. Before continuing, go through start-up checklist
____ 2. Fill LN2 sleeve
____ 3. Levels: Start: LHe _____ liters END: LHe _____ liters
 He _____ pounds He _____ pounds
____ 4. RGA scan, chart at 1cm/min
 Temperature _____ °K
 Pressure: IG _____ torr
 RGA _____ mb
____ 5. Top off LN2
____ 6. Heat gun and sunlamp on
____ 7. Connect He gas to LHe dewar
____ 8. Connect and secure transfer line to tank
____ 9. Connect to sample dewar
____ 10. Monitor temperature and pressure throughout run (lab book)
____ 11. Realign when mount temperature levels off (Alignment List)
____ 12. Scan as required (Consult Room Temperature Procedure #6)
____ 13. At end of measurements return mirror to home position
____ 14. List Path D:\ _____
 Filenames:

____ 15. Disconnect transfer line and seal LHe tank
____ 16. Mirror facing window with sunlamp on low
____ 17. Heating tape on dewar at 200 degrees
____ 18. Siphon off LN2 with tubes, insure against freezing seals
____ 19. Low pressure Nitrogen gas into LHe vent hole
____ 20. Bunsen valve LHe transfer connector

```

If LHe tank needs to be replaced during scan:

1. He gas off
2. Disconnect at dewar
3. Disconnect at tank
4. Connect new tank
5. Connect He gas to tank
6. Wait for white plume
7. Reconnect to dewar

**COLD TEMPERATURE RUN WITH**  
**e-BEAM IRRADIATIONS**

DATE: \_\_\_\_\_

SAMPLE: \_\_\_\_\_

OPERATOR: \_\_\_\_\_

CHECKED BY: \_\_\_\_\_

- \_\_\_\_\_ 1. Before continuing, go through start-up checklist
- \_\_\_\_\_ 2. RGA scan, chart at 1cm/min  
Temperature \_\_\_\_\_ °K  
Pressure: IG \_\_\_\_\_ torr  
RGA \_\_\_\_\_ mb
- \_\_\_\_\_ 3. Fill LN<sub>2</sub> sleeve
- \_\_\_\_\_ 4. Levels: Start: LHE \_\_\_\_\_ liters      END: LHE \_\_\_\_\_ liters  
He \_\_\_\_\_ pounds      He \_\_\_\_\_ pounds
- \_\_\_\_\_ 5. e-Beam on
- \_\_\_\_\_ 6. Oscilloscope on and settings set  
Channel 1 (left) for voltage monitor  
1 volt scale  
polarity up  
x20 attenuation  
Channel 2 (right) for current monitor  
0.5 volt scale  
polarity up  
x200 attenuation  
Time Base at 20 nanoseconds, single sweep triggered "--"
- \_\_\_\_\_ 7. Top off LN<sub>2</sub>
- \_\_\_\_\_ 8. Heat gun and sunlamp on
- \_\_\_\_\_ 9. He gas to LHe dewar
- \_\_\_\_\_ 10. Connect and secure transfer line to tank
- \_\_\_\_\_ 11. Connect to sample dewar
- \_\_\_\_\_ 12. Monitor temperature and pressure throughout run (lab book)
- \_\_\_\_\_ 13. Realign when mount temperature levels off (Alignment List)
- \_\_\_\_\_ 14. Scan as required (Consult Room Temperature Procedure #6)
- \_\_\_\_\_ 15. At end of measurements return sample to home position
- \_\_\_\_\_ 16. e-Beam Alignment
  - \_\_\_\_\_ a) Home Center
  - \_\_\_\_\_ b) Translate to Si wafer center Y= \_\_\_\_\_  
Z= \_\_\_\_\_
  - \_\_\_\_\_ c) Rotate 180 degrees
  - \_\_\_\_\_ d) Translate Y & Z previously moved distances
  - \_\_\_\_\_ e) Move X toward e-Beam: note position X = \_\_\_\_\_

- \_\_\_\_\_ f) All electrical equipment off and disconnected  
and cap off temperature monitor feed-through
  - \_\_\_\_\_ g) Fire e-Beam at 32%
  - \_\_\_\_\_ h) Back X off
  - \_\_\_\_\_ i) Rotate 90 degrees and inspect
  - \_\_\_\_\_ j) Correct Y & Z positions as necessary
  - \_\_\_\_\_ k) Rotate -90 degrees
  - \_\_\_\_\_ l) Return X to e) position
  - \_\_\_\_\_ m) Repeat steps f thru l until e-beam is on target
  - \_\_\_\_\_ n) Finish e-beam shots at each fluence on wafer
  - \_\_\_\_\_ o) Translate -(Z) and +(Y) amounts from step b  
(+Z 12.7mm to position A)
  - \_\_\_\_\_ o) Go to A ( Z = +12.7000 mm)
  - \_\_\_\_\_ p) Set fluence, irradiate with V/C trace \_\_\_\_\_
  - \_\_\_\_\_ q) Go to B ( Y = +10.9985 mm, Z = -19.0500 mm)
  - \_\_\_\_\_ r) Set fluence, irradiate with V/C trace \_\_\_\_\_
  - \_\_\_\_\_ s) Go to C ( Y = -21.9970 mm)
  - \_\_\_\_\_ t) Set fluence, irradiate with V/C trace \_\_\_\_\_
  - \_\_\_\_\_ u) Back X off from e-Beam
  - \_\_\_\_\_ v) Rotate 90 degrees and inspect (note in book)
  - \_\_\_\_\_ w) rotate -272 degrees then send home
  - \_\_\_\_\_ x) e-Beam off, Oscilloscope off, Electrical on
  - \_\_\_\_\_ 21. Scan as required on Post Irradiated Surface
  - \_\_\_\_\_ 22. At end of measurements return sample to home position
  - \_\_\_\_\_ 23. List Path D:\\_\_\_\_\_
- Filenames:
- |       |       |       |
|-------|-------|-------|
| _____ | _____ | _____ |
| _____ | _____ | _____ |
| _____ | _____ | _____ |
| _____ | _____ | _____ |
| _____ | _____ | _____ |
| _____ | _____ | _____ |
| _____ | _____ | _____ |
| _____ | _____ | _____ |
| _____ | _____ | _____ |
| _____ | _____ | _____ |
- \_\_\_\_\_ 24. Disconnect transfer line and seal LHe tank
  - \_\_\_\_\_ 25. Bunsen valve LHE transfer connector
  - \_\_\_\_\_ 26. Heating tape on dewar at 200 degrees
  - \_\_\_\_\_ 27. Siphon off LN<sub>2</sub> with tubes, insure against freezing seals
  - \_\_\_\_\_ 28. Low pressure Nitrogen gas into LHe vent hole

If LHe tank needs to be replaced during scan:

1. He gas off
2. Disconnect at dewar
3. Disconnect at tank
4. Connect new tank
5. Connect He gas to new tank
6. Wait for white plume
7. Reconnect to dewar

## VENTING AND SAMPLE REMOVAL

DATE: \_\_\_\_\_

SAMPLE: \_\_\_\_\_

OPERATOR: \_\_\_\_\_

CHECKED BY: \_\_\_\_\_

USE UPON COMPLETION OF ALL TESTS OR WHEN NECESSARY

- \_\_\_\_\_ 1. All monitoring gauges off
- \_\_\_\_\_ 2. Argon level Start \_\_\_\_\_ Stop \_\_\_\_\_ Used \_\_\_\_\_
- \_\_\_\_\_ 3. Argon pressure at 2 lbs.
- \_\_\_\_\_ 4. Sample in safe position
- \_\_\_\_\_ 5. High Vacuum off
- \_\_\_\_\_ 6. Vent on
- \_\_\_\_\_ 7. Check for relief valve release
- \_\_\_\_\_ 8. Vent off
- \_\_\_\_\_ 9. Rough down to 1000 microns
- \_\_\_\_\_ 10. Rough off
- \_\_\_\_\_ 11. Repeat 6 through 10 as necessary
- \_\_\_\_\_ 12. Argon to 1 lb.
- \_\_\_\_\_ 13. Rotate sample to face port
- \_\_\_\_\_ 14. Remove Port
- \_\_\_\_\_ 15. Loosen sample mount and remove sample (keep clean)
- \_\_\_\_\_ 16. Remove and label Si wafer
- \_\_\_\_\_ 17. Remove sample from mount while under flow-hood
- \_\_\_\_\_ 18. Prep sample for next test.
- \_\_\_\_\_ 19. If new sample is to be installed proceed immediately  
If chamber will remain unused for some time: Argon off,  
reseal chamber and rough down to 1000 microns or less.

## BEAM DUMP REPLACEMENT

DATE: \_\_\_\_\_

OPERATOR: \_\_\_\_\_

CHECKED BY: \_\_\_\_\_

- \_\_\_\_ 1. Set Specular with system as is
- \_\_\_\_ 2. Remove detector and place on safe surface
- \_\_\_\_ 3. Remove front mounting block and remove old beam dump
- \_\_\_\_ 4. Install detector into system and find specular signal  
note signal (no beam dump) \_\_\_\_\_ Volts
- \_\_\_\_ 5. Attach new Beam Dump to mounting block.
- \_\_\_\_ 6. Remove detector and set into HeNe path:
  - detector opening must be directly in HeNe beam
  - use back reflections visible on detector window from element surface.
  - retro-reflect HeNe: Back reflection from detector window  
to HeNe opening; and then back reflection from detector element onto detector window; both must be co-linear
- \_\_\_\_ 7. Beam Dump assembly carefully reconnected to detector almost tight
- \_\_\_\_ 8. Slide beam dump left and right until HeNe spot on window is maximum
- \_\_\_\_ 9. Tighten beam dump
- \_\_\_\_ 10. Install detector back into system
- \_\_\_\_ 11. Find and note specular signal: \_\_\_\_\_ Volts  
should be at least 50% or more of signal observed in step 4
- \_\_\_\_ 12. If signal is good, continue  
If signal is not good, retry steps 2 to 12
- \_\_\_\_ 13. If still no luck after two attempts, Mal-adjust beam dump to the right or the left and retry steps 2 to 13

**APPENDIX B**  
**MIRROR INVENTORY AT SPIRE CORPORATION**  
**AS OF 30 NOVEMBER 1990**

| NUMBER          | SIZE<br>(") | BRDF<br>Tested |
|-----------------|-------------|----------------|
| POCT74-V-1      | 7           | N              |
| POCT-56-W1-M1-1 | 2           | Y              |
| POCT-56-W1-M1-2 | 2           | Y              |
| POCT-56-W1-M1-4 | 2           | N              |
| POCT-57-W1-M2-1 | 2           | N              |
| POCT-58-W1-M6-1 | 2           | N              |
| POCT-58-W1-M6-3 | 2           | N              |
| POCT-2V-A-67-A  | 2           | Y              |
| POCT-2V-A-67-B  | 2           | N              |
| POCT-2V-A-68-A  | 2           | N              |
| POCT-6V-A-69-B  | 2           | N              |
| POCT-U-29       | 1.5         | N              |
| POCT-U-32       | 1.5         | Y              |
| POCT-U-42       | 2           | Y              |
| POCT-U-43       | 2           | Y              |
| POCT-U-52       | 2           | Y              |
| PE-Sn-11        | 2           | Y              |
| PE-Sn-14        | 2           | Y              |
| PE-Sn-15        | 2           | Y              |
| PE-Sn-16        | 2           | Y              |
| PE-Sn-19        | 1.5         | Y              |
| 93              | 2           | Y              |
| 94              | 2           | Y              |
| 95              | 2           | Y              |
| 100             | 2           | Y              |
| 102             | 2           | Y              |
| 105             | 2           | Y              |
| 108             | 2           | Y              |
| 114             | 2           | Y              |
| 119             | 2           | Y              |
| 121             | 2           | Y              |
| 124             | 2           | Y              |
| 63-10           | 2           | N              |
| Be050-01        | 1.5         | Y              |
| Be050-04        | 1.5         | Y              |
| SIC 6-21-89-1   | 2           | N              |
| SIC 6-21-89-5   | 2           | N              |
| OEC-017         | 1.5         | N              |

## **DISTRIBUTION LIST**

U.S. Army Strategic Defense Command  
P.O. Box 1500  
Huntsville, AL 35807-3801

Attention: CSSD-SD-P

U.S. Army Strategic Defense Command  
P.O. Box 1500  
Huntsville, AL 35807-3801

Attention: CSSD-H-SAV

U.S. Army Strategic Defense Command  
P.O. Box 1500  
Huntsville, AL 35807-3801

Attention: CSSD-H-MPL

Hughes Danbury Optical Systems, Inc.  
110 Woosler Heights Road  
MS848  
Danbury CT 06810

Attention: George Gardopee

Director  
United States Army Materials Technology Laboratory  
Arsenal Street  
Watertown, MA 02171-0001

Attention: Dr. John Dignam, SLCMT-BM

Martin Marietta Energy Systems, Inc.  
P.O. Box 2009  
Oak Ridge, TN 37831-8063

Attention: W.B. Snyder

Strategic Defense Initiative Organization  
The Pentagon, Room 30444  
Washington D.C. 20301-7000

Attention: T/SK

Mission Research Corporation  
4935 North 30th Street  
Colorado Springs, CO 80919

Attention: Mr. Phillip Jessen

BREAULT Research Organization, Inc.  
4601 East First Street  
Tucson, AZ 85711

Attention: Dr. Robert Breault

Rockwell International  
3370 Miraloma Avenue  
P.O. Box 3170  
Anaheim, CA 92803-3170

Attention: Paul Dahlgren

Rockwell International  
3370 Miraloma Avenue  
P.O. Box 3170  
Anaheim, CA 92803-3170

Attention: Harry Moreen

Lockeed Missile & Space Company, Inc.  
3251 Hanover Street, 0/93-10b/204  
Palo Alto, CA 94304-1187

Attention: Dr. Charles M. Packer

Teledyne Brown Engineering Co.  
300 Sparkman Drive  
Huntsville, AL 35807

Attention: Mr. J. Wells MS-19

Dynamics Research Corporation  
1755 Jefferson Davis Highway  
Crystal Square 5  
Arlington, VA 22202

Attn: SDIO Library, Suite 708

Defense Technical Information Center (DTIC)  
Cameron Station  
Alexandria, VA 22314